STUDIES ON SOME NICKEL COMPLEXES

A Thesis
Submitted for the Degree of
Doctor of Philosophy

By
ABHIK MUKHOPADHYAY

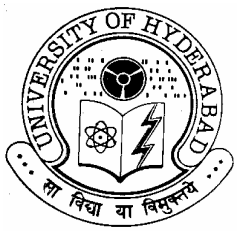

School of Chemistry
University of Hyderabad
Hyderabad 500 046
India

May 2006

STATEMENT

I hereby declare that the matter embodied in this thesis entitled "***Studies on Some Nickel Complexes"*** is the result of the investigations carried out by me in the School of Chemistry, University of Hyderabad, under the supervision of **Prof. Samudranil Pal**.

In keeping the general practice of reporting scientific observations, due acknowledgement has been made wherever the work is described is based on findings of other investigators. Any omission, which might have occurred by oversight or error, is regretted.

May 2006 **Abhik Mukhopadhyay**

PROF. SAMUDRANIL PAL
SCHOOL OF CHEMISTRY
UNIVERSITY OF HYDERABAD
HYDERABAD-500 046, INDIA

Phone: +91-40-23134756
(office)
Fax: +91-40-23012460
Email: spsc@uohyd.ernet.in

th May, 2006

CERTIFICATE

Certified that the work embodied in the thesis entitled "***Studies on Some Nickel Complexes"*** has been carried out by **Mr. Abhik Mukhopadhyay** under my supervision and the same has not been submitted elsewhere for any degree.

Prof. Samudranil Pal
(Thesis supervisor)

Dean
School of Chemistry
University of Hyderabad

Acknowledgement

I express my deep sense of gratitude and profound respect to my research supervisor Prof. Samudranil Pal for his invaluable guidance, support and constant encouragement. I have learned a great deal from him and consider my association with him to be a rewarding experience. He has allowed me to grow as a chemist by letting me work on my own ideas and having me learn from my own mistakes.

I would like to thank the former and present Dean, School of Chemistry, for their constant inspiration and for the available facilities. I am extremely thankful individually to all the faculty members of the school for their help, cooperation and encouragement at various stages of my stay in the school.

I convey my sincere thanks to Prof. M. Vairamani (IICT) for providing me the FAB mass data. I also convey my sincere thanks to Prof. Waterloo Fujita (Nagoya University) for providing me the variable temperature magnetic data.

I thank all the non-teaching staff of the school for their cooperation. They had all been quite helpful. I should mention two people in particular, Raghavaiah and Suresh.

Financial assistance from CSIR, New Delhi is gratefully acknowledged.

I am thankful to my childhood teachers Mr. Ashok Kr. Ghosh, Dr. Amitava Mukhopadhyay and Mrs. Swati Ghosh.

Each of the members of our group has helped me to enrich my experience in their own way. I thank all my seniors in the lab: Drs. Sangeetha, Satyanarayan, Tin, Mariappan, Gupta and Vamsee, with whom I am associated at various stages of my stay in the lab. I thank my juniors Raji, Anindita and Rajesh for creating cheerful atmosphere inside the lab. I will cherish my association with all of them. I was really lucky to have Sunirban, my friend and my M.Sc batch met, as my lab met. I will definitely miss our late night discussions from where I developed my perspectives towards science and life.

I am grateful to Binoyda, Dinuda, Sandy, Rahulda and Tamalda. I have learnt a lot from them in various stages of my research life. I also thank our great “2001” batch:

Archan, Manab, Subahsh, Moloy, Saikat, Prasun, Shatabdi, Bishwarup, Pavan and Padmanabhan. I will cherish those memorable days throughout my life. I wish to thank Balaraman, Venkatesh, Gireesh, Suresh, Narsi, Shyamraj, Pradeep, Prabhakar, Malla, Venu Anna, Senthil (Sr and Jr), Sreenivas Reddy, Sreenivasulu, Basovoju, Baluji, Sarat, Subbu didi, Aparna, Chadrasekhar, Anoop, Param, Deshigan, Rajesh, Madhu and Sunil for their help, cooperation and encouragement at various stages of my stay in the campus. I also thank my Juniors Jeths, Bhat, Ghana, Podu, Bachha, Tapto, Tanmoy, Ghanta, Ullas, Bipul, Assam Rifles, Pati, Arindam, Rakesh, Bhaswati, Suparna, Rumpa, Thakur, Sandip, Biju, Prasad and Jaggu. I will miss many people of this campus with whom I have shared the last five years of my life. Special thanks go to Nilesh, Som, Abhinandan, Kedarda, Ajayda, Masoom and Saonti.

I gratefully acknowledge my music club members: Bobs, Saki, Pachu and Tapto. I have really enjoyed many weekends jamming with them for hours after hours forgetting chemistry.

I would like to thank my friends Randhir, Chanchal, Kajjal, Supriyo, Deba, Bunty and many more for their constant encouragement and support.

Without my parent’s and my elder brother’s (dadabhai) relentless support and blessings, I would not have reached to this stage of my life. I owe every thing to them. I am grateful to my boudi for her constant encouragement. I thank my cousin Babuda, with whom I spent a good time during my stays here in Hyderabad. The blessings and wishes of my sweet dida have made me what I am. I am grateful to all of my family members for their support and encouragement at various stages of my life.

I convey my profound regards to all my teachers who taught me throughout my student life. I end by thanking each and everyone who helped me to reach here.

Abhik Mukhopadhyay

CONTENTS

Chapter 1

Introduction

1.1. Prelude

The coordination chemistry of the transition metal ions has been a challenge to the inorganic chemists since they were identified in the nineteenth century. The modern study of the coordination complexes started with two men, Alfred Warner and Sophus Mads Jørgensen. Both were astute chemists, not only in laboratory aspects but also in the areas of interpretation and theory. Nearly a century later, from our vantage point we are able to conclude that Warner was right[1] and Jørgensen was wrong in the interpretation of the experimental evidences they had. Werner was the first inorganic chemist to be awarded the Noble prize in chemistry. Nevertheless, Jorgensen's contribution can not be slighted. Today, these coordination complexes comprise a large body of current research activities covering a vast area of science. In fact coordination chemistry bridges almost all the branches of chemistry, which include inorganic, physical, organic, analytical, material, etc.[2-7] In addition, various complexed metal ions play vital roles in a number of biological processes. The fast evolving area "bioinorganic chemistry/biological chemistry/inorganic chemistry" covers these "bio-coordination compounds".

1.2. Motivation behind the present work

1.2.1. Importance of nickel chemistry

The coordination chemistry of nickel especially in high oxidation states is of considerable interest due to its importance not only in inorganic chemistry but also in other areas of chemistry and biology.[8] The structure and spectroscopy of high-valent nickel species have received much attention from inorganic chemists during the seventies and eighties, and promptly constituted a classical topic in

high-valent transition metal chemistry.[9] The continuing interest in the redox chemistry of nickel complexes is primarily due to the participation of high-valent nickel species in the catalytic redox cycle of some enzymes in certain microorganisms.[10] These include the well-known Ni–Fe hydrogenase[11] and Ni–tetrahydrocorphinoid cofactor (F430) of methyl-coenzyme M reductase (MCR),[12] and a recently discovered Ni-containing superoxide dismutase (NiSOD).[13] Likewise, high-valent nickel species have been postulated as reactive intermediates in the catalytic oxidative cleavage of nucleic acids[14] and in a variety of catalytic oxidative processes of organic synthesis, including Ni-catalyzed alkene epoxidation and arene hydroxylation reactions.[15,16] Whether for their significance as biomimetic models[17] or their potential use as catalytic oxidants,[18] the list of coordination complexes of nickel has continued to grow during the last decade. Thus, a number of well-characterized nickel complexes with diverse ligand types and coordination geometries are available nowadays.[19-24]

1.2.2. Role of nickel in biology

The slow-footed struggle to ascertain the importance of nickel in biology was fraught with contrarieties and surprise, but it was just may be “a matter of time” before nickel was found to be an element of biological importance. Dr. James B. Summer was the first scientist to isolate an enzyme. The enzyme he has isolated was urease.[25] Summer demonstrated urease to be a protein devoid of organic coenzymes and, of interest here, metal ions. Thus it was quite surprising when Dixons and co-workers 49 years later announced that urease is a nickel containing metalloenzyme.[26] All the Ni proteins known to date are from plants or bacteria. However, ~80 years elapsed between the crystallization of jack-bean urease in 1925 and the identification of the nickel component in plant protein. Thus it is premature to exclude the possibility of Ni-proteins in animal. Apart

from urease few other recently discovered nickel containing enzymes are hydrogenase and methycoenzyme M reductase (MCR).

Hydrogenases (H_2ases) are metalloenzymes that catalyze the reversible oxidation of H_2 and, as such, are important enzymes in anaerobic metabolism for both chemotrophic and phototrophic bacteria.[27-29] Because they are involved in producing H_2 from water,[30] nitrogen fixation,[31] methane production,[32] and sulfate reduction,[29] they have attracted attention as biological catalysts involved in reactions that are of considerable commercial importance. Hydrogenases contain a complex assembly of metal cofactors and fall into three classes according to the cofactor present, these enzymes are divided into three main groups: (i) Fe – only hydrogenase, (ii) [FeNi] hydrogenase and (iii) [FeNiSe] hydrogenase. The active site of [FeNi] hydrogenase contains 1 equivalent of nickel in addition to Fe–S clusters. EPR studies on different [FeNi] hydrogenases indicate that the nickel center or centers in these enzymes serve as the binding sites for the substrate hydrogen.[33] Carbon monoxide, an inhibitor of the enzyme, also binds at the nickel center reversibly. When Ni is present in the enzyme, it is often detected by an unusual $S = ½$ EPR signal that has been assigned to formally Ni(III) or Ni(I) centers.[34] This EPR signal has provided a tool for investigating the role of the Ni centers and the evidence linking Ni to the binding of H_2 and inhibitors (e.g. CO), and has been used to demonstrate the redox activity of the Ni site. Recent spectroscopic studies have indicated that the nickel center in [FeNi] hydrogenase from *Thiocapsa roseoperscinia* exists in a distorted pentacoordinated geometry with three nitrogen/oxygen and two sulfur atoms in its first coordination sphere.[35]

The methyl-coenzyme M reductase (MCR) catalyzes the last chemical step of methane formation by methanogenic organisms (*methanoarchaea*). The reaction involves a two-electron reduction of the methylthioether coenzyme M (CH_3-S-CoM) by *N*-7-mercaptoheptanoyl-threonine phosphate (CoB-SH). A key

component of the active site of MCR is F430, a nickel(II) tetrapyrrole cofactor, whose Ni(I) form is present in the active form of the enzyme, MCR_{red1}.[36-39]

1.2.3. Nickel in catalysis

The epoxidation of olefins with terminal oxidants such as peroxides, iodosylbenzene, hypochlorite, amine oxides, etc. is catalyzed by a variety of metal complexes.[40] The same catalytic epoxidations are mimicked by metal complexes of macrocycles in which (a more or less) square-planar array of nitrogen and oxygen atoms are coordinated to the metal center.[41] The most accepted pathway for the catalytic epoxidation of olefins is the oxygen rebound process outlined in Scheme I.[42] According to Scheme I, the metal catalyst (M) serves as a relay for oxygen atom transfer from the oxygen donor (TO) via of an oxo-metal species (M=O) as the intermediate. The shuttling of the metal complex between the two states formally corresponds to an oxidative-addition-reductive-elimination sequence. As such, it is generally found that those metals that are capable of readily undergoing two-electron changes are effective in this catalysis. Generally square-planar nickel(II) complexes with tetracoordinating ligands such as several macrocycles and also with bidentate ethylenediammine, where the higher oxidation state(+4) of the nickel can be accessed, are good candidates for olefin epoxidation.[43]

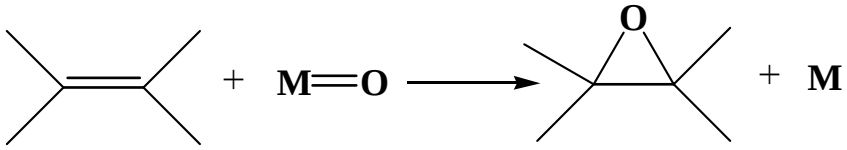

$$M + TO \longrightarrow T + M{=}O$$

Scheme 1

1.2.4. Intra-molecular C-H···M interaction in d^8 complexes

Short distance between a hydrogen atom, attached to nitrogen or carbon, and a metal has been known for a while and was first identified by Trofimenko.[44] They were often interpreted as a manifestation of agostic interactions.[45] Such interaction was mainly observed in square planar Group VIII metal ion complexes, formally 16-electron species, where the X–H bond approached the metal from one of the axial positions.[46] Brammer *et al.* were among the first to assign X–H···M short contacts as hydrogen bonds.[47] Weak X–H···M interactions are important in the context of metal protonation and reactivity, especially when square planar metal centers are involved.[48]

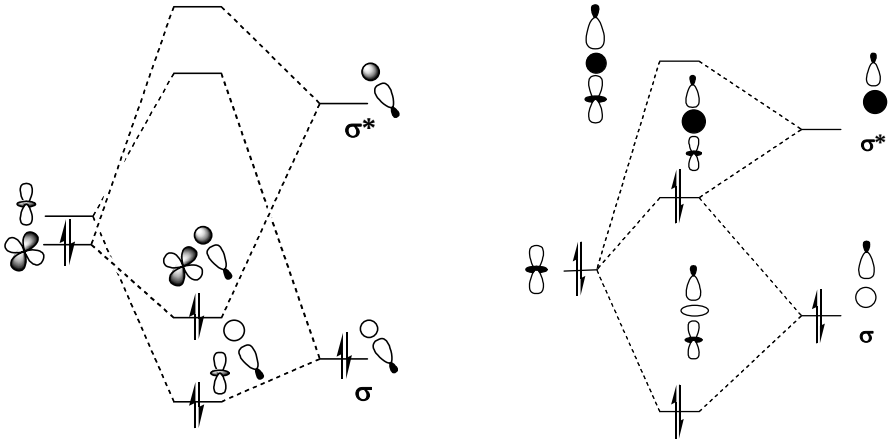

3c-2e agostic bond 3c-4e hydrogen bond

Scheme 2

In a typical agostic interaction, the metal centre is electron deficient and receives electrons from a C–H···σ orbital with a back donation from the metal to the σ* of C–H bond. Such bonds can be described as three-centre-two-electron bonds[49] (C–H→M), as sketched in Scheme 2. Thus Electron deficient transition metals are good candidates for agostic interaction. Whereas in a C-H···M hydrogen bond, an electropositive H-atom acts as a bridge between two

electronegative centers.[50] Electron rich metal atoms, typically late transition metals in low oxidation states, can act as acceptors in this type of hydrogen bonds and the interaction is three-center-four-electron one (Scheme-2). However, the situation is not entirely straightforward, particularly in the case of 16-electron metal centers as found in square-planar d^8 systems, where in principle axial C–H···M interactions could be either 3c–4e or 3c–2e in nature,[51] because the metal center has available lone pair as well as an empty orbital. Proton NMR was used to distinguish between agostic and hydrogen bond interactions in 16-electron square planar complexes, as the proton resonance is shifted upfield for the first case, and downfield for the second case, compared to the free ligand.[52] Crabtree and co-workers examined the available experimental evidences for square-planar d^8 systems and concluded that the nature of axial C-H···M interaction is still ambiguous because of the weakness of the interaction[53] compared to N-H···M and O-H···M interactions, which are clearly hydrogen bonds. Despite the doubt weak hydrogen bond description of C-H···M in d8 systems is favored.[54]

1.2.5. Noncovalent interactions

One of the main goal of present day chemistry is the construction of larger and larger structures.[55] These structures are the numerous synthetic targets in the domain of covalent chemistry. But the limitations of traditional covalent bond-forming chemistry must also be questioned – just how far can molecular synthesis[56] be taken? This realization prompts us to seek alternative strategies for the construction of extended structures and leads us to consider the chemistry of the noncovalent bond, and consequently, interactions between molecules, i.e. supramolecular chemistry[57] and hence supramolecular synthesis.[58] A detailed knowledge and realization of the molecular recognition processes, particularly those based upon hydrogen bonding,[59,60] π–π interactions,[61] hydrophobic,[62] ion pairing[63] and van der Walls interactions,[64] allows us to design small, relatively

simple building blocks that are capable of assembling into large super structures. Application of the chemistry of the noncovalent interactions has proved to be very effective, in the creation of the numerous supramolecular architectures,[65] in the realization of molecular topologies,[66] as well as describing several complex phenomena in biological systems.[67]

1.3. About the present investigation

The known chemistry of nickel spans all oxidation states from -1 to +4.[68] Among these the -1 states is ill-defined and a search of the literature reveals that the known examples do not exceed those catalogued in recent textbooks.[69,70] The common chemistry of nickel is the chemistry of it in the +2 oxidation state. An extensive chemistry also exists for zero-valent nickel.[58] The oxidation states +1, +3 and +4 can be considered as comparatively sparse but enough is now known mainly due to the efforts during the last two decades. Our principal aim was to synthesize stable nickel(II) and nickel(III) species with Schiff bases containing higher-oxidation state promoting functionalities such as phenolic-OH and amide. The Schiff bases used are shown in Scheme-3. We were able to isolate higher valent species in one case and nickel(II) complexes with the rest. All the complexes prepared were characterized by analytical, spectroscopic and X-ray crystallographic techniques.

The Schiff bases of type I have been derived from 2-pyridinecarboxaldihyde and *ortho*-substituted aminobenzene. Bis complexes of nickel(II) with this tridentate ligand system have been synthesized. Chapter 2 deals mainly with the supramolecular architectures formed by these complexes via intermolecular non-covalent interactions.

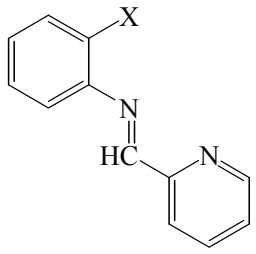

X = OH, COOH
(**I**)

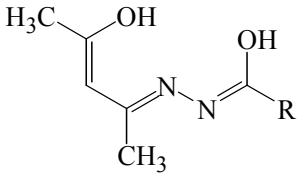

R = CH_3, Ph
(**II**)

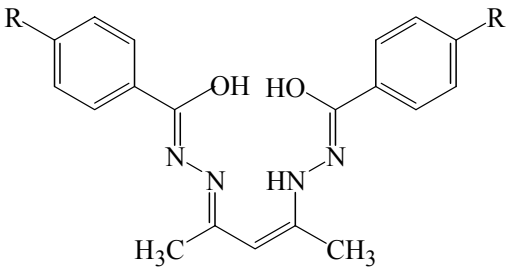

R = H, OCH_3, $N(CH_3)_2$
(**III**)

Scheme 3

Ternary square-planar nickel(II) complexes with the tridentate Schiff bases of type II and monodentate N-heterocycles are described in Chapter 3 and 4. Self-assembly via intermolecular Ni···H-C interaction in these complexes have been investigated and discussed in details.

We have tried to synthesize the tetradentate Schiff base system (type III) from two mole equivalents of 4-substituted benzoylhydrazines and one mole equivalent of acetylacetone. The isolated product was substituted pyrazolines. Using these pyrazolines and nickel acetate we have synthesized a series of square planar nickel(II) and nickel(II) stabilized radical species. Chapter 5 contains the description of these complexes.

1.4. References

1. A. Werner, *Z. Anorg. Chem*., 1893, **3**, 267.
2. A. A. Grinberg, *Russ. Chem. Rev*., 1961, 30
3. A. Albert, *Aust. J. Sci*., 1967, **30**, 1.
4. J. Schubert, *Sci. Amer*., 1966, **214(5)**, 40.
5. M. J. Seven and L. A. Johnson, Ed., *Metal binding in medicines;* Lippincot Co., Philadelphia, Pa., 1960.
6. F. P. Dwyer and D. P. Mellor, Ed., *Chelating agents and metal chelates*; Academic Press, London., 1960
7. Collection of metalloenzyme reviews, *Struct. Bonding*. (Berlin), 1970,8.
8. F.Meyer and H. Kozlowski, *Comprehensive Coordination ChemistryII: From Biology to Nanotechnology*, ed. J. A. McCleverty and T. J. Meyer, Elsevier, Oxford, 2004, vol. 6, p. 247.
9. (*a*) W. Levason and C. A. McAuliffe, *Coord. Chem. Rev.*, 1974, **12**, 105; (*b*) J. Willemse, J. A. Crass, J. J. Steggerda and C. P. Keijzers, *Struct. Bonding (Berlin)*, 1976, **28**, 83; (*c*) K. Nag and A. Chakravorty, *Coord. Chem. Rev.*, 1980, **33**, 87; (*d*) R. I.Haines and A. McAuley, *Coord. Chem. Rev.*, 1981, **39**, 77; (*e*) J. A. Ibers, L. J. Pace, J. Martinsen and B.M. Hoffman, *Struct. Bonding (Berlin)*, 1982, **50**, 3; (*f*) A. Chakravorty, *Isr. J. Chem.*, 1985, **25**, 99; (*g*) A. McAuley and P. R. Norman, *Isr. J. Chem.*, 1985, **25**, 106; (*h*) L. Fabbrizzi, M. Licchelli, A. Perotti, A. Poggi and S. Soresi, *Isr. J. Chem.*, 1985, **25**, 112; (*i*) P. Cocolios and K. M. Kadish, *Isr. J. Chem.*, 1985, **25**, 138; (*j*) A. G. Lappin and A. McAuley, *Adv. Inorg. Chem.*, 1988, **32**, 241.
10. (*a*) C. T. Walsh and W. H. Orme-Johnson, *Biochemistry*, 1987, **26**, 4901; (*b*) *The Bioinorganic Chemistry of Nickel*; ed. J. R. Lancaster, Jr., VCH, New York, 1988.
11. A. Volbeda, M. H. Charon, C. Piras, E. C. Hatchikian, M. Frey and J. C. Fontecilla-Camps, *Nature*, 1995, **373**, 580.
12. U. Ermler, W. Grabarse, S. Shima, M. Goubeaud and R. K. Thauer, *Science*, 1997, **278**, 1457.

13 (*a*) J. W. Lee, J. H. Roe and S. O. Kang, *Methods Enzymol.*, 2002, **349**, 90; (*b*) B. Palenik, B. Brahamsha, F. W. Larimer, M. Land, L. Hauser, P. Chain, J. Lamerdin, W. Regala, E. E. Allen, J. McCarren, I. Paulsen, A. Dufresne, F. Partensky, E. A.Webb and J.Waterbury, *Nature*, 2003, **424**, 1037.

14. (*a*) C. C. Cheng, S. E. Rokita and C. J. Burrows, *Angew. Chem., Int. Ed. Engl.*, 1993, **32**, 277; (*b*) C. J. Burrows, J. G. Muller,G. T. Poulter and S. E. Rokita, *Acta Chem. Scand.*, 1996, **50**, 337; (*c*) J. G. Muller, R. P. Hickerson, R. J. Perez and C. J. Burrows, *J. Am. Chem. Soc.*, 1997, **119**, 1501.

15. (*a*) J. D. Koola and J. K. Kochi, *Inorg. Chem.*, 1987, **26**, 908; (*b*) J. F. Kinneary, J. S. Albert and C. J. Burrows, *J. Am. Chem. Soc.*, 1988, **110**, 6124; (*c*) H. Yoon and C. J. Burrows, *J. Am. Chem. Soc.*, 1988, **110**, 4087; (*d*) H. Yoon, T. R. Wagler, K. J. O'Connor and C. J. Burrows, *J. Am. Chem. Soc.*, 1990, **112**, 4568; (*e*) W. Nam and J. S. Valentine, *J. Am. Chem. Soc.*, 1993, **115**, 1772.

16. (*a*) E. Kimura, A. Sakonaka and R. Machida, *J. Am. Chem. Soc.*, 1982, **104**, 4255; (*b*) E.Kimura and R. Machida, *J. Chem. Soc., Chem. Commun.*, 1984, 499; (*c*) E. Kimura, R. Machida and M. Kodama, *J. Am. Chem. Soc.*, 1984, **106**, 5497; (*d*) R.Machida, E. Kimura and Y. Kushi, *Inorg. Chem.*, 1986, **25**, 3461; (*e*) D. Chenand and A. E.Martell, *J. Am. Chem. Soc.*, 1990, **112**, 9411; (*f*) D. Chen, R. J. Motekaitis and A. E. Martell, *Inorg. Chem.*, 1991, **30**, 1396.

17. (*a*) R.Cammack, *Adv. Inorg. Chem.*, 1988, **32**, 297; (*b*) M. A.Halcrow and G. Christou, *Chem. Rev.*, 1994, **94**, 2401.

18. (*a*) C. J. Burrows and S. E. Rokita, *Acc. Chem. Res.*, 1994, **27**, 295; (*b*) E. C. Long, *Acc. Chem. Res.*, 1999, **32**, 827.

19. (*a*) P. A. Connick and K. A. Macor, *Inorg. Chem.*, 1991, **30**, 4654; (*b*) S. Will, J. Lex, E. Vogel, H. Schmickler, J. P. Gisselbrecht, C. Haubtmann, M. Bernard and M. Gross, *Angew. Chem., Int. Ed. Engl.*, 1997, **36**, 357; (*c*) C. J. Campbell, J. F.Rusling and C. Bruckner, *J. Am. Chem. Soc.*, 2000, **122**, 6679; (*d*) K. M. Kadish, M. Lin, E. V. Caemelbecke, G. De Stefano, C. J. Medforth, D. J. Nurco, N. Y. Nelson, B.

Krattinger, C. M. Muzzi, L. Jaquinod, Y. Xu, D. C. Shyr, K. M. Smith and J. A. Shelnutt, *Inorg. Chem.*, 2002, **41**, 6673.

20. (*a*) M. A. A. F. C. T. Carrondo, B. De Castro, A. M. Coelho, D. Domingues, C. Freire and J. Morais, *Inorg. Chim. Acta*, 1993, **205**, 157; (*b*) F. Azevedo, M. A. A. F. C. T. Carrondo, B. De Castro, M. Convery, D. Domingues, C. Freire, M. T. Duarte, K.Nielsen and I. C. Santos, *Inorg. Chim. Acta*, 1994, **219**, 43; (*c*) E. Pereira, L. Gomes and B. De Castro, *Inorg. Chim. Acta*, 1998, **271**, 83; (*d*) C. Freire and B. De Castro, *J. Chem. Soc., Dalton Trans.*, 1998, 1491; (*e*) D. Pinho, P. Gomes, C. Freire and B. De Castro, *Eur. J. Inorg. Chem.*, 2001, 1483.
21. T. J. Collins, T. R. Nichols and E. S. Uffelman, *J. Am. Chem. Soc.*, 1991, **113**, 4708.
22. (*a*) H. J. Kruuger, G. Peng and R. H. Holm, *Inorg. Chem.*, 1991, **30**, 734; (*b*) J. Hanss and H. J. Kruger, *Angew. Chem. Int. Ed.*, 1998, **37**, 360; (*c*) C. L.Weeks, P. Turner, R. R. Fenton and P. A. Lay, *J. Chem. Soc., Dalton Trans.*, 2002, 931.
23. (*a*) H. J. Kruger and R.H. Holm, *J. Am. Chem. Soc.*, 1990, **112**, 2955; (*b*) N. Baidya, M. M. Olmstead and P. K. Mascharak, *J. Am. Chem. Soc.*, 1992, **114**, 9666; (*c*) C. A. Marganian, H. Vazir, N. Baidya, M. M. Olmstead and P. K. Mascharak, *J. Am. Chem. Soc.*, 1995, **117**, 1584; (*d*) A. K. Patra and R. Mukherjee, *Inorg. Chem.*, 1999, **38**, 1388; (*e*) B. De Bruin, E. Bill, E. Bothe, T. Weyhermuller and K. Wieghardt, *Inorg. Chem.*, 2000, **39**, 2936.
24. (*a*) S. Hikichi, M. Yoshizawa, Y. Sasakura, M. Akita and Y. Morooka, *J. Am. Chem. Soc.*, 1998, **120**, 10567; (*b*) S. Itoh, H. Bandoh, S. Nagatomo, T. Kitagawa and S. Fukuzumi, *J. Am. Chem. Soc.*, 1999, **121**, 8945; (*c*) K. Shiren, S. Ogo, S. Fujinami, H. Hayashi, M. Suzuki, A. Uehara, Y.Watanabe and Y. Moro-oka, *J. Am. Chem. Soc.*, 2000, **122**, 254; (*d*) B. Bag, N. Mondal, G. Rosair and S. Mitra, *Chem. Commun.*, 2000, 1729; (*e*) S. Hikichi, M. Yoshizawa, Y. Sasakura, H. Komatsuzaki, Y. Moro-oka and M. Akita, *Chem. Eur. J.*, 2001, **7**, 5012; (*f*) S. Itoh, H. Bandoh, M. Nakagawa, S. Nagatomo, T. Kitagawa, K. D. Karlin and S. Fukuzumi, *J. Am. Chem. Soc.*, 2001, **123**, 1168.

25. J. B. Summer, *J. Biol. Chem*., 1926, **69**, 435.
26. R. K. Andrews, R. L. Blakeley, B. L. Zerner, Urease-A nickel(II) metalloenzyme. In: J. R. Lancaster, Jr., Ed., *The Bioinorganic Chemistry of Nickel*; New York, VCH Publishers, 1988, vol 141, p 165.
27. M. W. Adams, L. E. Mortenson and J. S. Chen, *Biochim. Biophys. Acta.,* 1980**, 594,** 105.
28. P. M. Vignais, A. Colbeau, J. C. Willison and Y. Jouanneau, *Adu. Microb. Physiol.* 1985**, 26,** 155.
29. G. Fauque, H. D. Peck Jr., J. J. G. Moura, B. H. Huynh, Y. Berber, D. V. DerVartanian, M. Teixeira, A. E. Przybyla, P. A. Lespinat, I. Moura and J. LeGall, *FEMS Microbiol. Reu.,* 1988**, 54,** 299.
30. I. Okura, *Coord. Rev. Chem. Rev.,* 1985**, 68,** 53.
31. (*a*) E. N. Kondrat'eva, I. N. Gogotov and I. V. Gruzinskii, *Mikrobiologiia,* 1979**, 48,** 389 (*b*) I. N. Gogotov, *Biochimie,* 1978**, 60,** 267.
32. R. W. Spencer, L. Daniels, G. Fulton and W. H. Orme-Johnson, *Biochemistry,* 1980, **19,** 3678.
33. J. W. van der Zwan, J. M. C. C. Coremans, E. C. M. Bouwens and S. P. J. Albracht, *Biochim. Biophys. Acta*., 1990, **1041**, 101
34. R. Cammack, V. M. Fernandez and K. Schneider, In *The Bioinorganic Chemistry of Nickel;* Lancaster, J. R., Ed.; VCH Publishers, New York, 1988; Chapter 8.
35. M. J. Caroney, G. J. Colpas, C. Bagyinka, N. Baidya and P. K. Mascharak, *J. Am. Chem. Soc*., 1991, **113**, 3962
36. R. P. Gunsalus and R. S. Wolfe, *FEMS Microbiol. Lett*., 1978, **3**, 191.
37. A. Pfaltz, D. A. Livingston, B. Jaun, G. Diekert, R. K. Thauer, A. Eschenmoser, *Helv. Chim. Acta*., 1985, **68**, 1338
38. R. K. Thauer, *Microbiology,* 1998, **144**, 2377.
39. J. Telser, *Struct. Bonding,* 1998, **91**, 31.

40. R. A. Sheldon and J. K. Kochi, *Metal Catalyzed Oxidations of Organic Compounds;* Academic, New York, 1981**.**
41. E. G. Samsel, K. Srinivasan and J. K. Kochi, *J. Am. Chem. Soc.,* 1985**, 107,** 7606**.**
42. J. T. Groves and T. E. Nemo, *J. Am. Chem. Soc.,* 1983**, 105,** 5786.
43. J. D. Koola and J. K. Kochi, *Inorg. Chem*., 1987, **26**, 908.
44. (*a*) S. Trofimenko, *J. Am. Chem. Soc*., 1968, **90**, 4754; (*b*) S. Trofimenko, *Inorg. Chem*., 1970, **9**, 2493.
45. M. Brookhart and M. L. H. Green, *J. Organomet. Chem.*, 1983, **250**, 395.
46. (*a*) A. D. Ryabov, G. M. Kazankov, A. K. Yatsimirsky, L. G. Kuz'mina, O. Yu. Burtseva, N. V. Dvortsova and V. A. Polyakov, *Inorg. Chem.*, 1992, **31**, 3083; (*b*) A. D. Ryabov, *Chem. Rev.*, 1990, **90**, 403; (*c*) D. Drago, P. S. Pregosin, M. Tschoerner and A. Albinati, *J. Chem. Soc., Dalton Trans.*, 1999, 2279.
47. L. Brammer, J. M. Charnock, P. L. Goggin, R. J. Goodfellow, A. G. Orpen and T. F. Koetzle, *J. Chem. Soc., Dalton Trans.*, 1991, 1789.
48. A. J. Canty and G. van Koten, *Acc. Chem. Res.*, 1995, **28**, 406.
49. (*a*) O. Eisenstein and Y. Jean, *J. Am. Chem. Soc.*, 1985, **107**, 1177; (*b*) A. Demolliens, Y. Jean and O. Eisenstein, *Organometallics*, 1986, **5**, 1457.
50. G. C. Pimentel and A. L. McClellan, *The Hydrogen Bond*; W. H. Freeman, San Franscisco, 1960.
51. L. Brammer, Dalton Trans.,2003, 3145.
52. A. J. Canty and G. van Koten, *Acc. Chem. Res.*, 1995, **28**, 406.
53. W. Yao, O. Eisenstein and R. H. Crabtree, *Inorg. Chim. Acta*, 1997, **254**, 105.
54. M. J. Calhorda, *J. Chem. Soc. Chem. Commun*., 2001, 801.
55. K. Nag and A. Chakravorty, *Coord. Chem. Rev*., 1980, **33**, 87.
56. F. A. Cotton and G. Wilkinson, *Advanced Inorganic Chemistry; 4th ed*., New York, 1980.

57. D. Nicholls in J. C. Bailar, Jr., H. J. Emeléus, R. S. Nyholm and A. F. Trofman-Dickenson, Eds., *Comprehensive Inorganic Chemistry*; Pergamon, Oxford, 1973, **3**, 1115.
58. L. Malatesta and S. Cenni, *Zerovalent Compounds of Metals*; Academic Press London, 1974.
59. P. W. Jolly and G. Wilke, *The Organic Chemistry of nickel*; Academic Press, London, 1974,1.
60. G. R. Deshiraju and T Steiner, *The Weak Hydrogen Bond In Structural Chemistry and Biology*; Oxford University Press, New York, 1999
61. C. A. Hunter, *Chem. Soc. Rev*., 1994, **23**, 101.
62. A. Ben-Naim, *Hydrophobic Interactions*, Plenum Press, New York & London, 1980.
63. K. J. Masaib and C. I. F. Watt, *Chem Soc. Rev*. 1992, **21**, 437.
64. A. G. Street and S. L. Mayo, *Proc Natl. Acad. Sci. USA*, 1996, **96**, 9074.
65. M. C. T. Fyfe and J. F. Stoddart, *Coord. Chem. Rev*., 1999, **183**, 139.
66. D. B. Amabilino and J. F. Stoddart, Chem. Rev., 1999, **95**, 2725.
67. A. Sigel and H. Sigel, *Metal Ions in Biological System*; Dekker, New York, 1996.
68. K. Nag and A. Chakravorty, *Coord. Chem. Rev*., 1980, **33**, 87.
69. F. A. Cotton and G. Wilkinson, *Advanced Inorganic Chemistry; 4th ed*., New York, 1980.
70. D. Nicholls in J. C. Bailar, Jr., H. J. Emeléus, R. S. Nyholm and A. F. Trofman-Dickenson, Eds., *Comprehensive Inorganic Chemistry*, Pergamon, Oxford, 1973, **3**, 1115.

Chapter 2

Nickel(II) complexes with N,N,O-donor Schiff bases. Two-dimensional network via intermolecular hydrogen bonding[§]

2.1. Abstract

The syntheses, characterization and crystal structures of two mononuclear nickel(II) complexes are described. Reactions of $Ni(O_2CCH_3)_2{\cdot}4H_2O$ with the Schiff bases derived from 2-pyridinecarbaldehyde and *ortho*-aminophenol (Hpaap) and 2-pyridinecarbaldehyde and *ortho*-aminobenzoic acid (Hpaab) in methanolic media afford the complexes in good yields. The elemental analysis, magnetic moments, and spectral features of the complexes are consistent with the formulae $[Ni(paap)_2]{\cdot}CH_3COOH{\cdot}H_2O$ (**1**) and $[Ni(paab)_2]{\cdot}2H_2O$ (**2**). In each complex, two tridentate monoanionic meridionally spanning ligands form a distorted octahedral N_4O_2 coordination sphere around the metal ion. In $[Ni(paap)_2]{\cdot}CH_3COOH{\cdot}H_2O$, two metal coordinated phenolate-O atoms are hydrogen bonded to CH_3COOH and H_2O, respectively. Intermolecular C–H···O interactions involving the water molecule and the C–H groups from azomethine and aromatic fragments of the metal coordinated ligands lead to a 4.8^2 network of $[Ni(paap)_2]{\cdot}CH_3COOH{\cdot}H_2O$ in the crystal lattice. A uncoordinated carboxylate O-atom in $[Ni(paab)_2]{\cdot}2H_2O$ is hydrogen bonded to both water molecules. One of the water molecules is again hydrogen bonded to the corresponding symmetry related water molecule forming a dimer. The azomethine groups and the metal coordinated carboxylate-O atoms in $[Ni(paab)_2]$ are involved in intermolecular C–H···O interactions forming a chain-like arrangement of the molecules. The water dimers act as bridges between these chains and form a two-dimensional square-grid network of $[Ni(paab)_2]{\cdot}2H_2O$.

[§] A part of this work has been published in *J. Chem. Crystallogr.*, 2005, **35**, 737.

2.2. Introduction

In recent times, the scope of the metal mediated azomethine to carboxamide transformation, in several complexes with Schiff bases, is under scrutiny especially as a synthetic tool.[1] The complexes that display such metal coordinated azomethine to carboxamide oxidation are very rare.[2] They are of particular interest as the selective oxidation of ligand framework provides a valuable route to complexes and ligands otherwise difficult to synthesize. It appears that to realize such oxidation, the metal center must have two easily accessible oxidation states.[1,2]

The summation of numerous weak and subtle non-covalent interactions often has a decisive role in crystal packing. Self-assembly of transition metal ion complexes into a desired structural network has been realized by utilizing the metal ion's preference for a particular coordination geometry, design and use of suitable ligands and weak non-covalent intermolecular interactions.[3-5] The proton of polarized azomethine (-CH=N-) group in metal coordinated Schiff bases may help in self-assembly of the complex molecules by participating in intermolecular hydrogen bonding interactions.[6] The acceptor atom in this type of hydrogen bonding can be a part of the complex molecule or of the solvent molecule trapped in the crystal lattice. Thus the resulting network pattern can be influenced by the orientation of the acceptor atom with respect to the azomethine moiety.

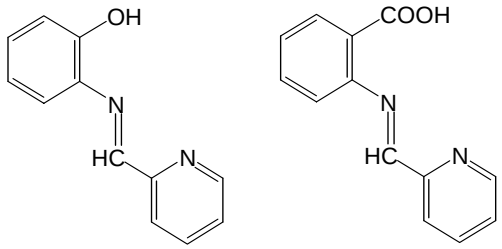

Hpaap **Hpaab**

Scheme 1

Herein, we report the syntheses, characterization and crystal structures of two hexacoordinated nickel(II) complexes with the Schiff bases obtained by condensation reactions of 2-pyridine-carbaldehyde with *ortho*-aminophenol (Hpaap) and with *ortho*-aminobenzoic acid (Hpaab) (Scheme 1). In the deprotonated state, these Schiff bases can coordinate a metal ion *via* the pyridine-N, the imine-N and the phenolate-O ($paap^-$) or the carboxylate-O ($paab^-$). The $paap^-$ will form two five-membered chelate rings, whereas the $paab^-$ will form one six- and one five-membered chelate ring. The reasons for the choice of these Schiff bases are as follows. They contain higher oxidation state promoting phenolic –OH moiety and carboxyl groups.[7] Thus if +3 oxidation state of the metal center can be accessed, metal mediated transformation of the azomethine group can be explored. In addition, we also wanted to investigate the intermolecular non-covalent interactions and the crystal packing patterns guided by these interactions.

The complexes that have been isolated are $[Ni(paap)_2]\cdot CH_3COOH\cdot H_2O$ (**1**) and $[Ni(paab)_2]\cdot 2H_2O$ (**2**). Although we are unsuccessful to find any metal ion mediated ligand oxidation process, but both species form interesting two-dimensional networks in the crystal lattice via intermolecular hydrogen bonding interactions involving the polarized azomethine moieties and the water molecules.

2.3. Experimental

2.3.1. Materials

The chemicals and solvents used in this work were of analytical grade available commercially and were used without further purification.

2.3.2. Physical measurements

Micro-analytical (C, H, N) data were obtained with a Perkin-Elmer Model 240C elemental analyzer. Room temperature solid state magnetic susceptibilities were measured by using a Sherwood Scientific magnetic

susceptibility balance. Diamagnetic corrections calculated from Pascal's constants[8] were used to obtain the molar paramagnetic susceptibilities. Solution electrical conductivities were measured with a Digisun DI-909 conductivity meter. Infrared spectra were collected by using KBr pellets on a Jasco-5300 FT-IR spectrophotometer. Electronic spectra were recorded on a Shimadzu 3101-PC UV/vis/NIR spectrophotometer. A CH−instrument model 620A electrochemical analyzer was used for cyclic voltammetric experiments.

2.3.3. Syntheses of the complexes

$[Ni(paap)_2]\cdot CH_3COOH\cdot H_2O$ (1)

To a methanol solution (20 mL) of 2-aminophenol (230 mg, 2.1 mmol), 0.2 mL (225 mg, 2.1 mmol) of 2-pyridinecarbaldehyde was added and the mixture was refluxed for ½ h. Powdered $Ni(O_2CCH_3)_2\cdot 4H_2O$ (260 mg, 1.05 mmol) was added to the clear light yellow solution. The resulting red mixture was refluxed for another ½ h and then cooled to room temperature. The red-brown crystalline solid separated was collected by filtration, washed with ice-cold methanol and finally dried in air. Yield obtained was 470 mg (84%). A single crystal suitable for X-ray structure determination was selected from this material. Anal. calcd. for $C_{26}H_{24}N_4O_5Ni$: C, 58.77; H, 4.55; N, 10.54%. Found: C, 58.43; H, 4.39; N, 10.29%. Selected infrared bands (cm^{-1}): 3046 br, 1703 s, 1586 s, 1559 m, 1537 m, 1479 s, 1456 s, 1362 m, 1317 m, 1300 w, 1281 s, 1250 m, 1184 m, 1144 s, 1044 m, 864 m, 806 m, 756 s, 637 w, 586 w, 515 s, 447 w, 417 w. Electronic spectral data in CH_3OH solution (λ_{max}, nm (ε, M^{-1} cm^{-1})): 855 (23), 480 (18,800), 323 (21,000), 241 (21,100). Solid state magnetic moment at 300 K (μ_{eff}, μ_B): 3.17.

$[Ni(paab)_2]\cdot 2H_2O$ (2)

$[Ni(paab)_2]\cdot 2H_2O$ (**2**) was prepared in methanolic medium from 2-aminobenzoic acid, 2-pyridinecarbaldehyde and $Ni(O_2CCH_3)_2\cdot 4H_2O$ (2:2:1 mole ratio) as brown microcrystalline solid in 75% yield by following the

same procedure as described above. Single crystal suitable for X-ray structure determination was obtained directly from the synthetic reaction mixture. Anal. calcd. for $C_{26}H_{22}N_4O_6Ni$: C, 57.26; H, 4.07; N, 10.27%. Found: C, 57.05; H, 3.96; N, 10.14%. Selected infrared bands (cm^{-1}): 3397 br, 1589 s, 1560 s, 1483 m, 1441 m, 1358 s, 1236 w, 1153 w, 1101 w, 1049 m, 1017 m, 918 s, 864 s, 824 s, 777 s, 745 m, 692 s, 640 m, 579 w, 546 w, 488 w, 417 m. Electronic spectral data in CH_3OH solution (λ_{max}, nm (ε, M^{-1} cm^{-1})): 900 (15), 350sh (15,300), 328 (19, 800), 243sh (16,700). Solid state magnetic moment at 300 K (μ_{eff}, μ_B): 3.19.

2.3.4. X-ray crystallography

The data were collected on an Enraf-Nonius Mach-3 single crystal diffractometer using graphite monochromated Mo Kα radiation (λ = 0.71073 Å) by ω-scan method. Unit cell parameters of **1** and **2** were determined by the least-squares fit of 25 reflections having 2θ values in the range 19-21^o and 18-22^o, respectively. Stability of the crystal was monitored by measuring the intensities of three check reflections after every 1.5 h during the data collection. No decay was observed in either case. In each case, the position of the unique nickel atom was determined from a Patterson map. The remaining non-hydrogen atoms were determined from successive Fourier difference syntheses. The model was then refined by full-matrix least-squares procedures on F^2. For both structures all the non-hydrogen atoms were refined anisotropically. The hydrogen atoms of the water molecule and the –COOH group in **1** were located in a difference map. For **2** hydrogen atoms of only one water molecule could be located in a difference map. Calculations were done using the programs of WinGX[9] for data reduction, and SHELX-97 programs[10] for structure solution and refinement. The Ortex6a[11] and Platon[12] packages were used for molecular graphics. Significant crystal data are summarized in Table 2.1.

Table 2.1. Crystallographic Data

Compound	**1**	**2**
Empirical formula	$NiC_{26}H_{24}N_4O_5$	$NiC_{26}H_{22}N_4O_6$
Crystal system	Monoclinic	Triclinic
Space group	$P2_1/c$	$P\bar{1}$
a (Å)	9.675(2)	9.834(3)
b (Å)	17.109(5)	11.319(3)
c (Å)	14.403(4)	13.130(4)
α (°)	90	84.68(3)
β (°)	92.903(11)	67.54(3)
γ (°)	90	85.49(2)
V (Å^3)	2381.1(11)	1343.4(6)
Z	4	2
$\rho_{calcd.}$ (g cm^{-3})	1.482	1.348
μ (mm^{-1})	0.861	0.768
Reflections collected	4287	4487
Unique reflections	4033	4487
$R_{(int)}$	0.214	0.00
Reflections ($I > 2\sigma(I)$)	2594	2797
Parameters	326	334
$R1$[a], $wR2$[b] ($I > 2\sigma(I)$)	0.0747, 0.1899	0.0790, 0.1908
$R1$[a], $wR2$[b] (all data)	0.1206, 0.2249	0.1292, 0.2275
Goodness-of-fit[c] on F^2	1.060	1.009
Largest peak, hole (e Å^{-3})	0.747, –0.748	0.694, –0.392

[a] $R1 = \sum||F_o| - |F_c||/\sum|F_o|$. [b] $wR2 = \{\sum[(F_o^2 - F_c^2)^2]/\sum[w(F_o^2)^2]\}^{1/2}$.
[c] GOF = $\{\sum[w(F_o^2 - F_c^2)^2]/(n - p)\}^{1/2}$ where 'n' is the number of reflections and 'p' is the number of parameters refined.

2.4. Results and discussion

2.4.1. Synthesis and some properties

Two new hexacoordinated nickel(II) complexes have been synthesized in good yields by reacting one mole equivalent of $Ni(O_2CCH_3)_2 \cdot 4H_2O$ with the Schiff bases Hpaap and Hpaab preformed in methanolic media by refluxing two mole equivalents each of 2-pyridinecarbaldehyde and the corresponding *ortho* substituted anilines. The elemental analysis data for the isolated crystalline solids are consistent with the formulae $[Ni(paap)_2] \cdot CH_3COOH \cdot H_2O$ and $[Ni(paab)_2] \cdot 2H_2O$. The solid state room temperature (300 K) magnetic moments of **1** and **2** are 3.17 and 3.19 μ_B, respectively. These values are consistent with an S = 1 spin state of the metal ion in each complex. Both species are electrically non-conducting in methanol solutions. Thus the ligands are monoanionic and the oxidation state of the metal ion is +2 in each complex. Cyclic voltammetric studies revealed that both complexes are redox active.

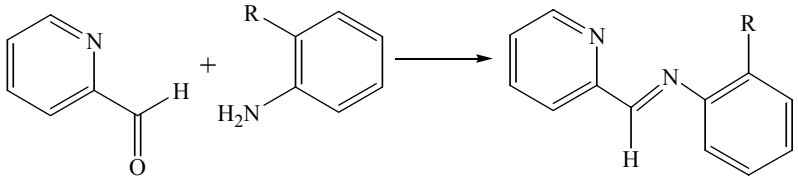

when R = –OH, Hpaap.
when R = –COOH, Hpaab.

2.4.2. Infrared spectral characteristics

The infrared spectrum of **1** displays a broad band centered at 3046 cm^{-1} and a strong band at 1703 cm^{-1}. These two bands are ascribable to the carboxyl group[13] of the acetic acid molecule that is hydrogen bonded to the metal coordinated phenolate-O of one of the two ligands (*vide infra*). The strong and sharp band observed at 1586 cm^{-1} is most likely due to the azomethine C=N stretching.[14] The medium to strong bands in the range

1559–1456 cm^{-1} are possibly due to the vibrations associated with the aromatic C=C fragments of the ligands.[15] The broad band observed at 3397 cm^{-1} in the infrared spectrum of **2** is most likely due to the lattice water molecules.[13] The origin of the strong band with a shoulder at 1589 cm^{-1} and another strong band at 1358 cm^{-1} might involve the metal coordinated carboxylate functionalities present in the ligands. The former is assigned to the ν_{as} stretch and the latter is assigned to the ν_s stretch.[16] The shoulder at the higher energy band is possibly due to the -HC=N- group of the ligand. Like **1**, **2** also displays medium to strong bands in the range 1560–1441 cm^{-1} attributable to the aromatic parts of the ligands.

2.4.3. Electronic spectral characteristics

In methanol solutions, **1** and **2** display a weak absorption at 855 and 900 nm, respectively (Figure 2.1). This absorption is assigned to the ν_1 transition for an octahedral nickel(II) complex.[17] The difference in this band position suggests that $paap^-$ is a stronger ligand than $paab^-$. The other two coordinating atoms being same in both ligands the better σ-bonding ability of the phenolate-O compared to that of the carboxylate-O is likely to be one of the major reasons for this observation. In addition to this weak absorption, **2** displays three intense absorptions in the range 480–240 nm, whereas **1** displays a strong peak at 343 nm and two shoulders at 328 and 243 nm, respectively (Figure 2.1). These higher energy absorptions are most likely due to ligand-to-metal charge transfer and intra-ligand transitions.

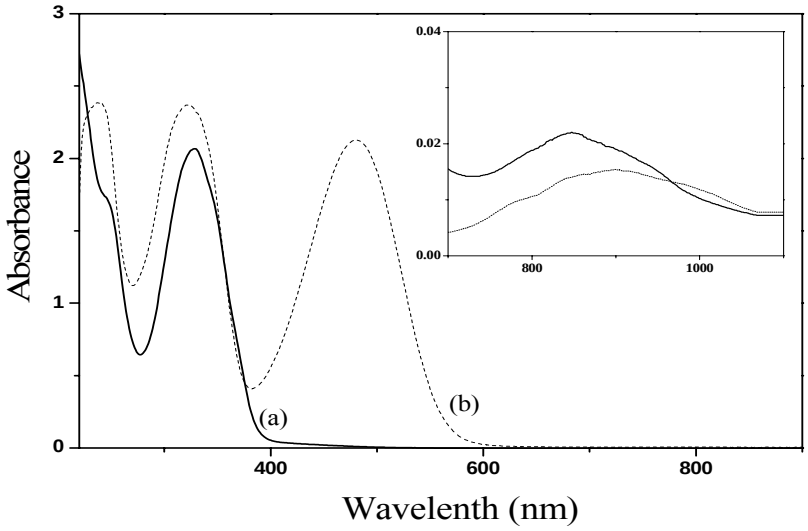

Fig.2.1. Electronic spectra of **1** (a) and **2** (b) in methanol. Inset: ν_1 transition band for both the complexes.

2.4.4. Description of molecular structures

The structures of **1** and **2** are depicted in Figure 2.2 and 2.3, respectively. In each complex, these tridentate ligands bind the metal ion meridionally and form a N_4O_2 coordination sphere. The bond parameters associated with the metal ion (Tables 2.2) suggest a distorted octahedral coordination geometry around the metal ion. The average chelate bite angle (78.23°) in the five-membered ring formed by the pyridine-N and the imine-N in $[Ni(paap)_2]$ is slightly smaller than that (80.57°) in $[Ni(paab)_2]$. The same for the other five-membered ring constituted by the imine-N and the phenolate-O in $[Ni(paap)_2]$ is 81.32°. On the other hand, for **2** average chelate bite angle (89.36°) in the six-membered ring formed by the imine-N and the

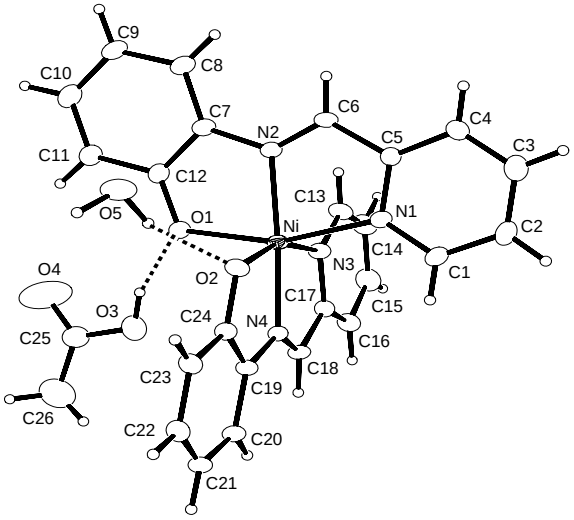

Fig. 2.2. Structure of **1** with the atom labeling scheme. All non-hydrogen atoms are represented by their 15% probability thermal ellipsoids. Hydrogen bonding interactions are shown by dashed lines.

carboxylate-O is very close to the ideal value of 90°. As a consequence, the average *trans* N–Ni–O angle (169.62°) in [Ni(paab)$_2$] is significantly larger than that (159.41°) in [Ni(paap)$_2$]. However, the *trans* N(imine)–Ni–N(imine) angles are very similar in both complexes. The values are 176.13(19) and 176.6(2)° for [Ni(paap)$_2$] and [Ni(paab)$_2$], respectively. The Ni-N(pyridine), Ni-N(imine), Ni-O(phenolate), and Ni-O(carboxylate) bond distances observed in these complexes are within the range reported for nickel(II) complexes having the same coordinating atoms.[17a,18] In **1**, the acetic acid molecule is hydrogen bonded to one of the phenolate-O atoms (Figure 2.2). The O1···O3 distance and the O1···H–O3 angle are 2.605(8) Å and 148.5°, respectively. The water molecule is hydrogen bonded with the other phenolate-O atom. The O2···O5 distance and the O2···H–O5 angle are 2.721(8) Å and 112.2°, respectively. On the other hand, both water molecules

are hydrogen bonded to the same uncoordinated carboxylate-O in **2** (Figure 2.3). The O2···O5 and O2···O6 distances are 2.728(13) and 3.25(2) Å, respectively. The O2···H–O5 angle is 143.2°. There is no interaction between the two water molecules.

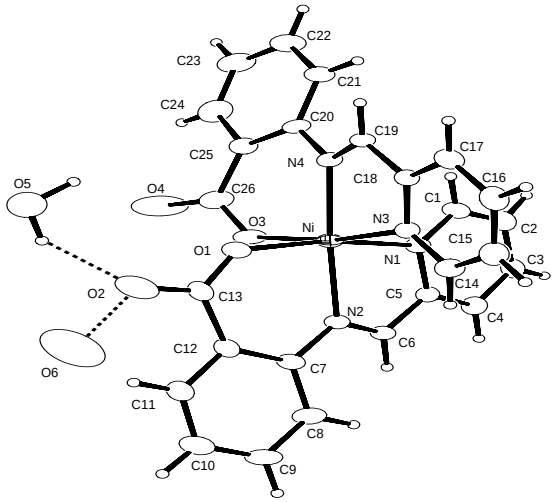

Fig. 2.3. Structure of **2** with the atom labeling scheme. All non-hydrogen atoms are represented by their 15% probability thermal ellipsoids. Hydrogen bonding interactions are shown by dashed lines.

Table 2.2. Selected bond lengths (Å) and angles (°) of 1·$CH_3COOH·H_2O$ and 2·$2H_2O$.

1·$CH_3COOH·H_2O$			
Ni-N(1)	2.114(5)	Ni-N(4)	2.005(5)
Ni-N(2)	2.007(5)	Ni-O(1)	2.053(4)
Ni-N(3)	2.122(5)	Ni-O(2)	2.086(4)
N(1)-Ni-N(2)	78.17(19)	N(2)-Ni-O(2)	98.65(19)
N(1)-Ni-N(3)	90.0(2)	N(3)-Ni-N(4)	78.3(2)
N(1)-Ni-N(4)	105.68(19)	N(3)-Ni-O(1)	91.51(19)
N(1)-Ni-O(1)	159.01(18)	N(3)-Ni-O(2)	159.82(18)
N(1)-Ni-O(2)	92.99(18)	N(4)-Ni-O(1)	95.12(18)
N(2)-Ni-N(3)	101.5(2)	N(4)-Ni-O(2)	81.64(19)
N(2)-Ni-N(4)	176.13(19)	O(1)-Ni-O(2)	92.77(18)
N(2)-Ni-O(1)	81.01(18)		
2·$2H_2O$			
Ni-N(1)	2.085(5)	Ni-N(4)	2.045(5)
Ni-N(2)	2.064(4)	Ni-O(1)	2.011(5)
Ni-N(3)	2.079(5)	Ni-O(3)	2.011(5)
N(1)-Ni-N(2)	81.26(19)	N(2)-Ni-O(3)	92.20(18)
N(1)-Ni-N(3)	96.09(18)	N(3)-Ni-N(4)	79.89(19)
N(1)-Ni-N(4)	96.00(19)	N(3)-Ni-O(1)	87.6(2)
N(1)-Ni-O(1)	169.87(18)	N(3)-Ni-O(3)	168.38(18)
N(1)-Ni-O(3)	90.4(2)	N(4)-Ni-O(1)	93.94(18)
N(2)-Ni-N(3)	98.31(19)	N(4)-Ni-O(3)	89.86(19)
N(2)-Ni-N(4)	176.6(2)	O(1)-Ni-O(3)	87.7(2)
N(2)-Ni-O(1)	88.87(19)		

2.4.5. Hydrogen bonding and self-assembly

The self-assembly of **1** and **2** *via* intermolecular hydrogen bonding interactions leads to the two-dimensional network in each case (Figures 2.4 and 2.5). For **1**, acetic acid has no role in the formation of the network. As mentioned before it is only connected to one of the phenolate-O in $[Ni(paap)_2]$ through a hydrogen bond. In the crystal lattice, the water molecules are the basic units for linking the $[Ni(paap)_2]\cdot CH_3COOH$ units into a two-dimensional sheet arrangement with a 4.8^2 topology (Figure 2.4). Each water molecule acts as a three connector node between three $[Ni(paap)_2]\cdot CH_3COOH$ units by participating in three hydrogen bonding interactions. These are one O–H···O and two C–H···O interactions. In the O–H···O interaction, the O-atom of the water molecule acts as the donor atom and one of the phenolate-O atoms of the first $[Ni(paap)_2]$ moiety acts as the acceptor atom (*vide supra*). In the C–H···O interactions, the water O-atom acts as the acceptor atom. The aromatic C-atom (C20) *meta* to the phenolate-O of the second $[Ni(paap)_2]$ unit and the C-atom (C6) of the azomethine fragment of the third $[Ni(paap)_2]$ unit act as the donor atoms in the two C–H···O interactions. The C20···O5 and C6···O5 distances are 3.364(10) and 3.424(8) Å, respectively. The corresponding C–H···O angles are 161.1 and 163.8°, respectively.

In the self-assembly of **2**, the azomethine groups of the ligands play the crucial role. Two azomethine fragments and the two metal coordinated carboxylate-O atoms in each $[Ni(paab)_2]$ unit are involved in two pairs of reciprocal C–H···O interactions with its two neighbors on both sides (Figure 2.5). The C6···O3 and C19···O1 distances are 3.172(7) and 3.256(7) Å, respectively. The corresponding C–H···O angles are 142.9 and 150.3°, respectively. Due to these interactions **2** exists in a one-dimensional infinite

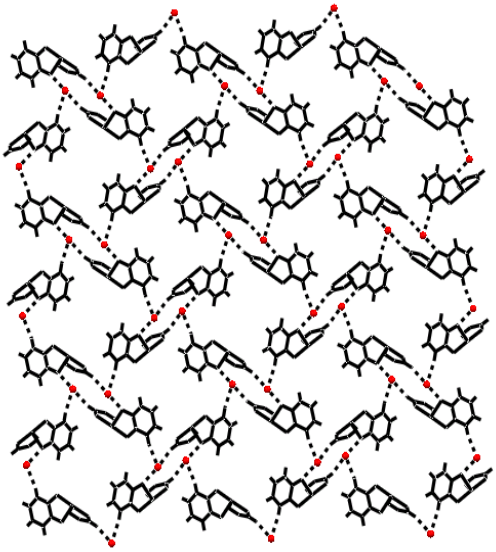

(a)

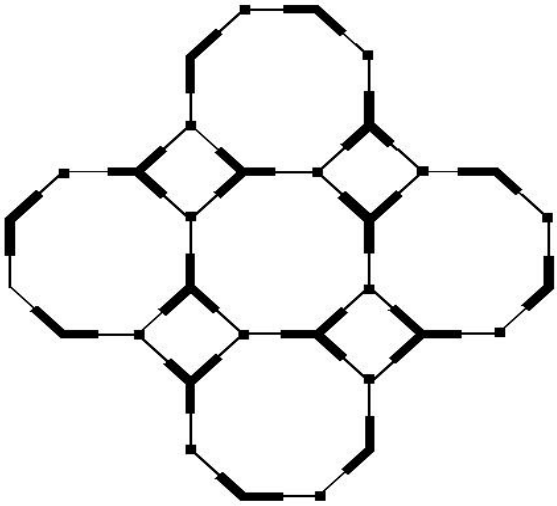

(b)

Fig. 2.4. (a) Two-dimensional 4.8^2 network of **1**. The acetic acid molecules are not shown for clarity. (b) Schematic representation of this 4.8^2 net.

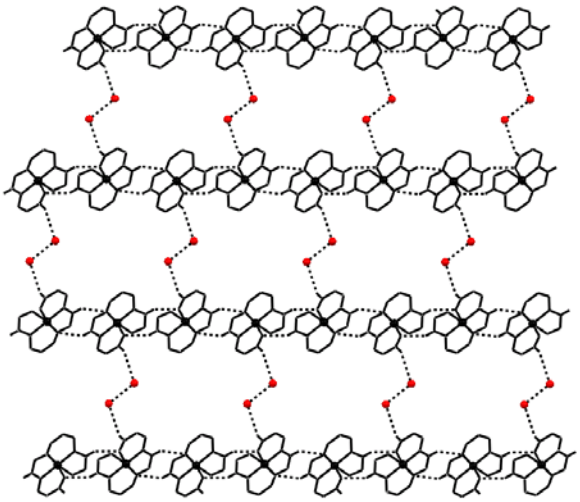

(a)

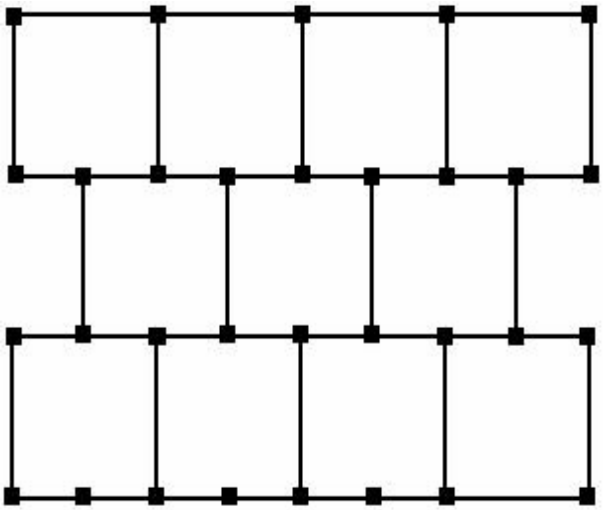

(b)

Fig. 2.5. (a) Two-dimensional brick−wall network of **2**. The water molecule not involved in the formation of the network is not shown for clarity. (b) Schematic representation of the square brick network.

chain-like arrangement. Both water molecules are hydrogen bonded to one of the uncoordinated carboxylate-O atom (*vide supra*). The O-atom (O6) of one of these two water molecules is at a distance of 3.10(3) Å from the O-atom of the corresponding symmetry related water molecule. This distance suggests that they exist as hydrogen bonded water dimer. These water dimers provide the bridges between the chains of $[Ni(paab)_2]\cdot H_2O$ moieties and complete the two dimensional brick-wall network of **2** (Figure 2.5).

2.5. Conclusion

Two new bis complexes of nickel(II) with the N, N, O- donor Schiff bases Hpaap and Hpaab have been synthesized. The complexes have been isolated as $[Ni(paap)_2]\cdot CH_3COOH\cdot H_2O$ (**1**) and $[Ni(paab)_2]\cdot 2H_2O$ (**2**). Analytical, magnetic, spectroscopic and electrochemical measurements are used for the characterization of **1** and **2**. Our original goal was to examine whether these ligands can provide access to the +3 oxidation state of the nickel center or not and if higher-valent species is obtained whether that can lead to metal ion mediated ligand transformation or not. Both complexes turned out to be redox inactive. However, X-ray structures of **1** and **2** reveal O-H···O and C-H···O interactions assisted two-dimensional networks in the crystal lattice. In the case of **1**, the water molecules act as three connector nodes and help to form a two-dimensional 4.8^2 network. On the other hand, in the case of **2**, the metal coordinated azomethine moiety plays the crucial role in forming infinite chains of hydrated complex molecules. These parallel chains are inter-connected by water dimmers and a two-dimensional brick-wall network is formed.

2.6. References

1 (*a*) B. K. Dirghangi, M. Menon, S. Banerjee and A. Chakravorty, *Inorg.Chem*., 1997, **36**, 3595; (*b*) H. L. Chum and P. Krumholz, *Inorg.Chem.,* 1974, **13**, 519.

2 (*a*) B. K. Dirghangi, M. Menon, A. Pramanik and A.; Chakravorty, *Inog. Chem.,* 1997, **36**, 1095; (*b*) M. Menon, S. Choudhury, A. Pramanik, A. K. Deb, S. W. Chandra, N. Bag, S. Goswami and A. Chakravorty, *J. Chem. Soc., Chem.Commun.,* 1994, 57; (*c*) E. Gallo, E. Solari, N. Re, C. Floriani, A Chiesi-Villa and C. Rizzolie, *Agnew Chem. Int. Ed. Engl.,* 1996, **35**, 1981; (*d*) M. Menon, A. Pramanik and A. Chakravorty, *Inorg. Chem.,* 1995, **34**, 3310; (*e*) M. Menon, A. Pramanik, M. Bag, and A. Chakravorty, *Inorg. Chem.,* 1994, **33,** 403.

3. (*a*) Proceedings of the Inorganic Crystal Engineering (Dalton Discussion No. 3) *J. Chem. Soc., Dalton Trans.,* 2000, 3705; (*b*) J. –M. Lehn, *Supramolecular Chemistry*; VCH, Weinheim, 1995; (*c*) T. J. Marks, *Angew. Chem. Int. Ed. Engl.,* 1990, **29**, 857; (*d*) T. Mallah, S. Thiébault, M. Verdaguer and P. Veillet, *Science,* 1993, **262**, 1554; (*e*) B. Schoentjes and J. –M. Lehn, *Helv. Chim. Acta,* 1995, **78**, 1; (*f*) *Magnetism: A Supramolecular Function*; Kahn O., Ed.; Kluwer, Dordrecht, NATO ASI Series, 1996, vol. C-484; (*g*) M. Clemente-León, E. Coronado, P. Delhaes, J. R. Galán Mascarós, C. J Gómez-García and C. Mingotaud, in *Supramolecular Engineering of Synthetic Metallic Materials. Conductors and Magnets*; J. Veciana, C. Rovira and D. B. Amabilino, Eds.; Kluwer, Dordrecht, NATO ASI Series, 1998, vol. **C-518**, pp. 291-312; (*h*) O. Kahn and C. J. Martinez, *Science,* 1998, **279**, 44; (*i*) O. R. Evans and W. Lin, *Acc. Chem. Res.,* 2002, **35**, 511.

4 (*a*) L. Carlucci, G, Cianni,D. M. Proserpio and S. Rizzato, *Chem. Commun.,* 2000, 1319; (*b*) M. Moon, I. Kim and M. S. Lah, *Inorg. Chem.,* 2000, **39**, 2710; (*c*) D. Ghoshal, T. K. Maji, G. Mostafa, T. –H. Lu and N. Ray Chaudhuri, *Cryst. Growth Des.,* 2003, **3**, 9.

5. (*a*) P. N. W. Baxter, J. –M. Lehn, B. O. Kneisel and D. Fenske, *Angew. Chem. Int. Ed. Engl.,* 1997, **36**, 1978; (*b*) D. Braga, F. Grepioni and G. R. Desiraju, *Chem. Rev.,* 1998, **98**, 1375; (*c*) R. J. Puddephatt, *Chem. Commun.,* 1998, 1055; (*d*) O. M. Yaghi, H. Li, H. C. Davis, D. Richardson and T. L. Groy, Acc. Chem. Res., 1998, **31**, 474; (*e*) C. J. Janiak, *Chem. Soc., Dalton Trans.*, 2000, 3885.

6. (*a*) N. R. Sangeetha and S. Pal, *Polyhedron,* 2000, **19**, 1593; (*b*) S. N. Pal, K. R. Radhika and S. Pal, *Z. Anorg. Allg. Chem.,* 2001, **627**, 1631; (*c*) K. Heinze, *J. Chem. Soc.*, *Dalton Trans.,* 2002, 540; (*d*) K. Heinze and V. Jacob, *J. Chem. Soc.*, *Dalton Trans.,* 2002, 2379.
7. (*a*) D. W. Margerrum, *Pure Appl. Chem.*, 1983, **55**, 23; (*b*) D. P. Kessissoglou, X. Li, W. M. Butler and V. L. Pecoraro, *Inorg. Chem*., 1987, **26**, 2487, (*c*) S. Dutta, P. Basu and A. Chakravorty, *Inorg. Chem*., 1991, **30**, 4031.
8. W. E. Hatfield, in *Theory and Applications of Molecular Paramagnetism*; E. A. Boudreaux; L. N. Mulay, Eds.;Wiley, New York, 1976, p. 491.
8. L. J. Farrugia, *J. Appl. Crystallogr.,* 1999, **32**, 837.
10. G. M. Sheldrick, *SHELX-97*, *Structure Determination Software*; University of Göttingen: Göttingen, Germany, 1997.
11. P. McArdle, *J. Appl. Crystallogr.,* 1995, **28**, 65.
12. A. L. Spek, *PLATON-A Multipurpose Crystallographic Tool*; Utrecht University, Utrecht, The Netherlands, 2002.
13. W. Kemp, *Organic Spectroscopy*; ELBS/Macmillan: Hong Kong, 1987; p 60.
14. (*a*) S. G. Sreerama, S. N. Pal and S. Pal, *Inorg. Chem. Commun.,* 2001, **4**, 656; (*b*) S. N. Pal and S. Pal, *Polyhedron,* 2003, **22**, 867.
15. K. Nakamoto, *Infrared and Raman Spectra of Inorganic and Coordination Compounds*; Wiley: New York, 1986, p. 228.
16. N. R. Sangeetha and S. Pal, *Polyhedron,* 2000, **19**, 1593.
17. (*a*) G. V. Karunakar, N. R. Sangeetha, V. Susila and S. Pal, *J. Coord. Chem,.* 2000, **50**, 51; (*b*) S. Mukhopadhyay and D. Ray, *J. Chem. Soc.*, *Dalton Trans.,* 1995, 265.
18. (*a*) S. Seth, S. Chakraborty, *Acta Cryst. Sect. C,* 1984, **40,** 1530; (*b*) M. H. Moore, L. R. Nassimbeni and M. L. Niven, *J. Chem. Soc.*, *Dalton Trans.,* 1987, 2125; (*c*) M. J. van der Merwe, J. C. A. Boeyens and R. D. Hancock, *Inorg. Chem.,* 1983, **22**, 3489; (*d*) E. Coronado, M. Drillon, A. Fuertes, D. Beltran, A. Mosset and J. Galy, *J. Am. Chem. Soc.,* 1986, **108**, 900; (*e*) T. Aono, H. Wada, Y. Aratake, N. Matsumoto, H. Ökawa and Y. Matsuda, *J. Chem. Soc.*, *Dalton Trans.,* 1996, 25.

Chapter 3

Square-planar nickel(II) complexes with a tridentate O,N,O-donor Schiff base and monodentate N-heterocycles[§]

3.1. Abstract

A couple of nickel(II) complexes having the general formula [Ni(bhac)hc] with tridentate acetylacetone benzoylhydrazone (H_2bhac) and monodentate heterocycles (hc = 3,5-dimethylpyrazole (Hdmpz) and imidazole (Himdz)) are reported. The complexes were synthesized in ethanol media by reacting $Ni(O_2CCH_3)_2 \cdot 4H_2O$, H_2bhac and hc in 1:1:1 mole ratio and characterized by analytical, magnetic and spectroscopic methods. X-ray crystal structures of both complexes have been determined. In each complex, the metal ion is in square-planar N_2O_2 coordination geometry. In the solid state, a one-dimensional assembly of the [Ni(bhac)(Himdz)] molecules is formed *via* intermolecular hydrogen bonds between the imidazole N−H groups and the uncoordinated N-atoms of the deprotonated amide functionalities. On the other hand, two [Ni(bhac)(Hdmpz)] molecules are involved in a pair of complementary hydrogen bonds between the pyrazole N−H groups and the coordinated O-atoms of the deprotonated amide functionalities forming a dinuclear species.

[§] A part of this work has been published in *Inorg. Chem. Commun.*, 2003, **6**, 381.

3.2. Introduction

In recent years, extended assemblies of complexed metal ions are receiving immense attention primarily due to their photophysical, magnetic and conducting properties.[1-4] The general strategies used for the self-assembly of transition metal ion complexes into such extended assemblies are the metal ion's preference for different coordination geometry, use of suitable ligands and weak intermolecular interactions such as hydrogen bonding and π-π interaction.[1,5-7] In this chapter, we report the self-assembly of two square-planar mixed-ligand nickel(II) complexes. The common ligand in both complexes is the deprotonated acetylacetone benzoylhydrazone (H_2bhac, two H represent the dissociable enolic-OH and the amide proton) that can coordinate the metal ion through the enolate-O, the imine-N and the deprotonated amide-O atoms. Neutral N-donor imidazole (Himdz) or 3,5-dimethylpyrazole (Hdmpz) has been used as the ancillary ligand to satisfy the fourth coordination number around the metal ion. The reasons behind the choice of these ligands are as follows. The tridentate planar $bhac^{2-}$ will enforce the square-planar coordination geometry and it will also satisfy the +2 charge of the metal ion so that a neutral monodentate ligand can occupy the fourth site. The heterocycles (Himdz and Hdmpz) used as the monodentate ligands can be either coplanar with the {Ni(bhac)} moiety or can have a different orientation. In the first case, there is a distinct possibility for a π-stacked one-dimensional assembly of the molecules. In the second case, the acidic N−H protons of Hdmpz and Himdz can participate in intermolecular hydrogen bonding with the O- or N-atoms of the tridentate ligand to form extended assemblies. Herein, we describe the synthesis, characterization and solid state structures of [Ni(bhac)(Himdz)] (**3**) and [Ni(bhac)(Hdmpz)] (**4**). The self-assembly of the complex molecules via intermolecular N−H···O and N−H···N interactions has been demonstrated.

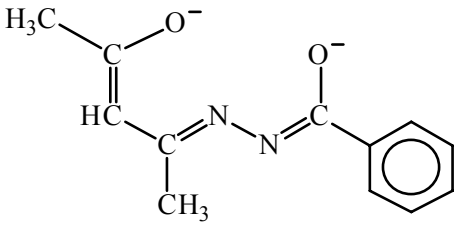

bhac^{2-}

3.3. Experimental

3.3.1. Materials

The Schiff base H_2bhac was prepared as reported before.[8] All other chemicals and solvents were of analytical grade available commercially and were used as received.

3.3.2. Physical measurements

Elemental (C, H, N) analysis data were obtained with a Perkin-Elmer Model 240C elemental analyzer. Infrared spectra were collected by using KBr pellets on a Jasco-5300 FT-IR spectrophotometer. Room temperature solid state magnetic susceptibilities were measured by using a Sherwood Scientific magnetic susceptibility balance. Solution electrical conductivities were measured with a Digisun DI-909 conductivity meter. A Shimadzu 3101-PC UV/vis/NIR spectrophotometer was used to record the electronic spectra. Proton NMR spectra of the complexes in $CDCl_3$ solutions were recorded on a Bruker 200 MHz spectrometer using $Si(CH_3)_4$ as an internal standard.

3.3.3. Synthesis of nickel(II) square planar complexes

[Ni(bhac)(Himdz)] (3)

This complex was synthesized in 55% yield by using the same procedure as described above by reacting $Ni(O_2CCH_3)_2{\cdot}4H_2O$, H_2bhac and Himdz in ethanol. Single crystal for X-ray structure determination was

selected from the crystalline product obtained directly from the reaction mixture. *Anal.* Calc. for $C_{15}H_{16}N_4O_2Ni$: C, 52.52; H, 4.70; N, 16.33. Found: C, 52.35; H, 4.53; N, 16.17. Electronic spectral data in CH_3CN solution (λ_{max}, nm (ε, M^{-1} cm^{-1})): 530sh (125), 482 (450), 382 (15100), 298 (4900), 235sh (19000). ^1H NMR (200 MHz) data in $CDCl_3$: δ 1.91 (s, 3H, -(H_3C)C=N-); 2.34 (s, 3H, H_3C-C(-O^-)=); 5.09 (s, 1H, =CH- of $bhac^{2-}$); 7.29 (m, 3H, phenyl ring protons); 7.89 (t, 2H, phenyl ring protons); 6.93, 7.11, 7.72 (s, s, s, imidazole C−H protons), 9.71 (s, imidazole N−H proton).

[Ni(bhac)(Hdmpz)] (4)

An ethanol solution (10 ml) of $Ni(O_2CCH_3)_2{\cdot}4H_2O$ (125 mg, 0.5 mmol) was added to another ethanol solution (15 ml) of H_2bhac (110 mg, 0.5 mmol) and Hdmpz (48 mg, 0.5 mmol). The resulting brown solution was refluxed for 3 h. Slow evaporation of this reaction mixture at room temperature in air afforded the complex as brown crystalline material. This material was collected by filtration, washed with ice-cold ethanol and dried in air. Yield obtained was 85 mg (46%). Single crystal for X-ray structure determination was selected from this material. *Anal.* Calc. for $C_{17}H_{20}N_4O_2Ni$: C, 55.02; H, 5.43; N, 15.10. Found: C, 55.24; H, 5.12; N, 14.91. Electronic spectral data in CH_3CN solution (λ_{max}, nm (ε, M^{-1} cm^{-1})): 540sh (120), 378 (17 400), 292sh (5 700), 222 (25 000). ^1H NMR (200 MHz) data in $CDCl_3$: δ 1.80 (s, 3H, -(H_3C)C=N-); 2.17 (s, 3H, 3-methyl of dmpz); 2.26 (s, 3H, H_3C-C(-O^-)=); 2.52 (s, 3H, 5-methyl of dmpz); 5.03 (s, 1H, =CH- of $bhac^{2-}$); 5.80 (s, 1H, =CH- of dmpz); 7.26 (m, 3H, phenyl ring protons); 7.78 (m, 2H, phenyl ring protons); 10.67 (s, 1H, -NH- of dmpz).

3.3.4. X-ray crystallography

For crystals of both **3** and **4** data were collected on an Enraf-Nonius Mach-3 single crystal diffractometer using graphite monochromated Mo $K\alpha$ radiation (λ = 0.71073 Å) by ω-scan method at 298 K. In each case, unit cell

parameters were determined by least-squares fit of 25 reflections having 2θ values in the range 18-22°. Intensities of 3 check reflections were measured after every 1.5 h during the data collection to monitor the crystal stability. In both cases, there is no siginificant change in the intensities of the check reflections. Empirical absorption corrections were applied to both datasets based on the ψ-scans.[9] The structures were solved by direct methods and refined on F^2 by full-matrix least-squares procedures. In each case, the asymmetric unit contains one molecule of the complex. All non-hydrogen atoms were refined using anisotropic thermal parameters. Hydrogen atoms were included in the structure factor calculation at idealised positions by using riding model, but not refined. The programs of WinGX[10] were used for data reduction and absorption correction. Structure solution and refinement were performed with the SHELX-97 programs[11]. The platon package was used for molecular graphics.[12] Selected crystal and refinement data are listed in Table 3.1.

Table 3.1. Crystallographic data for 3 and 4

Compound	**3**	**4**
Empirical formula	$C_{15}H_{16}N_4O_2Ni$	$C_{17}H_{20}N_4O_2Ni$
Formula weight	343.03	371.08
Crystal system	Monoclinic	Orthorhombic
Space group	$P2_1/c$	*Pbcn*
a (Å)	14.384(4)	19.058(4)
b (Å)	5.8031(13)	11.318(2)
c (Å)	18.082(4)	15.931(4)
α (^{o})	90	90
β (^{o})	93.56(3)	90
γ (^{o})	90	90
V (Å^3)	1506.4(6)	3436.4(14)
Z	4	8
ρ_{calc} (g cm^{-3})	1.513	1.435
μ (mm^{-1})	1.300	1.146
Crystal size (mm^3)	0.48 x 0.36 x 0.12	0.51 x 0.48 x 0.36
θ range (^{o})	1.42 to 27.47	2.09 to 27.45
Reflections collected/unique	3796/3448	4417/3945
Reflections having $I \geq 2\sigma(I)$	1874	2521
Data/restr./parameters	3448/0/201	3945/0/221
*R*1[a], *wR*2[b] [$I \geq 2\sigma(I)$]	0.0625, 0.1533	0.0435, 0.0837
*R*1[a], *wR*2[b] (all data)	0.1348, 0.1914	0.0861, 0.0976
Goodness-of-fit[c]	1.020	1.001
Largest peak/hole (*e* Å^{-3})	0.679/-0.598	0.350/-0.263

[a] $R1 = \sum||F_o| - |F_c||/\sum|F_o|$. [b] $wR2 = \{\sum[(F_o^2 - F_c^2)^2]/\sum[w(F_o^2)^2]\}^{1/2}$.
[c] GOF = $\{\sum[w(F_o^2 - F_c^2)^2]/(n - p)\}^{1/2}$ where 'n' is the number of reflections and 'p' is the number of parameters refined.

3.4. Results and discussion

3.4.1. Synthesis and some properties

The dark brown complexes were synthesized in moderate yields by reacting $Ni(O_2CCH_3)_2 \cdot 4H_2O$, H_2bhac and Hdmpz or Himdz in 1:1:1 mole ratio in boiling ethanol. Elemental analysis data are consistent with the molecular formula [Ni(bhac)hc] (hc = Himpz, Hdmpz). Both complexes are non-conducting in acetonitrile solutions. The complexes are diamagnetic and NMR active. Thus in each complex, the nickel ion is in +2 oxidation state and the coordination geometry around the metal centre is square-planar.

3.4.2. Spectral characteristics

The infrared spectra of the complexes do not display any amide or secondary amine N−H stretch in the range 3300-3500 cm^{-1}.[13] Several sharp weak peaks observed in the range 2855-3180 cm^{-1} are likely to be due to the aromatic C-H stretches. The absence of any peak assignable to the heterocycle N-H group is consistent with their involvement in strong intermolecular hydrogen bonding (*vide infra*). The C=O stretch (1675 cm^{-1}) of the amide functionality[14] in free H_2bhac is also absent in both spectra. Thus the Schiff base is completely deprotonated ($bhac^{2-}$) and acts as a dibasic enolate-O, imine-N and amide-O donor ligand in both complexes. The X-ray structures confirm such coordination. A strong peak at ~1600 cm^{-1} might involve the C=N stretches.[15]

Electronic spectral profiles of both complexes in acetonitrile solutions are very similar (Figure 3.1). A weak absorption band observed at ~535 nm is assigned to the spin-allowed d-d transition ($^1A_{1g} \rightarrow {}^1A_{2g}$) for a square-planar nickel(II) complex.[16] At higher energy, several strong absorptions are observed in the range 482-222 nm. Each of the three ligands (H_2bhac, Himdz and Hdmpz) in methanol solution displays a single absorption in the range 250-

215 nm. Thus the higher energy absorptions displayed by **3** and **4** are most likely due to charge transfer and ligand band transitions.

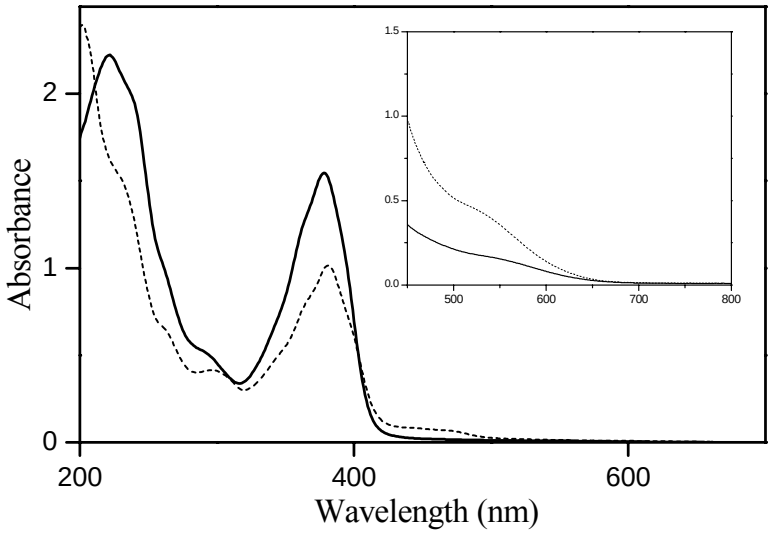

Fig.3.1. Electronic spectra of **3** (---) and **4** (—) in acetonitrile.

The ^{1}H NMR spectra of the complexes in $CDCl_3$ solutions are consistent with the [Ni(bhac)L] formulation. Protons of the two methyl groups on the $bhac^{2-}$ moiety appear as singlets at δ 1.92 and 2.34 for **3** and δ 1.80 and 2.26 for **4**. The =CH- proton of the $bhac^{2-}$ appears at δ 5.09 and 5.03 for **3** and **4**, respectively. For both complexes, the five phenyl protons appear in two groups at δ ~7.3 and ~7.8. The imidazole C−H protons in **3** are observed as three singlets at δ 6.93, 7.11 and 7.72. On the other hand, the lone C-H proton of Hdmpz in **4** appear as a singlet at δ 5.80. Two singlets observed at δ 2.17 and 2.52 for **4** are assigned to the 3- and 5-methyl group protons of the Hdmpz ligand, respectively. The heterocycle N−H proton appears as a singlet at δ 9.71 and 10.67 for **3** and **4**, respectively.

3.4.3. Molecular structures

The solid state molecular structures of **3** and **4** are shown in Figures 3.2 and 3.3, respectively. Selected bond parameters associated with the metal ions are listed in Table 3.2. In each complex, the tridentate bhac^{2-} coordinates the metal ion via the enolate-O, the imine-N and the deprotonated amide-O atoms forming one five- and one six-membered chelate ring. The fourth site is occuppied by the sp^2 N-atom of the heterocycle to complete a square-planar geometry around the metal centre. In both complexes, there is no deviation of the metal centre from the N_2O_2 square-plane. For **3**, the maximum and minimum deviations from the mean plane constituted by O1, O2, N1, N2 and Ni are 0.032(2) and 0.017(2) Å, respectively. For **4**, the corresponding values are 0.091(1) and 0.028(1), respectively. The N-N, N-C and C-O bond distances

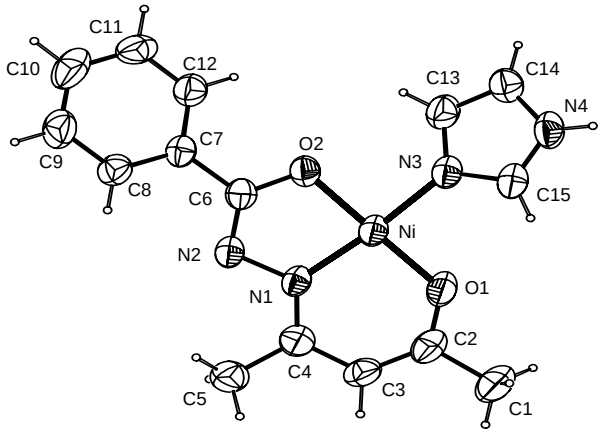

Fig. 3.2. Molecular structure of **3** with the atom-labeling scheme. Non-hydrogen atoms are represented by their 50% probability thermal ellipsoids.

(Table 3.2) in the =N-N=C(O$^-$)- fragment of bhac^{2-} are consistent with the enolate form of the amide functionalities.[8,15] The Ni-N_{imine} and Ni-O_{amide} distances are comparable with those observed in other Ni(II) complexes with

aroylhydrazones.[17,18] In both structures, the Ni-$O_{enolate}$ bond distances are similar to those reported for Ni(II) complexes where the metal centres have the same coordinating atom.[19] Structurally characterized mononuclear tetracoordinated Ni(II) complexes containing neutral pyrazole or imidazole as a ligand are extremely rare.[20,21] The Ni-$N_{pyrazole}$ bond distance in **4** is comparable with the distances observed in the lone example of a tetracoordinated Ni(II) complex containing monodentate neutral pyrazole moiety.[20] In **3**, the Ni-$N_{imidazole}$ bond distance is normal, as observed in a similar square-planar Ni(II) complex with a tridentate ligand and a neutral imidazole.[21]

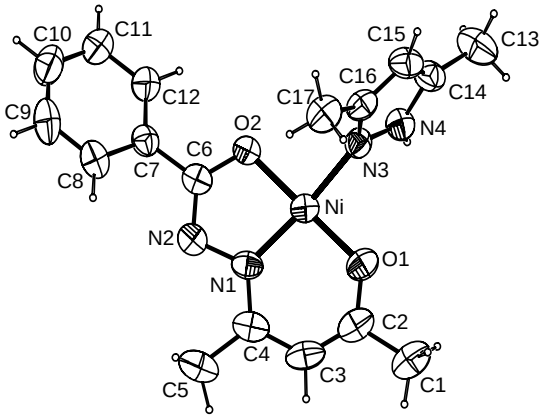

Fig. 3.3. Molecular structure of **4** showing 50% probability thermal ellipsoids for the non-hydrogen atoms and the atom-labeling scheme.

Table 3.2. Selected bond lengths (Å) and bond angles (º) of 3 and 4

	3	**4**
Ni-O1	1.824(4)	1.814(2)
Ni-O2	1.841(4)	1.850(2)
Ni-N1	1.8 25(4)	1.819(2)
Ni-N3	1.904(5)	1.915(2)
N1-N2	1.412(5)	1.404(3)
N2-C6	1.307(7)	1.292(4)
C6-O2	1.302(6)	1.319(3)
O1-Ni-O2	179.19(6)	177.05(9)
O1-Ni-N1	96.66(19)	96.59(11)
O1-Ni-N3	88.68(18)	88.92(10)
O2-Ni-N1	83.90(17)	83.89(10)
O2-Ni-N3	90.71(18)	90.97(9)
N1-Ni-N3	173.54(18)	171.06(10)

3.4.4. Hydrogen bonding and self-assembly

As mentioned earlier we were expecting a square-planar Ni(II) complex with the planar tridentate ligand $bhac^{2-}$ and a neutral monodentate heterocycle. The main quest was to see the orientation of the heterocycle plane with respect to the {Ni(bhac)} plane. If both are coplanar there is a possibility of π-stacked assembly of the molecules. In case of their non-coplanarity, self-assembly of the molecules via intermolecular hydrogen bonding between the heterocycle N-H and the O- or N-atoms of $bhac^{2-}$ is the next possibility. Indeed the coordination geometry around the metal centres are square-planar (*vide supra*) in **3** and **4**. For a π-stacked arrangement planarity of the whole molecule is one of the prerequisites.[22,23] However, excluding the phenyl ring atoms all other

atoms in the {Ni(bhac)} moiety are satisfactorily planar in both molecules. The mean deviations are 0.05 and 0.01 Å for **3** and **4**, respectively. In each case, the phenyl ring plane is significantly twisted. The dihedral angles between the phenyl ring plane and the plane constituted by Ni, O1, O2, N1, N2, C1-C6 are 21.1(2)^{o} and 34.4(1)^{o} for **3** and **4**, respectively. In addition to the twisting of the phenyl ring, the heterocycle plane also has a different orientation with respect to the plane containing Ni, O1, O2, N1, N2, C1-C6. However, these orientations are different for the two complexes (Figures 3.2 and 3.3). In case of **3**, the dihedral angle between the imidazole plane (mean deviation 0.003 Å) and the above mentioned plane is 19.5(3)^{o}. On the other hand, the dihedral angle between the pyrazole plane (mean deviation 0.017 Å) and the same plane is 69.12(7)^{o} in **4**. Most likely the two methyl groups in **4** on the Hdmpz make it sterically more unfavourable and hence the dihedral angle is larger. As a result of this non-planarity of both the molecules neither of them is involved in intermolecular π-π interactions in the crystal lattice. However, as we have anticipated the acidic heterocycle N−H in both molecules are involved in strong intermoleculer hydrogen bonding. In the case of **3**, the uncoordinated N-atom of the deprotonated amide functionality acts as the acceptor atom in the hydrogen bonding and a one-dimensional assembly (Figure 3.4) of the molecules is formed via this N−H···N interactions. The N4···N2 distance and the N4−H···N2 angle are 2.893(6) Å and 163.26^{o}, respectively. The Ni···Ni distance in this uniform chain-like arrangement is 9.079(2) Å. On the other hand, the metal coordinated amide-O atom acts as the acceptor atom in the hydrogen bonding in **4**. However, instead of a one-dimensional assembly two **4** molecules participate in a pair of complementary N4−H···O2 hydrogen bonds and form a dimeric structure (Figure 3.5). The N4···O2 distance and the N4−H···O2 angle are 2.830(3) Å and 162.95^{o}, respectively. In this dimeric arrangement, the Ni···Ni distance is 3.209(1) Å.

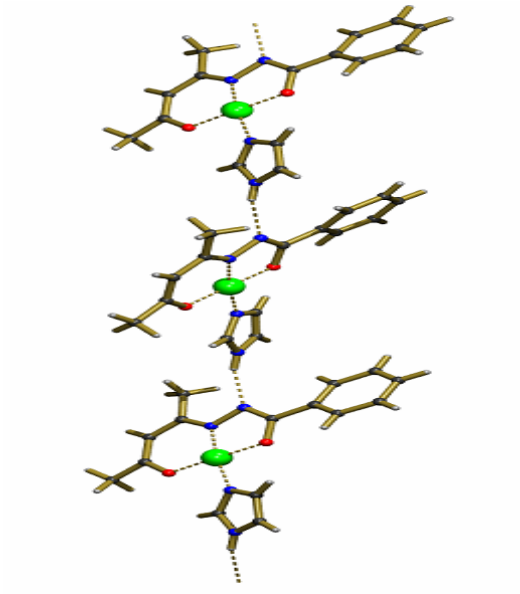

Fig. 3.4. One-dimensional ordering of **3**.

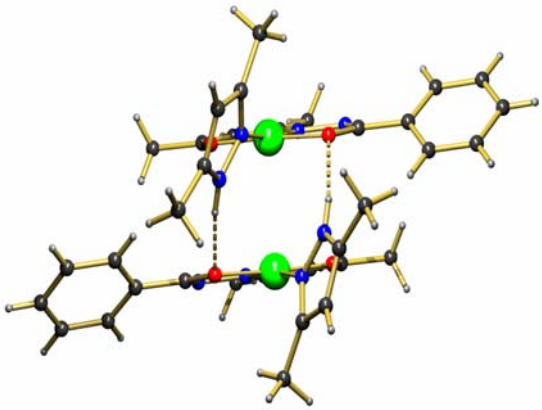

Fig. 3.5. Hydrogen bonded dimer of **4**.

The possible reasons for the difference in the hydrogen bonding pattern and hence in the self-assembly are as follows. The orientations of the heterocycle plane with respect to the plane containing Ni, O1, O2, N1, N2, C1-C6 are very different in the two complex molecules. In addition, the N−H proton in Himdz is one C-atom apart from the coordinating heterocycle N-atom compared to that in Hdmpz. Thus the direction of the Himdz N−H group as well as relatively more planar nature of the molecules of **3** lead to intermolecular N−H···N interactions and a one-diemensional assembly in the solid state. Whereas in case of **4**, the orientation of Hdmpz plane and the close proximity of Hdmpz N−H group and the coordinating N-atom leads to a dimeric arrangement via two reciprocal N4−H···O2 interactions.

3.5. Conclusions

We have synthesized and characterized two new mixed-ligand nickel(II) complexes with a tridentate enolate-O, imine-N and amide-O donor ligand and N-donor heterocycles such as imidazole (Himdz) and 3,5-dimethylpyrazole (Hdmpz). In both complex molecules, the metal ions are in a square-planar N_2O_2 coordination geometry. However, none of the molecules is planar primarily due to different orientation of the heterocycle plane with respect to the rest of the molecule. The extent of this difference in orientation is less for the complex containing Himdz than the complex containing Hdmpz. As a result of this variance in orientation and also due to different types of heterocycles, the molecules of these two essentially similar complexes display two different types of self-assembly via two different intermolecular hydrogen bonding interactions involving the acidic heterocycle N−H group in the solid state. The Himdz containing complex molecules form a one-dimensional chain via N−H···N_{amide} hydrogen bonds and two molecules of the Hdmpz containing complex form a dimer via a pair of N−H···O_{amide} hydrogen bonds.

3.6. References

1. Inorganic Crystal Engineering (Dalton Discussion No. 3), *J. Chem. Soc., Dalton Trans.,* 2000, 3705.
2. O.R. Evans and W. Lin, *Acc. Chem. Res*., 2002, **35**, 511.
3. O. Kahn (Ed.), *Magnetism: A Supramolecular Function;* Kluwer, Dordrecht, NATO ASI Series, 1996, vol. **C-484**.
4. M. Clemente-León, E. Coronado, P. Delhaes, J.R. Galán Mascarós, C.J. Gómez-García, C. Mingotaud, in: J. Veciana, C. Rovira and D.B. Amabilino (Eds.), *Supramolecular Engineering of Synthetic Metallic Materials. Conductors and Magnets;* Kluwer, Dordrecht, NATO ASI Series, 1998, vol. **C-518**, pp. 291-312.
5. O.M. Yaghi, H. Li, H.C. Davis, D. Richardson and T.L. Groy, *Acc. Chem. Res.*, 1998, **31**, 474.
6. P.N.W. Baxter, J.-M. Lehn, B.O. Kneisel and D. Fenske, *Angew. Chem. Int. Ed. Engl.*, 1997, **36**, 1978.
7. D. Braga, F. Grepioni and G. R. Desiraju, *Chem. Rev*., 1998, **98**, 1375.
8. N.R. Sangeetha, C.K. Pal, P. Ghosh and S. Pal, *J. Chem. Soc., Dalton Trans.*, 1996, 3293.
9. A.C.T. North, D.C. Philips and F.S. Mathews, *Acta Crystallogr., Sect. A*, 1968, **24**, 351.
10. L.J. Farrugia, *J. Appl. Crystallogr*., 1999, **32**, 837.
11. G.M. Sheldrick, SHELX-97, University of Göttingen, Göttingen, Germany, 1997.
12. A. L. Spek, *PLATON-A Multipurpose Crystallographic Tool*; Utrecht University, Utrecht, The Netherlands, 2002.
13. W. Kemp, *Organic Spectroscopy;* Macmillan, Hampshire, 1987, pp. 62-66.
14. K. Nakamoto, *Infrared and Raman Spectra of Inorganic and Coordination Compounds;* Wiley, New York, 1986, pp. 241-242.
15. S.N. Pal and S. Pal, *J. Chem. Soc., Dalton Trans.*, 2002, 2102.

16. A. la Cour, M. Findeisen, R. Hazell, L. Hennig, C.E. Olsen and O. Simonsen, *J. Chem. Soc., Dalton Trans*., 1996, 3437.
17. S. Seth and S. Chakraborty, *Acta Crystallogr*., 1984, **C40**, 1530.
18. G.V. Karunakar, N.R. Sangeetha, V. Susila and S. Pal, *J. Coord. Chem.*, 2000, **50,** 51.
19. M.B. Hursthouse, M.A. Laffey, P.T. Moore, D.B. New, P.R. Raithby and P. Thornton, *J. Chem. Soc., Dalton Trans.*, 1982, 307.
20. I.A. Krol, V.M. Agre, V.K. Trunov and O.V. Ivanov, *Koord. Khim.*, 1980, **6**, 1891.
21. S. Gou, X. You, Z. Xu, Z. Zhou and K. Yu, *Polyhedron,* 1991, **10**, 2659.
22. C.A. Hunter and J.K.M. Saunders, *J. Am. Chem. Soc.*, 1990, **112**, 5525.
23. C. Janiak, *J. Chem. Soc., Dalton Trans.*, 2000, 3885.

Chapter 4

Intramolecular apical M···H–C interaction in square-planar nickel(II) complexes with dibasic tridentate ligands and 2-phenyl-imidazole

4.1. Abstract

Two square-planar mixed-ligand nickel(II) complexes [Ni(bhac)(phim)] (**5**) and [Ni(ahac)(phim)] (**6**) with tridentate O,N,O-donor Schiff bases (acetylacetone benzoylhydrazone (H_2bhac) and acetylacetone acetylhydrazone (H_2ahac)) and monodentate sp^2 N-donor 2-phenyl-imidazole (phim) as the ancillary ligand have been synthesized and characterized by analytical, spectroscopic, magnetic and electrochemical methods. The solid state structures of both the complexes have been determined by X-ray crystallography. The asymmetric unit of **5** contains a single complex molecule while that of **6** contains four complex molecules with different conformations. The molecular structures of both complexes reveal that one of the two *ortho* C–H groups of the pendant phenyl ring of phim is very close to the metal centre at the apical site indicating the presence of intramolecular Ni···H–C interaction. A survey of the reported X-ray structures of similar d^8 metal ion complexes containing intramolecular M···H–C interaction has been performed to compare with the structural features of **5** and **6**. The optimized molecular structures of **5** and **6** generated by calculations based on density functional method are compared with the experimental structures. Calculations also reveal that the four molecules present in the asymmetric unit of **6** are very close in energy. The nature of the highest occupied molecular orbital and the down-field shift of the proton resonance on cooling in the NMR spectra suggest a three-centre four-electron hydrogen bond character of the observed Ni···H–C interaction in **5** and **6**.

4.2. Introduction

The long standing interest in the interaction of transition metal ions with proximate C–H fragments is primarily due to the C–H activation processes involved in many catalytic reactions. Such interactions have been scrutinized intensively for a better understanding of their structural and bonding features.[1–12] The nature of the apical M···H–C interactions in square-planar 16-electron complexes of d^8 metal ions is not very clear.[9–12] In such species, these interactions can be agostic bond (three-centre two-electron) as well as non-classical hydrogen bond (three-centre four-electron) in character due to the availability of the empty orbital and also the lone pair of electrons on the metal ion. Such apical M···H–C interactions in square-planar d^8 systems have variously been described as weakly agostic bonds, non-classical hydrogen bonds and also as repulsive due to filled metal d_{z^2} and C–H σ-orbitals.[2,12–14] Compared to the agostic interaction, non-classical hydrogen bond is not common in metal complexes. For a metal centre to participate as the proton acceptor in a hydrogen bond, it is essential for it to be electron rich. Examples of such complexes are more with d^8 and d^{10} metal centres. It has been demonstrated that such hydrogen bond can facilitate the oxidative addition of H–X to a metal centre.[15]

In the preceding chapter, we have seen that the square planar complexes of nickel, with the tridentate ligand $bhac^{2-}$ and monodentate heterocycles, are not planar due to the different orientation of the heterocycle ring compared to the rest of the molecules. Here we have chosen the ancillary ligand 2-phenyl-imidazole specifically so that one of the two *ortho* C–H groups of the phenyl ring will be in close proximity with the metal ion at the apical site.

In the present chapter, we report two square-planar nickel(II) complexes with the tridentate Schiff bases H_2bhac and H_2ahac and the monodentate 2-phenyl-imidazole as the ancillary ligand. The deprotonated planar Schiff bases ($bhac^{2-}$ and $ahac^{2-}$) satisfy the +2 charge on the metal ion

and three coordination sites. The sp^2 N-atom of the neutral 2-phenyl-imidazole (phim) occupies the fourth coordination site and completes the square-plane around the metal ion. The complexes, [Ni(bhac)(phim)] (**5**) and [Ni(ahac)(phim)] (**6**) have been characterized by analytical, magnetic, spectroscopic and electrochemical measurements. The X-ray structures of **5** and **6** indeed reveal the presence of apical M···H–C interaction in both complex molecules. We have examined the reported structures of the square-planar d^8 systems with similar intramolecular M···H–C interactions available in the Cambridge Structural Database (CSD) to compare with the structural features of **5** and **6**. Calculations based on density functional method (B3LYP) have been performed to understand the molecular conformations observed in the X-ray structures of **5** and **6**. We have also carried out variable temperature NMR measurements to probe the nature of this interaction in solution. We believe the findings described in the following account will be useful in understanding the nature of M···H–C interaction in the late first row transitional metal ion complexes.

4.3. Experimental

4.3.1. Materials

The Schiff bases H_2bhac and H_2ahac were prepared by condensation reactions of acetylacetone with benzoylhydrazine and acetylhydrazine, respectively.[16] All other chemicals and solvents used in this work were of analytical grade available commercially and were used without further purification.

4.3.2. Physical measurements

Microanalytical (C, H, N) data were obtained with a Thermo Finnigon Flash EA1112 series elemental analyzer. Infrared spectra were collected by using KBr pellets on a Jasco-5300 FT-IR spectrophotometer. A Shimadzu 3101-PC UV/vis/NIR spectrophotometer was used to record the electronic

spectra. The proton NMR spectra were recorded using a Bruker 400 MHz spectrometer. Solution electrical conductivities were measured with a Digisun DI-909 conductivity meter. A Sherwood Scientific balance was used for magnetic susceptibility measurements. A CH-Instruments model 620A electrochemical analyser was used for cyclic voltammetric experiments with acetonitrile solutions of the complexes containing tetrabutylammonium perchlorate (TBAP) as supporting electrolyte. The three electrode measurements were carried out at 298 K under a dinitrogen atmosphere with a platinum disk working electrode, a platinum wire auxiliary electrode and an Ag/AgCl reference electrode.

4.3.3. Synthesis of the complexes

[Ni(bhac)(phim)] (5)

A dry methanol solution (15 cm^3) of $Ni(O_2CCH_3)_2{\cdot}4H_2O$ (125 mg, 0.5 mmol) was added to a dry methanol solution (10 cm^3) of H_2bhac (110 mg, 0.5 mmol) and 2-phenyl-imidazole (72 mg, 0.5 mmol). The resulting deep brown mixture was kept under reflux for 2 h and then evaporated on a steam bath to approximately half of the original volume. The brown needles separated after cooling to room temperature were collected by filtration, washed with little ice-cold methanol and finally dried in air. Yield was 160 mg (76%). A single crystal suitable for X-ray structure determination was selected from this material. Anal. Calc. for $NiC_{21}H_{20}N_4O_2$: C, 60.18; H, 4.81; N, 13.37. Found: C, 59.95; H, 4.78; N, 13.24%. Electronic spectral data in CH_3OH (λ_{max}, nm (ε, M^{-1} cm^{-1})): 565 (94)^{sh}, 380 (14 200), 366 (12 700)^{sh}, 267 (19 800), 234 (21 100)^{sh}.

[Ni(ahac)(phim)] (6)

A dry methanol solution (15 cm^3) of $Ni(O_2CCH_3)_2{\cdot}4H_2O$ (125 mg, 0.5 mmol) was added to a dry methanol solution (10 cm^3) of H_2ahac (70 mg, 0.5 mmol) and 2-phenyl-imidazole (72 mg, 0.5 mmol) and the mixture was kept

under reflux for 2 h. A brown crystalline material was deposited on the wall of the round−bottomed flask along the surface of the solvent and formed a ring. The reaction mixture was cooled to room temperature and the almost colorless and clear mother liquor was removed carefully by using a dropper. The crystalline material was collected after drying in air. Yield was 110 mg (62%). A single crystal suitable for X-ray structure determination was selected from this material. Anal. Calc. for $NiC_{16}H_{18}N_4O_2$: C, 53.82; H, 5.08; N, 15.69. Found: C, 53.54; H, 4.86; N, 15.47%. Electronic spectral data in CH_3OH (λ_{max}, nm (ε, M^{-1} cm^{-1})): 425 (370)^{sh}, 358 (3 500)^{sh}, 344 (4 700), 330 (4 400)^{sh}, 267 (18 400), 235 (18 600)^{sh}.

4.3.4. X-ray crystallography

Complexes **5** and **6** crystallize in the space groups C2/c and $P2_1/c$, respectively. Unit cell parameters and the intensity data were obtained on a Bruker-Nonius SMART APEX CCD single crystal diffractometer, equipped with a graphite monochromator and a Mo $K\alpha$ fine-focus sealed tube (λ = 0.71073 Å) operated at 2.0 kW. The detector was placed at a distance of 6.0 cm from the crystal. Data were collected at 298 K with a scan width of 0.3º in ω and an exposure time of 30 sec/frame. The SMART software was used for data acquisition and the SAINT-Plus software was used for data extraction.[17] In each case, an absorption correction was performed with the help of SADABS program.[18] The structures were solved by direct methods and refined on F^2 by full-matrix least-squares procedures. In both structures, all non-hydrogen atoms were refined with anisotropic thermal parameters. Hydrogen atoms were added at idealized positions by using a riding model. For **5** the hydrogen atoms were refined isotropically while for **6** they were not refined. The SHELX-97 programs[19] of the WinGX package[20] were used for structure solution and refinement. The ORTEX6a[21] and Platon[22] packages were used for molecular graphics. Significant crystallographic data for **5** and **6** are summarized in Table 4.1.

4.3.5. Computational methods

Molecules of **5** and **6** were fully optimized without geometry constraints using the B3LYP[23,24] density functional method. Basis set used for geometry optimizations and energy calculations was LANL2DZ.[25] The Gaussian 03[26] suite of programs were used for all calculations.

4.3.6. CSD database study

We have performed a database search on CSD to compare few structural trends found in **5** and **6** with similar types of structures already deposited in CSD. The search was based on the following criteria: (i) the metal ion is always coordinated to a N-atom which is bonded to the atom X (elements of groups 14–16), (ii) X is connected to an unsubstituted/substituted phenyl ring by a single bond (Scheme 1), (iii) the phenyl ring *ortho* C–H at the δ position is involved in the M···H–C interaction, (iv) the M···H separation is in the range 2.0–3.0 Å, (v) the N_α–X_β–Cγ angle is within 110–140°, (vi) the N_α–X_β–C_γ–C_δ torsion angle (ψ) is in the range 0–180° and (vii) structures with *R* factor > 10 are excluded. Forty-four hits were obtained. Selected structural parameters for these forty four X-ray structures are listed in Table AI.1 (Appendix I).

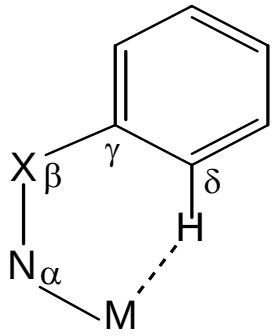

Scheme 1

Table 4.1. Crystallographic data for **5** and **6**

Complex	**5**	**6**
Empirical formula	$C_{21}H_{20}N_4O_2Ni$	$C_{16}H_{18}N_4O_2Ni$
Formula weight	419.12	357.05
Crystal system	Monoclinic	Monoclinic
Space group	*C*2/*c*	$P2_1/c$
a/Å	43.532(3)	24.450(2)
b/Å	11.8872(9)	8.5337(7)
c/Å	7.6363(6)	33.518(3)
(/o	99.3510(10)	108.985(2)
V/Å3	3899.1(5)	6613.2(9)
Z	8	16
(/mm(1	1.019	1.188
Reflections collected	19894	49271
Unique reflections	3853	8643
Reflections [*I* (2((I)]	3013	4844
Parameters	333	841
R1,[a] wR2[b] [I (2((I)]	0.0361, 0.0889	0.0713, 0.1155
R1,[a] wR2[b] (all data)	0.0488, 0.0970	0.1408, 0.1375
GOF[c] on F^2	0.913	1.025
Largest peak, hole/ e Å^{-3}	0.388, –0.201	0.400, –0.332

[a] $R1 = \sum||F_o| - |F_c||/\sum|F_o|$. [b] $wR2 = \{\sum[(F_o^2 - F_c^2)^2]/\sum[w(F_o^2)^2]\}^{1/2}$.
[c] GOF = $\{\sum[w(F_o^2 - F_c^2)^2]/(n - p)\}^{1/2}$ where 'n' is the number of reflections and 'p' is the number of parameters refined.

4.4. Results and discussion

4.4.1. Synthesis and some properties

Reactions of one equivalent each of $Ni(O_2CCH_3)_2{\cdot}4H_2O$, the Schiff bases ($H_2$bhac and H_2ahac) and 2-phenyl-imidazole in boiling methanol afford the dark brown complexes in moderate to good yield. Elemental analysis data are consistent with the molecular formula [Ni(bhac)(phim)] (**5**) and [Ni(ahac)(phim)] (**6**). Both **5** and **6** are electrically non-conducting in methanol solutions. The complexes are diamagnetic and NMR active. Thus in each complex, the nickel ion is in +2 oxidation state and the coordination geometry around the metal centre is square-planar.

4.4.2. Spectral characteristics

The infrared spectra of **5** and **6** do not display any band assignable to the amide or secondary amine N–H stretch.[27] Several sharp weak bands observed in the range 2900–3150 cm^{-1} are likely to be due to the C–H stretches. The absence of any band for the N–H group of the ancillary ligand phim is consistent with its involvement in strong intermolecular hydrogen bonding (*vide infra*). Free H_2bhac and H_2ahac display the amide C=O stretch[28] near ~1675 cm^{-1}. The absence of any such band in the spectra of **5** and **6** indicates complete deprotonation of the Schiff bases in the complexes. Thus in both complexes, the dibasic tridentate ligands ($bhac^{2-}$ and $ahac^{2-}$) act as the enolate-O, the imine-N and the deprotonated amide-O donor. A strong band observed near 1590 cm^{-1} might involve the C=N stretches.[29]

The electronic spectra were collected using methanol solutions of the complexes. The weak absorption observed at 565 nm for **5** and at 425 nm for **6** is assigned to the spin-allowed d–d transition ($^1A_{1g} \rightarrow {}^1A_{2g}$) for a square-planar nickel(II) complex (Figure 4.1).[30] The density functional calculations show that in both **5** and **6** the lowest unoccupied molecular oribital (LUMO) is primarily localized on the ancillary ligand phim and the highest occupied molecular orbital (HOMO) is composed of d- and p-orbitals of the metal and

coordinated O-atoms, respectively (*vide infra*). The spectra of the free Schiff bases and 2-phenyl-imidazole in methanol solutions display a single absorption in the range 250–215 nm. Thus the strong absorptions observed in the range 380–234 nm for **5** and **6** are possibly due to the metal-to-ligand and inter- or intra-ligand charge transfer transitions.

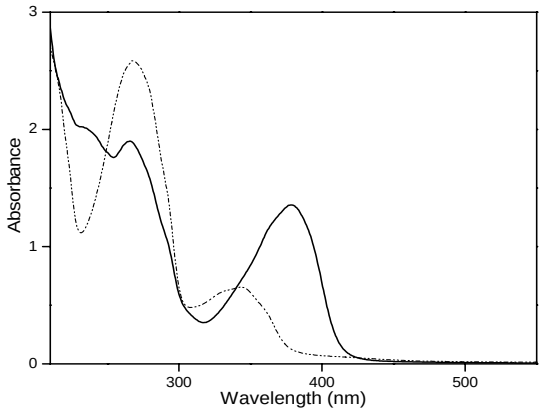

Fig. 4.1. Electronic spectra of **5** (—) and **6** (---) in methanol.

4.4.3. Redox Properties

Electron transfer properties of **5** and **6** have been investigated by cyclic voltammetry using acetonitrile solutions of the complexes. Both **5** and **6** display an irreversible oxidation response at 0.69 and 0.71 V, respectively. The current height of this response is comparable with known one electron redox processes under identical conditions.[31] No such response is observed for the deprotonated Schiff bases and 2-phenyl-imidazole under the same conditions. The iron(III) and copper(II) complexes with $bhac^{2-}$ show metal-centered oxidation responses in the potential range 0.4–0.8 V.[16,32,33] Therefore, the oxidation responses observed for **5** and **6** are assigned to Ni(II) $\rightarrow$ Ni(III) process. The nature of HOMO (*vide infra*) in both complexes also supports this assignment. The irreversible nature of the response suggests that in each case the corresponding oxidized species is unstable on the cyclic voltammetry time scale.

4.4.4. Description of X-ray structures and Ni···H–C interactions

The molecular structures of **5** and **6** are depicted in Figure 4.2. Bond parameters associated with the metal ions are listed in Table 4.2. The asymmetric unit of **5** contains one complex molecule while that of **6** contains four complex molecules. There is no deviation of the metal centre from the N_2O_2 square-plane. The Ni–O(enolate), Ni–N(imine), Ni–O(amide) and Ni–N(imidazole) bond lengths are comparable with those observed in nickel(II) complexes having the same coordinating atoms.[34–36]

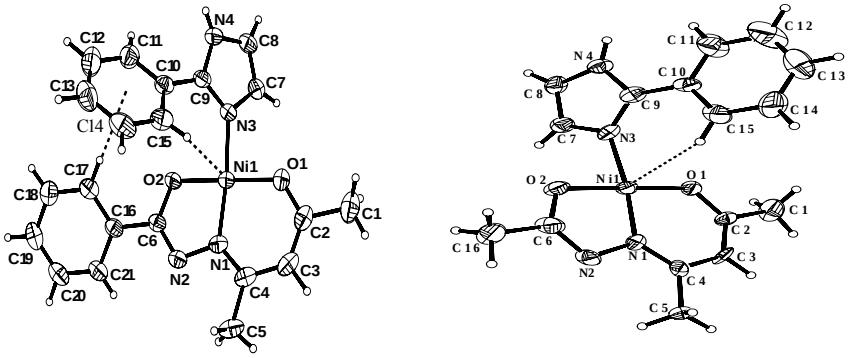

(**a**) (**b**)

Fig. 4.2. Molecular structures of (a) **5** and (b) **6** with the atom labeling scheme. All non-hydrogen atoms are represented by their 40% probability thermal ellipsoids.

In **5**, the tridentate ligand $bhac^{2-}$ is not planar due to twisting of the phenyl ring plane along the C6–C16 bond (Figure 4.2). It is also interesting to note that one of the two *ortho* C–H groups of the phenyl ring of $bhac^{2-}$ is involved in a C–H···π interaction with the phenyl ring of the ancillary ligand phim (Figure 4.2). The H···Cg distance and the C–H···Cg angle are 2.962 Å and 152.8°, respectively. Possibly this C–H···π interaction is primarily responsible for the twisting of the phenyl ring plane of $bhac^{2-}$ along the C6–C16 bond. The O1–Ni1–N3–C9 torsion angle (θ) is 48.9^0 (Table 4.3). Thus the chelate forming fragment (O1,O2,N1,N2,C1–C6) of $bhac^{2-}$ and the

metal coordinated imidazole ring plane are not orthogonal (Figure 4.2). The phim moiety is not planar due to the twisting of the imidazole ring plane and the phenyl ring plane along the C9–C10 bond (Figure 4.2). The extent of this twisting (ψ) is measured by taking the average of the N3–C9–C10–C15 and N4–C9–C10–C11 torsion angles. The value of ψ is found as 35.8°. As a result an *ortho* C–H of the phim phenyl ring is close to the metal centre at the apical site (Figure 4.2). The Ni···H and Ni···C distances and the Ni···H–C angle are 2.79(2), 3.321(3) Å and 116.8(2)°, respectively (Table 4.3).

The bond lengths and bond angles of the four molecules present in the asymmetric unit of **6** are very similar (Table 4.2). However, the orthogonality (θ) between the chelate forming fragment of $ahac^{2-}$ and the metal coordinated imidazole ring plane and the twisting of phim (ψ) differ significantly. The θ and ψ values are in the ranges 72.9–91.6° and 1.6–21.6°, respectively (Table 4.3). Most importantly in two molecules the orientation of the phim phenyl ring with respect to the {Ni(ahac)} plane is on one side and in the other two molecules it is on the other side (Figure 4.3). As in **5**, one of the two *ortho* C–H groups of the phim phenyl ring is close to the metal centre at the apical site in each of the four molecules. The Ni···H and Ni···C distances and the Ni···H–C angles are within 2.42–2.69 Å, 3.20–3.36 Å and 130.1–142.2°, respectively (Table 4.3).

The following trends are very clear from the above observations on the molecular structures of **5** and **6**. In **5**, only one complex molecule is present in the asymmetric unit and both the phenyl ring and the imidazole ring planes of phim are tilted toward the phenyl ring of the benzoyl fragment of $bhac^{2-}$ (Figure 4.2). In spite of being weak in nature we believe the intramolecular C–H···π interaction plays a major role in restricting the phim moiety from taking random orientations and a single conformation of it is stabilized in **5**. Due to the replacement of the phenyl group of $bhac^{2-}$ by a methyl group in $ahac^{2-}$ the intermolecular C–H···π interaction observed in **5** is not possible in **6**. Complex **6** crystallizes with four molecules in the asymmetric unit and the

phim moieties are randomly oriented on both sides of the plane containing the {Ni(ahac)} moiety. Thus lack of the C–H···π interaction here facilitates free rotation of phim about the Ni–N(imidazole) bond. In addition, the imidazole plane in **6** is closer to the orthogonal arrangement with the two chelate ring planes (θ = 72.9–91.6^o) compared to that in **5** (θ = 48.9^o). This difference is also likely to be due to the C–H···π interaction in **5**. The internal twisting of phim in **5** (ψ = 35.8^o) is significantly larger than that in **6** (ψ = 1.6–21.6^o). Possibly this difference is also partly due to the intramolecular C–H···π interaction in **5**. Despite the differences in the θ- and ψ-values one of the two *ortho* C–H groups of phim phenyl ring is near to the apical position of the metal ion in all the structures. In this context, it may be noted that the crystal structure of the protonated 2-phenyl-imidazole (Hphim$^+$) is known.[37] Here the ψ value is 22.32^o. Thus in all probability significantly different twisting of phim in **5** and **6** compared to that in Hphim$^+$ is due to the intramolecular C–H···π and Ni···H–C interactions observed in the present complex molecules.

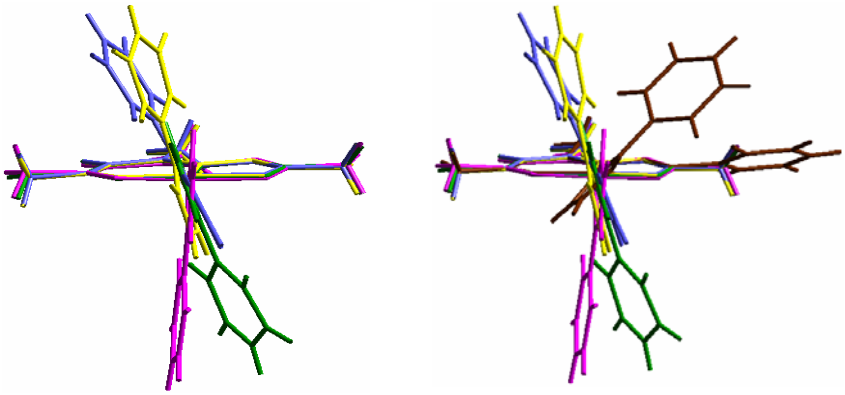

(**a**) (**b**)

Fig. 4.3. Overlay diagrams of (a) the four molecules present in the asymmetric unit of **6** and (b) the molecule of **5** and the four molecules of **6**.

Table 4.2. Selected bond lengths (Å) and bond angles (°) for 5 and 6

		(**5**)	
Ni(1)-O(1)	1.8195(17)	Ni(1)-O(2)	1.8443(16)
Ni(1)-N(1)	1.8269(18)	Ni(1)-N(3)	1.9136(18)
O(1)-Ni(1)-O(2)	175.76(7)	O(1)-Ni(1)-N(1)	96.15(7)
O(1)-Ni(1)-N(3)	89.07(7)	O(2)-Ni(1)-N(1)	84.13(7)
O(2)-Ni(1)-N(3)	91.08(7)	N(1)-Ni(1)-N(3)	172.37(8)
		(**6**)	
Molecule 1			
Ni(1)-O(1)	1.829(5)	Ni(1)-O(2)	1.851(5)
Ni(1)-N(1)	1.826(6)	Ni(1)-N(3)	1.923(6)
O(1)-Ni(1)-O(2)	178.3(2)	O(1)-Ni(1)-N(1)	95.6(3)
O(1)-Ni(1)-N(3)	91.4(2)	O(2)-Ni(1)-N(1)	84.0(2)
O(2)-Ni(1)-N(3)	89.0(2)	N(1)-Ni(1)-N(3)	173.0(3)
Molecule 2			
Ni(2)-O(3)	1.818(5)	Ni(2)-O(4)	1.852(5)
Ni(2)-N(5)	1.821(7)	Ni(2)-N(7)	1.909(6)
O(3)-Ni(2)-O(4)	177.8(2)	O(3)-Ni(2)-N(5)	96.0(3)
O(3)-Ni(2)-N(7)	90.3(3)	O(4)-Ni(2)-N(5)	83.8(3)
O(4)-Ni(2)-N(7)	89.8(3)	N(5)-Ni(2)-N(7)	173.6(3)
Molecule 3			
Ni(3)-O(5)	1.820(5)	Ni(3)-O(6)	1.855(5)
Ni(3)-N(9)	1.820(6)	Ni(3)-N(11)	1.918(6)
O(5)-Ni(3)-O(6)	178.3(3)	O(5)-Ni(3)-N(9)	95.6(3)
O(5)-Ni(3)-N(11)	89.4(3)	O(6)-Ni(3)-N(9)	84.3(3)
O(6)-Ni(3)-N(11)	90.5(3)	N(9)-Ni(3)-N(11)	174.2(3)
Molecule 4			
Ni(4)-O(7)	1.832(6)	Ni(4)-O(8)	1.853(5)
Ni(4)-N(13)	1.838(6)	Ni(4)-N(15)	1.928(7)
O(7)-Ni(4)-O(8)	179.6(3)	O(7)-Ni(4)-N(13)	96.0(3)
O(7)-Ni(4)-N(15)	89.4(3)	O(8)-Ni(4)-N(13)	83.7(3)
O(8)-Ni(4)-N(15)	91.0(3)	N(13)-Ni(4)-N(15)	173.5(3)

Table 4.3. Structural parameters[a] related to Ni···H–C interactions and molecular conformations of **5** and **6**

Parameters	(5)	(6)			
		Mol-1	Mol-2	Mol-3	Mol-4
Ni···H distance/Å	2.79(2) (2.84)	2.54 (2.86)	2.42 (2.86)	2.47 (2.86)	2.69 (2.86)
Ni···C distance/Å	3.321(3) (3.429)	3.288(9) (3.49)	3.207(9) (3.49)	3.236(12) (3.49)	3.364(11) (3.49)
Ni···H–C angle/^{o}	116.8(2) (117.5)	137.7 (116.7)	142.2 (116.7)	139.3 (116.7)	130.1 (116.7)
$\psi^{b}/^{o}$	35.8 (32.4)	12.9 (33.4)	1.6 (33.4)	11.3 (33.4)	21.6 (33.4)
$\theta^{c}/^{o}$	48.9 (38.0)	73.1 (38.9)	91.6 (38.9)	76.4 (38.9)	72.9 (38.9)

[a] Calculated values are in parentheses.
[b] Average of N3–C9–C10–C15 and N4–C9–C10–C11 (Fig.4.2) torsion angles.
[c] O1–Ni–N3–C9 (Fig. 4.2) torsion angles.

A close scrutiny of the structural parameters (Table 4.3) related to the Ni···H–C interactions and the molecular conformations of **5** and **6** reveals the following. The longer is the Ni···H distance the shorter is the Ni···H–C angle. There is a satisfactory linear correlation between the Ni···H distance and the Ni···H–C angle. In general, the Ni···H distance increases and the Ni···H–C angle decreases with the increase of the twisting of phim (ψ) and the decrease of the orthogonality (θ) between the imidazole ring plane and the plane containing the two chelate forming fragments of the tridentate ligands (Table 4.3). The Ni···H distance is linearly related with the Ψ values as well as θ values with opposite slopes (Figure 4.4). Thus large twist of phim forces a T-shape of the Ni···H–C interaction with an increase in the Ni···H distance, while small twist of phim makes the Ni···H–C interaction more linear with a decrease in the Ni···H distance. It is clear from the above facts that the geometrical arrangement of the Ni···H–C interaction largely depends on the twist of the phim in **5** and **6**. A detailed theoretical study reported previously has supported the idea that the axial M···H interactions in d^{8} metal ion

complexes are mainly repulsive in nature.[10] But a minor attractive contribution to the M···H–C interaction can not be ruled out in the present complexes. The Ni···H distances in both complexes and shorter Ni···H distances in **6** compared to that in **5** unaided and unhindered by any geometrical constraint in the former substantiate this idea.

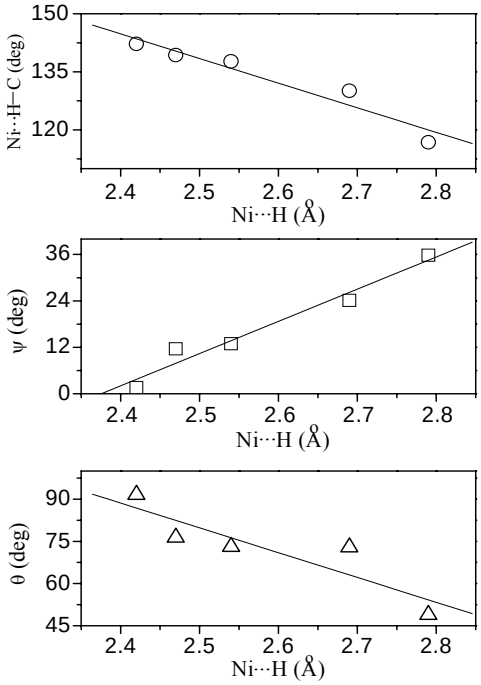

Fig. 4.4. The plots of Ni···H–C angles (O), twist angles (ψ) of 2-phenyl-imidazole (phim) (□), and the torsion angles (θ) reflecting the orthogonality between the planes containing the chelate rings and the imidazole ring (Δ) against the Ni···H distances observed in the X-ray structures of [Ni(bhac)(phim)] (**5**) and [Ni(ahac)(phim)] (**6**). The straight lines represent the least-squares fits.

4.4.5. Intermolecular hydrogen bonds and self-assembly of 5 and 6

Both complex molecules contain the imidazole N–H group and metal coordinated O-atoms which are conventional hydrogen bond donor and acceptor, respectively. In the crystal lattice, the molecules of each of the two complexes are involved in intermolecular N–H···O hydrogen bonding interactions involving the imidazole N–H groups and the metal coordinated amide O-atoms of the tridentate ligands. In the case of **5**, the N···O distance and the N–H···O angle are 2.856(3) Å and 160(2)^{o}, respectively. There are some variations in the structural parameters related to the N–H···O interaction for the four molecules present in the asymmetric unit of **6**. The N···O distances are in the range 2.788(8)–2.846(9) Å and the N–H···O angles are within 148–163^{o}. In each case, self-assembly of the complex molecules via these intermolecular N–H···O hydrogen bonds leads to one-dimensional supramolecular structure in the crystal lattice (Figure 4.5).

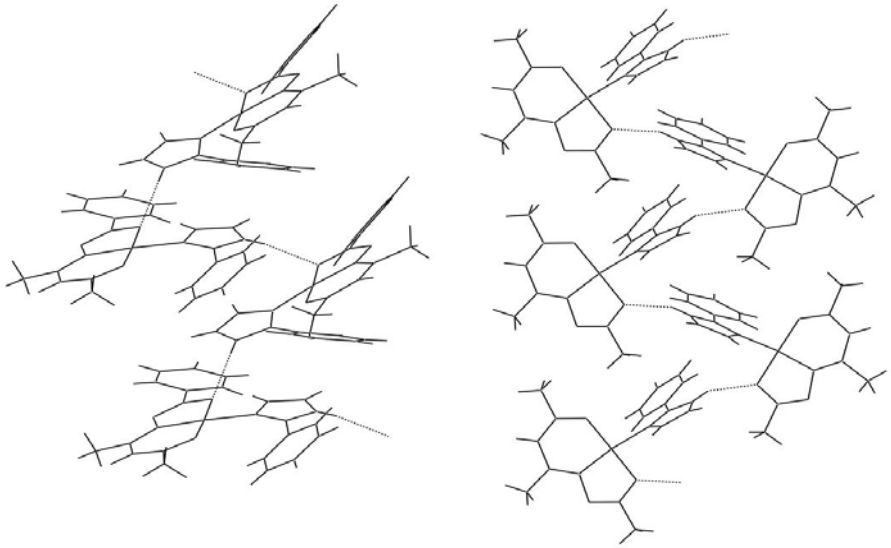

(**a**) (**b**)

Fig. 4.5. One-dimensional ordering of (a) **5** and (b) **6** via intermolecular N–H···O hydrogen bonds.

4.4.6. Survey of the d^8 metal ion complexes with intramolecular M···H–C interaction

To verify whether the trends observed for **5** and **6** are general or not we have performed a Cambridge Structural Database (version 5.26) search for d^8 metal ion complexes having intramolecular M···H–C interactions. In the structures collected in Table A1.1 of appendix I, the mean M···H distance increases in the order Ni(II) < Pd(II) < Pt(II). These values are 2.795, 2.841, and 2.932 Å for Ni(II), Pd(II), and Pt(II), respectively. This order is expected as the van der Waals radius increases in the order Ni(II) < Pd(II) < Pt(II).[10] In contrast to the structures of **5** and **6**, there is no readily apparent relationship between the M···H distance and the N_α–X_β–C_γ–C_δ torsion angle (ψ). However, the M···H distance generally increases with the decrease of the M···H–C angle (Figure 4.6) as observed for **5** and **6**. On the other hand, the scattergram of ψ against M···H distance shows the prevailing trend of long M···H distances for large ψ values (Figure 4.6). In other words, the M···H–C interaction becomes more T-shaped with the increase of the M···H distance.

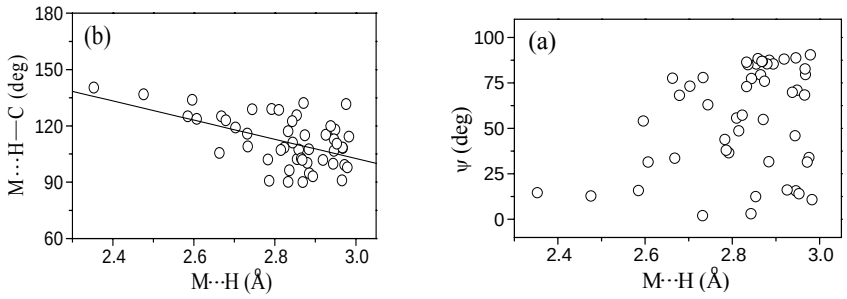

(**a**) (**b**)

Fig. 4.6. Scattergrams of (a) Ni···H–C angle versus Ni···H distance and (b) ψ (see text for definition) versus Ni···H distance. The straight line in (a) represents the least-squares fit.

4.4.7. Computational results

DFT calculations have been performed for structural optimizations of **5** and **6**. Each of the two complex molecules was computed as a complete system to consider all steric and electronic factors of the tridentate ligand ($bhac^{2-}$ or $ahac^{2-}$) and of the monodentate ancillary ligand 2-phenyl-imidazole (phim). In both cases, the atomic coordinates of the molecules obtained in the crystal structures were used as the starting points and references for geometry optimization. In the case of **5**, the overall conformation of the molecule in the optimized structure is in qualitatively good agreement with the experimental structure. The calculated Ni···H distance, Ni···H–C angle, the twisting of phim (ψ), and the orthogonality (θ) between the imidazole ring plane and the two chelate ring planes are in good agreement with the corresponding values found in the X-ray structure (Table 4.3). The only major difference between the optimized and the experimental structures is in the dihedral angle between the phenyl ring plane and the plane containing rest of the atoms in $bhac^{2-}$. In the optimized structure, the whole tridentate ligand is essentially planar. It may be noted that the X-ray structure of **5** shows an intramolecular C–H···π interaction between the phenyl ring of $bhac^{2-}$ and that of phim (*vide supra*). It is very likely that this interaction is responsible for the non-planarity of $bhac^{2-}$ in the experimental structure. In the present level of calculation we could not reproduce the C–H···π interaction in the optimized geometry.

The same optimized structure is obtained from the X-ray structural coordinates of the four molecules present in the asymmetric unit of **6**. However, the conformation of the optimized molecule is not exactly identical with that of any of the four starting molecular structures of **6**. In general, the Ni···H distances are significantly shorter, the Ni···H–C angles are more obtuse, the twisting of phim (ψ) is much less, and the imidazole ring plane and the two chelate ring planes are more orthogonal (θ) in the experimental structures than those in the optimised structure (Table 4.3). Not surprisingly the optimized molecule of **6** is very similar with that of **5** with respect to the

Ni···H distances, Ni···H–C angles, ψ- and θ-values (Table 4.3). Thus the Ni···H–C interaction in the optimised structures is close to the T-shape while it is more linear in the experimental structures.

The dependence of the conformational energies of **5** and **6** on the twisting (ψ) of phim has been analyzed by performing single point energy calculations by varying ψ from 0^0 to 90^0. The experimental structures of **5** and molecule 2 of **6** are used for these calculations. The relative energies (ΔE) with respect to the lowest energy (at ψ ~35^o for **5** and ~30^o for **6**) are plotted against the ψ values (Figure 4.7). For **5** it is a well shaped plot. On the other hand, for **6** below 30^o the change in energy is very low compared to that above 30^o. The energy increases by only 0.40 kcal/mole due to the gradual decrease of ψ form 30^o to 0^o. This small increase of energy possibly indicates the absence of any significant steric or electronic constraint for the twisting of the phim in this range of ψ. Most probably due to this reason four molecules with ψ values in the range 1.6–21.6^o have been found in the asymmetric unit of **6**.

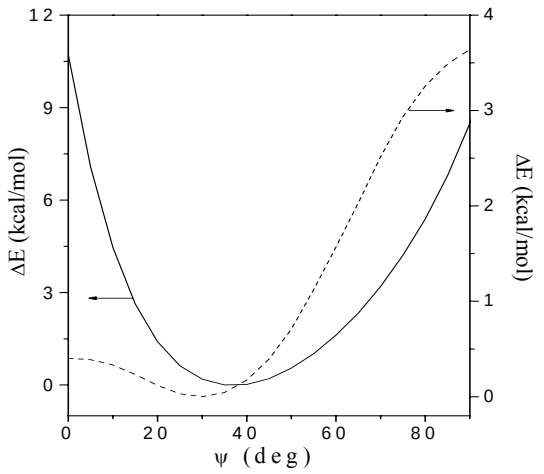

Fig. 4.7. Relative energies of **5** (—) and **6** (----) as a function of twist angles (ψ) of 2-phenyl-imidazole (phim).

For further understanding of the Ni···H–C interaction we have examined the nature of the highest occupied molecular orbital (HOMO) in both **5** and **6**. The experimental structures of **5** and molecule 2 of **6** are used for this purpose. The drawings are presented in Figure 4.8. In both cases, the HOMO is constituted by mainly the metal d-orbitals and also by the p-orbitals of the coordinated amide- and enolate-O atoms. The electron density localised in the vicinity of the metal centre (primarily on metal d_{z2} orbital) is underneath an *ortho* C–H of the phim phenyl ring. The other metal orbital which can overlap with the C–H σ-electron density is p_z. However it is at higher energy in each of the two cases. Thus these drawings highlight the predominantly hydrogen bond or three-centre four-electron nature of the Ni···H–C interaction in both **5** and **6.**

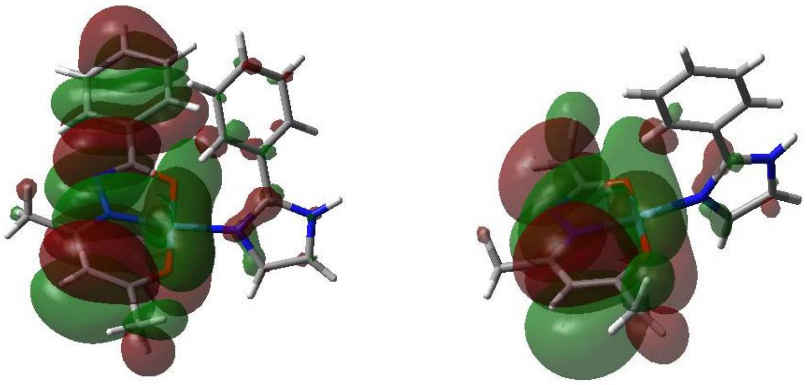

(**a**) (**b**)

Fig. 4.8. Highest occupied molecular orbitals (HOMO) in (a) **5** and (b) **6**.

4.4.8. Proton NMR studies

The NMR is an useful tool for the diagnosis of the agostic or hydrogen bond character of an apical M···H–C interaction in square-planar d^8 metal ion complexes. The proton resonance shifts to up-field for agostic interaction while it shifts to down-field for hydrogen bond interaction, compared to the free C–H.[9,11,38] The room temperature proton NMR spectra were recorded using $(CD_3)_2CO$ solutions of **5** and **6**. The protons of the two methyl groups of the acetylacetone fragment in **5** appear as two singlets at 1.47 and 2.20 δ. The singlet observed at 5.07 δ is assigned to the –CH= group. The imidazole N–H proton resonates as a doublet at 8.87 δ (J = 8 Hz). The multiplet observed in the range 7.2–7.6 δ is likely to be due to the imidazole ring C–H and aromatic protons. The absence of any cross-coupled peak in the 2D NMR spectrum of **5** indicates that the C–H···π interaction is probably absent in the solution state. In addition to all the above signals a broad singlet is observed at 12.07 δ. This down-field signal is attributed to the phim phenyl ring *ortho* C–H proton which is proximal to the metal centre. It may be noted that the free phim or the Schiff bases do not show any resonance in this region. The protons of the three methyl groups of $ahac^{2-}$ in **6** are observed as three singlets at 2.01, 2.11, and 2.27 δ. The proton of the –CH= group in the acetylacetone fragment resonates as a singlet at 5.51 δ. A broad singlet at 8.89 δ is assigned to the imidazole N–H proton. As observed for **5** the signal due to the phim phenyl ring *ortho* C–H proton close to the apical site of the metal centre shifts to down-field (11.63 δ) and appears as a broad singlet. The multiplet in the range 7.1–7.8 δ corresponds to the imidazole ring C–H and rest of the aromatic protons in the molecule.

We have recorded the spectra of both **5** and **6** in the temperature range 20 to -80^{o} C and monitored the broad singlet observed at 12.07 and 11.63 δ for **5** and **6**, respectively. In each case, the signal becomes sharper and it is shifted to further down-field on cooling (Figure 4.9). The extent of shift in the said temperature range is 0.75 and 0.90 δ for **5** and **6**, respectively. The

observation of the down-field signal and its behavior with lowering of temperature suggest that the Ni···H–C interaction present in the solid state structures of both **5** and **6** is also present in solution and it is essentially hydrogen bond in character.

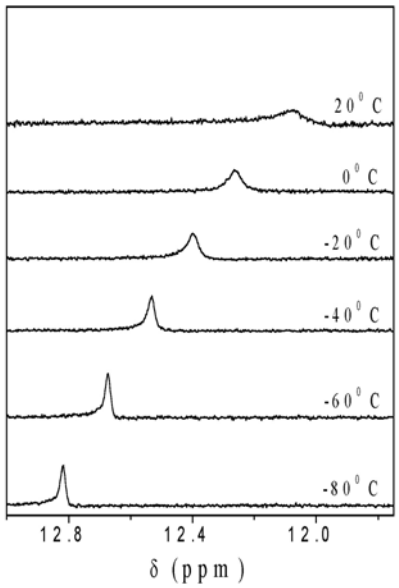

Fig. 4.9. Temperature dependence of the down-field signal in the proton NMR spectrum of **5**.

4.5. Conclusion

The tridentate O,N,O-donor benzoyl- and acetylhydrazone of acetylacetone (H_2bhac and H_2ahac) and monodentate 2-phenyl-imidazole (phim) yielded mononuclear square-planar mixed ligand nickel(II) complexes [Ni(bhac)(phim)] (**5**) and [Ni(ahac)(phim)] (**6**). X-ray crystal structures reveal that the asymmetric unit of **5** contains a single molecule while that of **6** contains four molecules having different conformations. The conformation of **5** is significantly different compared to that of any of the four molecules of **6**.

Perhaps the intramolecular C–H···π interaction present in **5** is responsible for this difference. In both **5** and **6**, the proton of one of the two *ortho* C–H groups of the phim phenyl ring is very close to the metal centre at the apical site suggesting an intramolecular Ni···H–C interaction. The shape of the Ni···H–C interaction and hence the Ni···H distance and the Ni···H–C angle depend on the twisting (ψ) of the phim and the extent of the orthogonality (θ) between the {Ni(ONO)} and the imidazole planes. The observed trends are compared with the structures of similar species reported in literature. Theoretically optimized structures of both **5** and **6** are very similar and they are very close to the experimental structure of **5**. Energy calculations by varying ψ from 0 to 90° for both **5** and **6** have been performed. The conformer of **5** having ψ value about 35° (experimental ψ = 35.8°) is at the lowest energy and the plot of relative energies (ΔE) of various conformers against ψ provides a reasonably symmetric well shaped curve. For **6** the lowest energy molecule has ψ value ~30°. However the energy change is very little below ψ = 30°. This observation explains the presence of four molecules having ψ in the range 1.6–21.6° in the asymmetric unit of **6**. The nature of the highest occupied MO suggests hydrogen bond description of the Ni···H–C interaction in both **5** and **6** is more appropriate. In the NMR spectra of **5** and **6**, the appearance of this proton at down-field and further down-field shift due to lowering of temperature substantiates the hydrogen bond character of this interaction.

4.6. References

1. M. Brookhart and M. L. H. Green, *J. Organomet. Chem.*, 1983, **250**, 395.
2. J.-Y. Saillard and R. J. Hoffman, *J. Am. Chem. Soc.*, 1984, **106**, 2006.
3. M. Brookhart, M. L. H. Green and L. L. Wong, *Prog. Inorg. Chem.*, 1988, **36**, 1.
4. R. H. Crabtree and D. G. Hamilton, *Adv. Organomet. Chem.*, 1988, **28**, 299.
5. A. D. Ryabov, *Chem. Rev.*, 1990, **90**, 403.
6. R. H. Crabtree, *Angew. Chem., Int. Ed. Engl.*, 1993, **32**, 789.

7. A. J. Canty and G. van Koten, *Acc. Chem. Res.*, 1995, **28**, 406.
8. D. Braga, F. Grepioni, E. Tedesco, K. Biradha and G. R. Desiraju, *Organometallics*, 1997, **16**, 1846.
9. W. Yao, O. Eisenstein and R. H. Crabtree, *Inorg. Chim. Acta.*, 1997, **254**, 105.
10. T. W. Hambley, *Inorg. Chem.*, 1998, **37**, 3767.
11. M. J. Calhorda, *Chem. Commun.*, 2000, 801.
12. L. Brammer, *Dalton Trans.*, 2003, 3145.
13. A. Albinati, P. S. Pregosin and F. Wombacher, *Inorg. Chem.*, 1990, **29**, 1812.
14. M. Bortolin, U. E. Bucher, H. Rüegger, L. M. Venanzi, A. Albinati, F. Lianza and S. Trofimenko, *Organometallics*, 1992**, 11**, 2514.
15. T. Hascall, M.-H. Baik, B. M. Bridgewater, J. H. Shin, D. G. Churchill, R. A. Friesner and G. Parkin, C*hem. Commun.*, 2002, 2644.
16. N. R. Sangeetha, C. K. Pal, P. Ghosh and S. Pal, *J. Chem. Soc.*, *Dalton Trans.*, 1996, 3293.
17. *SMART* V5.630 and *SAINT-plus* V6.45, Bruker-Nonius Analytical X-ray Systems Inc.: Madison, WI, USA, 2003.
18. G. M. Sheldrick, *SADABS*, Empirical Absorption Correction Program, University of Göttingen, Göttingen, Germany, 1997.
19. G. M. Sheldrick, *SHELX-97*, *Structure Determination Software*, University of Göttingen, Göttingen, Germany, 1997.
20. L. J. Farrugia, *J. Appl. Crystallogr.*, 1999, **32**, 837.
21. P. McArdle, *J. Appl. Crystallogr.*, 1995, **28**, 65.
22. A. L. Spek, *PLATON*, *A Multipurpose Crystallographic Tool*, Utrecht University, Utrecht, The Netherlands, 2002.
23. A. D. Becke, *J. Chem. Phys.*, 1993, **98**, 5648.
24. C. Lee, W. Yang and R. G. Parr, *Phys. Rev. B.*, 1988, **37**, 785.
25. T. H. Dunning Jr., and P. J. Hay, In *Modern Theoretical Chemistry*; Schaefer, H. F. III, Ed.; Plenum: New York, 1976; pp. 1–28.
26. M. J. Frisch et al, *Gaussian03 Revision B05*, Gaussian Inc., Pittsburgh, PA, 2004.
27. W. Kemp, In *Organic Spectroscopy*; Macmillan: Hampshire, 1987; pp. 62–66.

28. K. Nakamoto, In *Infrared and Raman Spectra of Inorganic and Coordination Compounds*; Wiley: New York, 1986; pp. 241–242.
29. S. Das and S. Pal, *J. Organomet. Chem.*, 2004, **689**, 352.
30. A. la Cour, M. Findeisen, R. Hazell, L. Hennig, C. E. Olsen and O. J. Simonsen, *J. Chem. Soc.*, *Dalton Trans.*, 1996, 3437.
31. S. G. Sreerama and S. Pal, *Eur. J. Inorg. Chem.*, 2004, 4718.
32. S. Das, G. P. Muthukumaragopal, S. N. Pal and S. Pal, *New J. Chem.*, 2003, **27**, 1102.
33. S. Das and S. Pal, *J. Mol. Struct.*, 2005, **741**, 183.
34. A. Mukhopadhyay, G. Padmaja, S. N. Pal and S. Pal, *Inorg. Chem. Commun.*, 2003, **6**, 381.
35. A. Mukhopadhyay and S. Pal, *Polyhedron*, 2004, ***23***, 1997.
36. G. V. Karunakar, N. R. Sangeetha, V. Susila and S. Pal, *J. Coord. Chem.*, 2000**,** **50**, 51.
37. D. R. Trivedi, A. Ballabh and P. Dastidar, *Cryst. Eng. Commun.*, 2003, **5**, 358.
38. A. J. Canty and G. van Koten, *Acc. Chem. Res.*, 1995, **28**, 406.

Chapter 5

Square−planar complexes of nickel with a non−innocent tetradentate ligand system[§]

5.1. Abstract

The condensation of acetylacetone with benzoylhydrazine in 1:2 mole ratio in methanol to prepare acetylacetone bis(benzoylhydrazone) (H_3L_1) resulted in the formation of the cyclized product 1-benzoyl-3,5-dimethyl-5-(1'-benzoyl-hydrazido)pyrazoline (**7**). The pyrazoline structure has been confirmed by X-ray crystallography. Treatment of this pyrazoline with $Ni(O_2CCH_3)_2{\cdot}4H_2O$ in 1:1 mole ratio in boiling methanol results into the pyrazoline ring opening and formation of a hydrated nickel(II) complex of formula $[Ni(HL_1)]{\cdot}H_2O$ (**8**). We have attempted to synthesize the analogous nickel(II) complexes with pyrazolines derived from in-situ condensation reactions of acetylacetone and 4-R-benzoylhydrazines (R = OMe and NMe_2). We have been able to isolate $[Ni(HL_2)]$ (**9**, where R = OMe). But in the case of R = NMe_2 the analogous nickel(II) species could not be isolated. However, in all the cases if the reaction mixtures were stirred in air at rom temperature for ~5 h, dinuclear species, $[NiL_1{-}L_1Ni]$ (**10**), $[NiL_2{-}L_2Ni]$ (**11**) and $[NiL_3{-}L_3Ni]$ (**12**, where R = NMe_2) were obtained. Here $(L_n\text{-}L_n)^{6-}$ represents the dinucleating ligand formed by oxidative C−C coupling involving the methine C−atom of the monomeric analog. The magnetic moments of **10**, **11**, and **12** indicate $S = 1/2$ spin state of each metal center in these dinuclear complexes. However, the EPR spectral features indicate that these species are in the borderline between genuine nickel(III) species and nickel(II) stabilized ligand radical systems. In wet dichloromethane–hexane mixture under aerobic condition each of **10**, **11** and **12** forms mononuclear nickel(II) complexes of general formula $[Ni(L_nO)]$ (**13** (n=1), **14** (n=2) and **15** (n=3)), where L_nO^{2-} is a tetradentate ligand formed from $(L_n{-}L_n)^{6-}$ by C−C bond cleavage accompanied by oxidation to keto

[§] A part of this work has been published in *Polyhedron*, 2003, **6**, 381.

group. All the complexes have been characterized by analytical, magnetic and various spectroscopic measurements. Moreover structures of **8**, **9**, **12-15** have been determined by X-ray crystallography.

5.2. Introduction

The chemistry of trivalent nickel complexes has been the subject of considerable interest due to the important roles played by nickel(III) in catalytic and biological processes.[1-4] The deprotonated amide functionality has been proved to be very effective in stabilizing nickel(III).[5] Several grossly planar nickel(III) complexes are available in literature with this kind of ligands. Schiff bases derived from semicarbazides/acyl- or aroylhydrazines and acetylacetone contain this high oxidation state promoting amide functionality as well as a non-innocent ligand framework.

In the last two chapters, square−planar nickel(II) complexes with the tridentate enolate-O, imine-N and deprotonated amide-O donor $bhac^{2-}$ and monodentate heterocycles have been described. Introduction of one more aroylhydrazine moiety to the framework of the tridentate Schiff base H_2bhac should provide a tetradentate Schiff base (H_3L_n). In principle this Schiff base has three dissociable protons (two amide protons and one –NH-proton) (Scheme 1). Thus the tetradentate ligand can be dianionic (HL_n^{2-}) and also trianionic (L_n^{3-}). In our attempt to prepare this Schiff base from one mole equivalent of acetylacetone and two mole equivalent of benzoylhydrazine, we have isolated a substituted pyrazoline compound (Scheme 1). Reactions of this substituted pyrazoline and other pyrazolines prepared in situ from acetylacetone and 4-R-benzoylhydraines (in 1:2 mole ratio) with $Ni(O_2CCH_3)_2{\cdot}4H_2O$ causes ring opening and the formation of the square−planar nickel(II) complexes of formula [$Ni(HL_n)$] of the desired tetradentate ligand system. Prolonged exposure to air causes oxidation of these complexes and dinuclear species having the formula [$NiL_n{-}L_nNi$] have been isolated. The formal oxidation state of the metal centers in these complexes is

+3. $(L_n{-}L_n)^{6-}$ represents the ligand formed by oxidative C−C bond formation between two L_n^{3-} (Scheme I). In presence of moisture these dinuclear species form mononuclear nickel(II) species, $[NiL_nO]$, where the ligand L_nO^{2-} is generated by the cleavage of the C−C bridge in $(L_n{-}L_n)^{6-}$ with the formation of a keto group. In the following sections, we have described the syntheses, physical properties and structures of these nickel complexes in details.

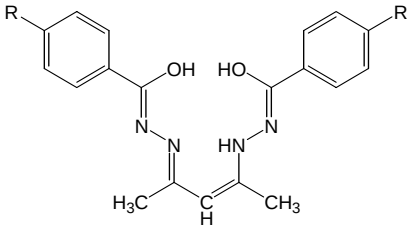

H_3L_n
(n = 1, R = H; n = 2, R = OMe;
n = 3, R = NMe_2)

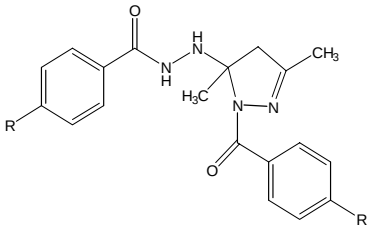

Substituted pyrazoline

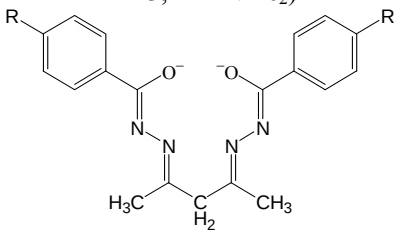

HL_n^{2-}

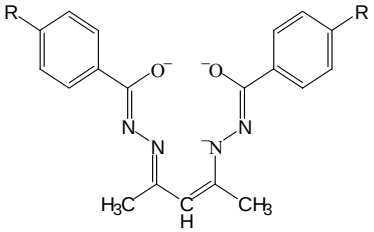

L_n^{3-}

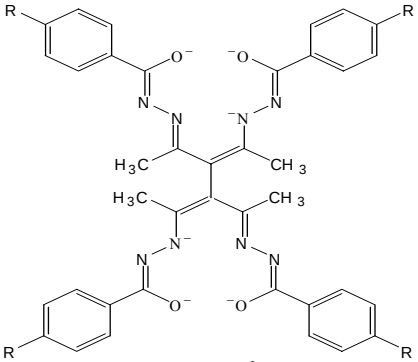

$(L_n{-}L_n)^{6-}$

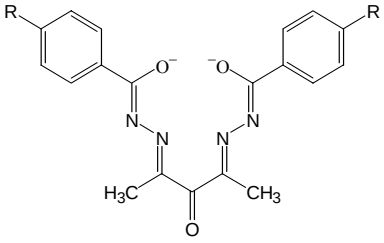

L_nO^{2-}

Scheme 1

5.3. Experimental

5.3.1. Materials

All the chemicals and the solvents used in this work were of analytical grade, available commercially and were used without further purification.

5.3.2. Physical measurements

Microanalytical (C, H, N) data were obtained with a Thermo Finnigon Flash EA1112 series elemental analyzer. Infrared spectra were collected by using KBr pellets on a Jasco5300 FT-IR spectrophotometer. Solution electrical conductivities were measured with a Digisun DI-909 conductivity meter. Room temperature (300 K) solid state magnetic susceptibilities were measured by using a Sherwood Scientific magnetic susceptibility balance. $Hg[Co(NCS)_4]$ was used as the standard. A SQUID magnetometer was used for the magnetic susceptibilities of $[NiL_1{-}L_1Ni]$ in the temperature range 2 – 300 K. Diamagnetic corrections calculated from Pascal's constants,[6] were used to obtain the molar paramagnetic susceptibilities. EPR spectra were recorded on a Jeol JES-FA200 spectrometer. A Shimadzu 3101-PC UV/Vis/NIR spectrophotometer was used to record the electronic absorption spectra. Proton NMR spectra were recorded on a Bruker 200 MHz spectrometer using $Si(CH_3)_4$ as an internal standard.

5.3.3. Synthesis of the compounds

1-benzoyl-3,5-dimethyl-5-(10-benzoyl-hydrazido)pyrazoline (**7**)

To a methanol solution (25 ml) of benzoylhydrazine (545 mg, 4 mmol) 0.21 ml of acetylacetone (205 mg, 2.05 mmol) was added. The mixture was refluxed for 6 h followed by evaporation to about 1/5th of the original volume on a rotary evaporator. It was then cooled to room temperature. The white solid thus obtained was collected by filtration and recrystallized from methanol. Yield, 430 mg (64%). A single crystal suitable for X-ray structure determination was selected from this material. Anal. Calc. for $C_{19}H_{20}N_4O_2$: C,

67.84; H, 5.99; N, 16.65. Found: C, 67.55; H, 5.82; N, 16.53%. Selected IR bands (cm^{-1}): 3277(s), 1659(s), 1605(s), 1572(m), 1537(m), 1489(w), 1456(s), 1427(s), 1375(s), 1329(s), 1306(m), 1134(m), 1105(m), 1061(w), 1026(m), 993(m), 934(w), 910(s), 862(s), 789(s), 708(s), 638(w), 488(m). ^{1}H NMR (200 MHz) data in CD_3OD (d): 1.88 (s, 3H, 5-CH3); 1.98 (s, 3H, 3-CH3); 2.90 and 3.22 (2H, CH_AH_B, J_{AB} = 18 Hz); 5.30 (s, 1H, 5-NH); 7.38–7.50 (m, 6H, aromatic protons); 7.73–7.84 (m, 4H, aromatic protons); 8.27 (s, 1H, NHNH).

[Ni(HL$_1$)] (**8**)

To a methanol solution (20 ml) of **7** (572 mg, 1.7 mmol) a methanol solution (20 ml) of $Ni(O_2CCH_3)_2{\cdot}4H_2O$ (425 mg, 1.7 mmol) was added drop wise over a period of 5 min. with stirring in air. The mixture was refluxed for one hour. The brown crystalline solid that precipitated was collected by filtration, washed thoroughly with methanol and dried in vacuum over anhydrous $CaCl_2$. Yield, 466 mg (70%). Selected IR bands (cm^{-1}): 2829(w), 1649(m), 1601(s), 1511(m), 1463(m), 1253(s), 1150(s), 849(s), 771(s), 675(m), 511(w).

[Ni(HL$_2$)] (**9**)

This compound was synthesized by following the same procedure as described for **8**, except that the pyrazoline was prepared in situ from acetylacetone and 4-methoxy-benzoylhydrazine (1:2 mole ratio). Yield, 451 mg (65%). Selected IR bands (cm^{-1}): 2820(w), 1643(m), 1604(s), 1508(m), 1458(m), 1371(s), 1249(s), 1167(s), 1028(s), 842(s), 752(s), 682(m), 652(m), 511(w).

[NiL$_1$-L$_1$Ni] (**10**)

To a methanol solution (20 ml) of **7** (572 mg,1.7 mmol) a methanol solution (20 ml) of $Ni(O_2CCH_3)_2{\cdot}4H_2O$ (425 mg, 1.7 mmol) was added drop wise over a period of 5 min. with stirring in air. The mixture was stirred in air

for 5 h. The green solid that precipitated was collected by filtration, washed thoroughly with methanol and dried in vacuum over anhydrous $CaCl_2$. Yield, 500 mg (75%). Selected IR bands (cm^{-1}): 1632(m), 1597(m), 1539(w), 1472(s), 1412(s), 1379(s), 1279(m), 1215(w), 1171(m), 1117(w), 1086(s), 1009(s), 920(s), 880(s), 787(m), 731(m), 698(s), 534(w).

[NiL_2-L_2Ni] (11)

This compound was synthesized by following the same method as described for **10**, except that the pyrazoline was prepared in situ from acetylacetone and 4-methoxy-benzoylhydrazine (1:2 mole ratio). 530 mg (72%). Selected IR bands (cm^{-1}): 1641(m), 1601(s), 1554(w), 1456(m), 1361(s), 1267(m), 1186(s), 1089(m), 1020(m), 1020(m), 933(m), 821(m), 752(s), 692(m).

[NiL_3-L_3Ni] (12)

This compound was also prepared by following the same procedure as described for **11**. Yield, 560 mg (81%). Selected IR bands (cm^{-1}): 1640(w), 1599(s), 1554(w), 1456(m), 1361(s), 1269(m), 1186(s), 1091(m), 1014(m), 929(m), 752(s)

[$Ni(L_1O)$] (13)

[NiL_1-L_1Ni] (**10**) (100 mg, 0.25 mmol) was dissolved in 25 ml of dichloromethane–acetonitrile (1:1) mixture and left in air at room temperature for slow evaporation. The initial green colour of the solution slowly became brown and in about 4–5 days a brown crystalline solid separated. The complex was collected by filtration and dried in air. Yield, 30 mg (29%). A single crystal suitable for X-ray structure determination was selected from this material. Selected IR bands (cm^{-1}): 1649(m), 1591(m), 1541(s), 1491(m), 1443(w), 1368(s), 1242(w), 1208(w), 1169(m), 1138(w), 1067(w), 1026(m), 955(w), 924(w), 870(w), 787(w), 700(s), 599(m), 474(w).

[Ni(L_2O)] (14)

This compound was prepared from **11** by following the same procedure as described for **13**. Yield, 20 mg (21%). Selected IR bands (cm^{-1}): 1647(m), 1604(m), 1556(m), 1508(s), 1458(m), 1373(s), 1249(s), 1208(w), 1167(m), 1028(m), 842(m), 752(w), 682(w).

[Ni(L_3O)] (15)

This compound was synthesized from **12** by following the same procedure as described for **13**. Yield, 25 mg (20%). Selected IR bands (cm^{-1}): 1649(m), 1591(m), 1541(s), 1491(m), 1443(w), 1368(s), 1242(w), 1208(w), 1169(m), 1138(w), 1067(w), 1026(m), 955(w), 924(w), 870(w), 787(w), 700(s), 599(m), 474(w).

5.3.4. X-ray crystallography

The data for the crystals of **7** and **13** were collected on an Enraf-Nonius Mach-3 single crystal diffractometer using graphite monochromated Mo Kα radiation (λ = 0.71073 Å) by ω-scan method at 298 K. In each case, the ψ-scans of selected reflections were used for an empirical absorption correction. The programs of the WinGX[7] package were used for data reduction and absorption correction. Unit cell parameters and the intensity data for each of **8**, **9**, **11**, **14** and **15** were obtained on a Bruker-Nonius SMART APEX CCD single crystal diffractometer, equipped with a graphite monochromator and a Mo Kα fine-focus sealed tube (λ = 0.71073 Å) operated at 2.0 kW. The detector was placed at a distance of 6.0 cm from the crystal. Data were collected at 100 K with a scan width of 0.3º in ω and an exposure time of 30 sec/frame. The SMART software was used for data acquisition and the SAINT-Plus software was used for data extraction.[8] An absorption correction was performed with the help of SADABS program.[9] In each case, the structure was solved by direct methods and refined on F^2 by full-matrix least-squares procedures. All non-hydrogen atoms were refined anisotropically. In the case

of **8**·H_2O, the protons of the water molecule were located in the difference map and refined with $U_{iso}(H) = 1.5U_{eq}(O)$. Other hydrogen atoms in all the structures were included in the structure factor calculation at idealized positions by using a riding model. The SHELX-97[10] programs were used for structure solution and refinement. The ORTEX6a[11] and Platon[12] packages were used for molecular graphics. Significant crystallographic data for all the structures are summarized in Tables 5.1 and 5.2.

Table 5.1. Crystallographic data for **7**, **8·H_2O** and **9**

Compound	**7**	**8·H_2O**	**9**
Empirical formula	$C_{19}H_{20}N_4O_3$	$C_{19}H_{21}N_4O_3Ni$	$C_{21}H_{22}N_4O_4Ni$
Formula weight	336.39	412.11	453.14
Crystal system	Orthorhombic	Orthorhombic	Monoclinic
Space group	*Pbca*	*Ccca*	$P2_1/c$
a/Å	10.287(2)	20.719(2)	7.7101(7)
b/Å	12.667(3)	23.480(2)	11.9373(10)
c/Å	27.550(6)	7.5740(7)	21.2125(18)
α/°	90	90	90
β/°	90	90	93.0520(10)
γ/°	90	90	90
V/Å^3	3590.2(15)	3684.6(6)	1949.6(3)
Z	8	8	4
μ/mm^{-1}	0.083	1.081	1.033
Reflections collected	4645	7182	19748
Unique reflections	4124	1215	3827
Reflections [$I \geq 2\sigma(I)$]	1943	989	3382
Parameters	236	127	359
R1,[a] wR2[b] [$I \geq 2\sigma(I)$]	0.0489, 0.0963	0.0412, 0.0980	0.0304, 0.0762
*R*1,[a] *wR*2[b] (all data)	0.1448, 0.1258	0.0513, 0.1034	0.0355, 0.0793
GOF[c] on F^2	1.003	1.070	1.069
Largest peak, hole/ e Å^{-3}	0.166, -0.189	0.760, -0.358	0.258, -0.371

[a] $R1 = \sum||F_o| - |F_c||/\sum|F_o|$. [b] $wR2 = \{\sum[(F_o^2 - F_c^2)^2]/\sum[w(F_o^2)^2]\}^{1/2}$.
[c] GOF = $\{\sum[w(F_o^2 - F_c^2)^2]/(n - p)\}^{1/2}$ where 'n' is the number of reflections and 'p' is the number of parameters refined.

Table 5.2. Crystallographic data for **12·$(CH_3)_2CO$**, **13**, **14** and **15·$CHCl_3$**

Compound	**12·$(CH_3)_2CO$**	**13**	**14**	**15·$CHCl_3$**
Empirical formula	$C_{49}H_{58}N_{12}O_5Ni_2$	$C_{19}H_{16}N_4O_3Ni$	$C_{21}H_{20}N_4O_5Ni$	$C_{24}H_{27}Cl_3N_6O_3Ni$
Formula weight	1012.49	407.07	467.12	612.57
Crystal system	Monoclinic	Triclinic	Monoclinic	Monoclinic
Space group	$P2_1/c$	$P\bar{1}$	$P2_1/n$	$P2_1/n$
a/Å	15.084(3)	7.5030(11)	7.9947(15)	17.2579(12)
b/Å	24.334(5)	11.1159(12)	16.915(3)	7.8024(5)
c/Å	14.952(3)	11.605(2)	14.735(3)	21.1395(14)
α/°	90	106.857(13)	90	90
β/°	118.669(3)	99.946(9)	93.714(4)	102.1760(10)
γ/°	90	102.851(13)	90	90
V/Å^3	4815.4(16)	873.4(2)	1988.4(6)	2782.5(3)
Z	4	2	4	4
(/mm(1	0.842	1.139	1.019	1.022
Reflections collected	36566	3453	18891	27836
Unique reflections	6299	3186	3511	5457
Reflections [$I \geq 2\sigma(I)$]	2419	2656	2290	4395
Parameters	627	244	360	442
R1,[a] wR2[b] [$I \geq 2\sigma(I)$]	0.0797, 0.1373	0.0387, 0.0959	0.0635, 0.1069	0.0487, 0.1444
R1,[a] wR2[b] (all data)	0.2217, 0.1909	0.0556, 0.1031	0.1076, 0.1224	0.0596, 0.1592
GOFc on F2	0.976	1.072	1.058	0.947
Largest peak, hole/ e Å^{-3}	0.288, -0.349	0.784, -0.405	0.462, -0.276	0.563, -0.421

[a] $R1 = \sum||F_o| - |F_c||/\sum|F_o|$. [b] $wR2 = \{\sum[(F_o^2 - F_c^2)^2]/\sum[w(F_o^2)^2]\}^{1/2}$.
[c] GOF = $\{\sum[w(F_o^2 - F_c^2)^2]/(n - p)\}^{1/2}$ where 'n' is the number of reflections and 'p' is the number of parameters refined.

5.4. Results and discussion

5.4.1. Synthesis and reactivity

To prepare the Schiff bases H_3L_1, H_3L_2 and H_3L_3 we have reacted one mole equivalent of acetylacetone and two mole equivalents of benzoylhydrazine, 4-methoxy−benzoylhydrazine and 4-N,N-dimethylamino−benzoylhydrazine in methanol, respectively. It is known that this type of reaction leads to cyclized 3,5-substituted pyrazoline.[13-15] This cyclized product undergoes a metal mediated ring opening reaction to form the N_2O_2−donor tetradentate ligand that can accommodate a metal ion in a square planar geometry. We have isolated the pyrazoline product (**7**) instead of the Schiff base H_3L_1. This compound (**7**) has been characterized by X-ray crystallography. ^{1}H NMR spectral features suggest the formation of 3,5-substituted pyrazolines in the other two cases also.

Reations of $Ni(O_2CCH_3)_2{\cdot}4H_2O$ with these pyrazolines over a period of 1 h in boiling methanol produced the brown crystalline square planar nickel(II) complexes $[Ni(HL_1)]$ (**8**) and $[Ni(HL_2)]$ (**9**). However, we could not isolate $[Ni(HL_3)]$. The elemental analysis data are consistent with the molecular formulae proposed for **8** and **9**. These complexes are diamagnetic and non-conducting in CH_2Cl_2 solution. Interestingly the stirring of the pyrazolines with $[Ni(O_2CCH_3)_2]{\cdot}4H_2O$ for 5 h in methanol under aerobic conditions produced paramagnetic green (when R = H and OMe) and purple ($R = NMe_2$) solids. The elemental analysis and other properties (vide infra) of these complexes suggest their formulae as $[NiL_n{-}L_nNi]$ (**10** (n=1), **11** (n=2) and **12** (n=3)). Here $(L_n{-}L_n)^{6-}$ represents a dinucleating ligand formed by C−C coupling between two L_n^{3-} ligands. Despite of our several attempts we could grow single crystals of **12** only. Furthermore when complexes **8** and **9** were stirred with an excess of H_2O_2 they produced the same paramagnetic green complexes **10** and **11 (**almost quantitatively), respectively.

In dichloromethane−hexane mixture under wet condition, the C−C bridge in $(L_n{-}L_n)^{6-}$ is cleaved for all the complexes (**10**, **11** and **12**) with the

formation of keto group leading to a new series of diamagnetic nickel(II) complexes with general formula [Ni(L_nO)] (**13** (n=1), **14** (n=2) and **15** (n=3)). The molecular structures of **13**, **14** and **15** were further confirmed by X-Ray crystallography.

5.4.2. Characterization of 7

Reaction of 1 mole equivalent of acetylacetone with 2 mole equivalents of benzoylhydrazine in methanol produced a white product in good yield. The elemental analysis data for this compound are consistent with the formula $C_{19}H_{20}N_4O_2$ for the desired acetylacetone bis(benzoylhydrazone) (H_3L_1). However, as it is known that this type of reaction leads to cyclized 3,5-substituted pyrazolines, we have determined the molecular structure of **7** by single crystal X-ray crystallography. The structure obtained confirms the cyclization reaction and formation of the pyrazoline derivative (Figure 5.1). Selected bond parameters are listed in Table 5.3. The intramolecular bond distances are comparable to other similar structurally characterized compounds.[14-17] The infrared spectrum of **7** shows a strong band at 3277 cm^{-1}, possibly due to the N–H groups.[18] Two strong bands observed at 1659 and 1605 cm^{-1} are assigned to the C=O and C=N stretches, respectively.[18,19] The electronic absorption spectrum of **7** in methanol solution displays three strong absorptions in the range 322–225 nm. The proton NMR spectrum of **7** in $CDCl_3$ solution is consistent with the pyrazoline structure. The 5-methyl and 3-methyl protons appear as two singlets at 1.88 and 1.98 δ, respectively. As observed in other similar compounds,[13–15,17] the methylene group protons of **7** are diastereotopic and observed as an AB type quartet centered at 3.06 δ. Each of the two N–H group protons appears as a singlet. They are observed at 5.30 and 8.27 δ. The aromatic protons appear as two multiplets centered at 7.44 and 7.78 δ.

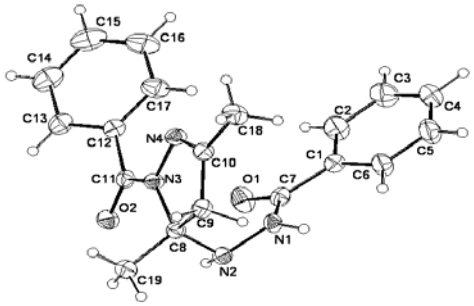

Fig. 5.1. Molecular structure of **7** with the atom labeling scheme. All non−hydrogen atoms are represented by their 40% probability thermal ellipsoids.

Table 5.3. Selected bond lengths (Å) and bond angles (°) for 7

Bond lengths			
O(1)–C(7)	1.231(2)	N(3)–N(4)	1.406(2)
O(2)–C(11)	1.233(2)	N(4)–C(10)	1.276(3)
N(1)–C(7)	1.344(3)	C(9)–C(10)	1.487(3)
N(1)–N(2)	1.414(2)	C(8)–C(9)	1.526(3)
N(2)–C(8)	1.459(3)	N(3)–C(8)	1.502(3)
N(3)–C(11)	1.355(3)	C(8)–C(18)	1.515(3)
Bond angles			
N(4)–N(3)–C(8)	112.36(15)	N(2)–C(8)–C(18)	108.02(17)
C(10)–N(4)–N(3)	107.56(17)	N(3)–C(8)–C(18)	113.46(17)
N(4)–C(10)–C(9)	114.54(18)	C(11)–N(3)–N(4)	122.19(17)
C(10)–C(9)–C(8)	103.94(17)	C(11)–N(3)–C(8)	124.50(17)
N(3)–C(8)–C(9)	99.96(16)	C(19)–C(10)–C(9)	123.54(19)
N(2)–C(8)–C(9)	110.91(16)	N(4)–C(10)–C(19)	121.9(2)

5.4.3. Self-assembly of 7

In the solid state, a one-dimensional assembly of **7**, is formed *via* intermolecular N−H···O hydrogen bonding (Figure 5.2). The oxygen atom (O2) of the benzoyl group attached to N3 and one of the hydrazide protons of the benzoylhydrazide group attached to C3 (Figure 5.1) are involved in this

hydrogen bonding. The N1···O2 distance and N1−H···O2 angle are 2.871(2) Å and 160.0(2)º, respectively.

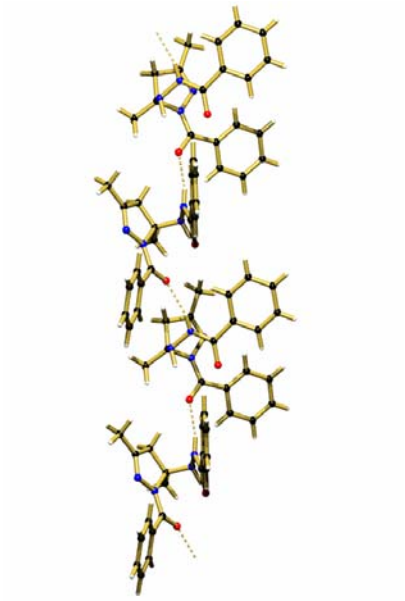

Fig. 5.2. One-dimensional ordering of **7** *via* N-H···O interactions.

5.4.4. Spectroscopic properties of [Ni(HL_n)] (8 and 9)

In the infrared spectra of **8** and **9** there are no bands that could be attributed to an N-H group or a C=O group. The absence of N-H and C=O stretches and diamagnetic nature of the complexes are consistent with the ring opening of the pyrazolines and complexation of the metal ion in a square−planar fashion by the N_2O_2 donor dianionic ligands (HL_n^{2-}).

The electronic spectral profiles of **8** and **9** in CH_2Cl_2 are very similar. The spectral data are listed in Table 5.4. A weak absorption at ~540 nm is assigned to the spin-allowed ($^1A_{1g} \rightarrow {}^1A_{2g}$) transition expected for a square-planar nickel(II) complex.[19] At higher energy, two more strong bands are observed in the range 440-292 nm. These higher energy absorptions are most likely due to metal−to−ligand charge transfer and intra-ligand transitions.

Table 5.4. Electronic spectral data for **8** and **9**

Complex	λ_{max} (nm) (ε ($M^{-1}cm^{-1}$))
8	533(70), 439(1060), 380^{sh}(590), 293(18500)
9	548^{sh}(20), 430^{sh}(1030),325^{sh}(390),283^{sh}(19150),268(21710)

sh=shoulder

5.4.5. Molecular structures of 8 and 9

Complexes **8** and **9** crystallize in the orthorhombic *Ccca* and monoclinic $P2_1/c$ space groups, respectively. The molecular structure of **8** and **9** are illustrated in Figures 5.3 and 5.4, respectively. Selected bond parameters associated with the metal ions are listed in Table 5.5. The asymmetric unit of **8** contains half of a complex molecule and half of a water molecule. In both complexes, there are two five- and one six- membered chelate rings. The chelate bite angles for the five membered rings are almost similar and are smaller than that of the six membered ring. There is essentially no displacement of the nickel(II) centre from the N_2O_2 plane in both of the complexes. However the molecule **9** as a whole is not perfectly planar. One of the phenyl ring (constituted by the atoms C8 to C13) is slightly tilted from the mean plane constituted by the rest of the molecules and the other phenyl rings (constituted by the atoms C14 to C19) is almost coplanar with this mean plane. The corresponding dihedral angles are 18.56(6)º and 2.42(9)º, respectively. In contrast the molecule of **8** is almost planar with very little twist of the phenyl rings. The Ni-N(imine) bond lengths are almost identical and similarly the Ni-O(amide) bond lengths are also very similar (Table 5.5). These bond lengths are comparable with the bond lengths observed for square-planar nickel(II) complexes having imine-N or deprotonated amide-O coordinating atoms.[17,20-23]

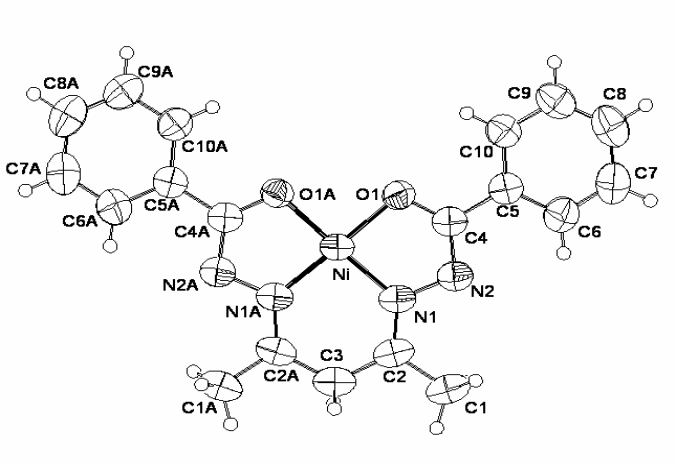

Fig. 5.3. Molecular structure of **8** with the atom labeling scheme. All non−hydrogen atoms are represented by their 40% probability thermal ellipsoids.

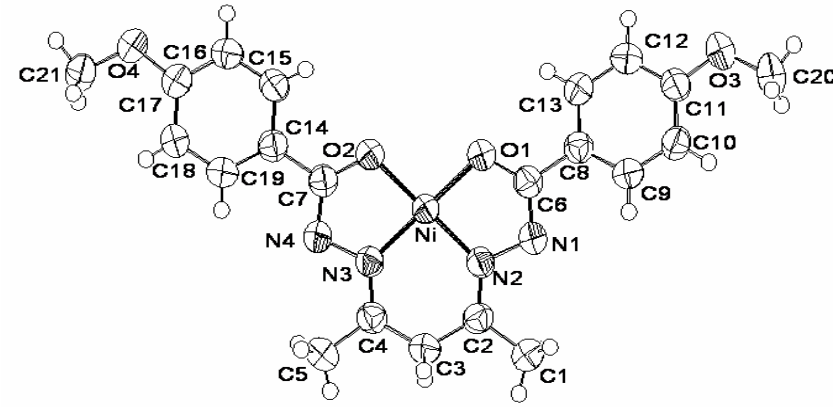

Fig. 5.4. Molecular structure of **9** with the atom labeling scheme. All non−hydrogen atoms are represented by their 40% probability thermal ellipsoids.

Table 5.5. Selected bond lengths (Å) and bond angles (°) for 8 and 9

Bond lengths			
8		**9**	
Ni(1)-N(1A)	1.828(3)	Ni(1)-N(2)	1.8342(14)
Ni(1)-N(1)	1.828(3)	Ni(1)-N(3)	1.8361(14)
Ni(1)-O(1)	1.851(2)	Ni(1)-O(1)	1.8585(12)
Ni(1)-O(1A)	1.851(2)	Ni(1)-O(2)	1.8599(12)
Bond Angles			
8		**9**	
N(1A)-Ni(1)-N(1)	96.84(19)	N(2)-Ni(1)-N(3)	96.18(6)
N(1A)-Ni(1)-O(1)	178.59(12)	N(2)-Ni(1)-O(1)	84.41(6)
N(1)-Ni(1)-O(1)	84.55(12)	N(3)-Ni(1)-O(1)	177.71(6)
N(1A)-Ni(1)-(1A)	84.55(12)	N(2)-Ni(1)-O(2)	179.60(6)
N(1)-Ni(1)-O(1A)	178.59(12)	N(3)-Ni(1)-O(2)	84.16(6)
O(1)-Ni(1)-O(1A)	94.06(15)	O(1)-Ni(1)-O(2)	95.24(5)

5.4.6. Self-assembly of [Ni(HL_n)]

In the solid state, a one−dimensional assembly of **8**, is formed *via* intermolecular C−H···O hydrogen bonding interaction (Figure 5.5). In this one−dimensional arrangement, two methyl C−H groups (C1 and its symmetry related counterpart) of each molecule are interacting with the amide oxygen atom (O1 and its symmetry related counterpart) of the two adjacent molecules in a reciprocal manner. The C1···O1 distance and C1−H···O1 angle are 3.485(7) Å and 154°, respectively.

We have investigated the crystal structure of **9** for non−covalent interactions. But no significant interaction is present in the crystal lattice of **9**.

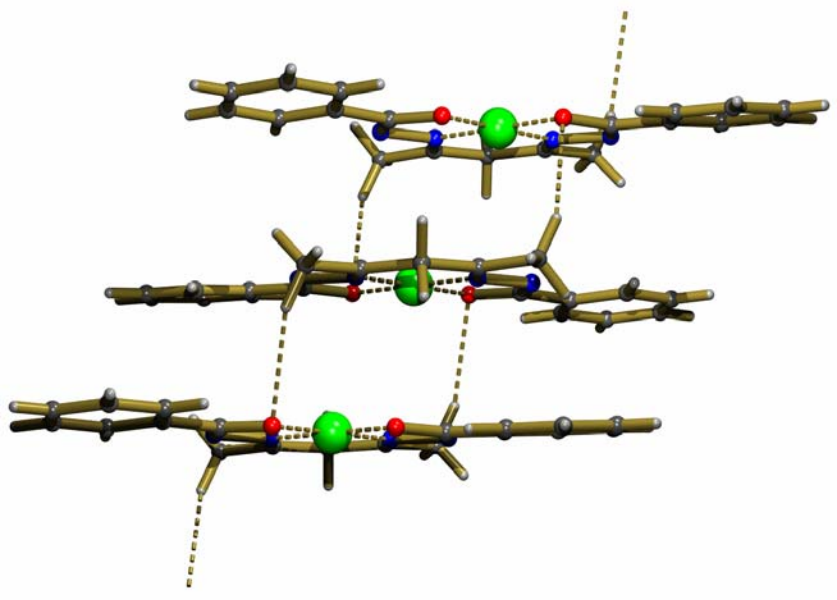

Fig. 5.5. One−dimensional ordering of **8** *via* C−H···O interactions.

5.4.7. Spectral properties of 10, 11 and 12

In the infrared spectra of **10**, **11** and **12,** there are no bands that could be attributed to N-H group or C=O groups. The nonappearance of the N–H and C=O stretches is consistent with the enolate form of the amide functionalities in the binucleating ligand. Two medium intensity bands observed in the range 1641-1632 cm^{-1} and 1601-1599 cm^{-1} are most likely due to the deprotonated O-coordinating amide functionalities and the C=N moieties of the ligands.[24-26]

It has been reported that in the presence of oxygen or iodine, oxidative C–C coupling involving the central C-atom of the acetylacetone residue in complexes with similar tetradentate Schiff bases leads to dinuclear species.[20,21,27,28] The ESI mass spectrum of **10** displays a doubly charged molecular ion peak at *m/z* = 392.[21]

Electronic spectral data of the complexes in CH_2Cl_2 are listed in Table 5.6. All the complexes show three weak to moderately intense bands in the range 970-595 nm followed by four relatively strong absorptions in the range 545-267 (Figure 5.6). For nickel(II) stabilized radical species weak bands in the same region, as observed for the present complexes, have been reported earlier.[29] The EPR and magnetic properties (vide infra) also indicate a similar situation in **10**, **11** and **12**. The remaining intense absorptions are most likely due to ligand-to-metal and intra-ligand charge transfer transitions.

Table 5.6. Electronic spectral data of **10**, **11** and **12**

Complex	**λ_{max} (nm) (ε ($M^{-1}cm^{-1}$))**
10	772(130), 644(640), 595^{sh}(330), 439(4600), 372^{sh}(4580), 346(5860), 267(9440)
11	825(3771), 692(3500), 654^{sh}(3100), 545(2220), 441(5920), 384(4960), 299(9210)
12	964(1560), 849^{sh}(1280), 605(1030), 476(3490), 417^{sh}(2050), 357^{sh}(3550), 320(7030).

sh=Shoulder

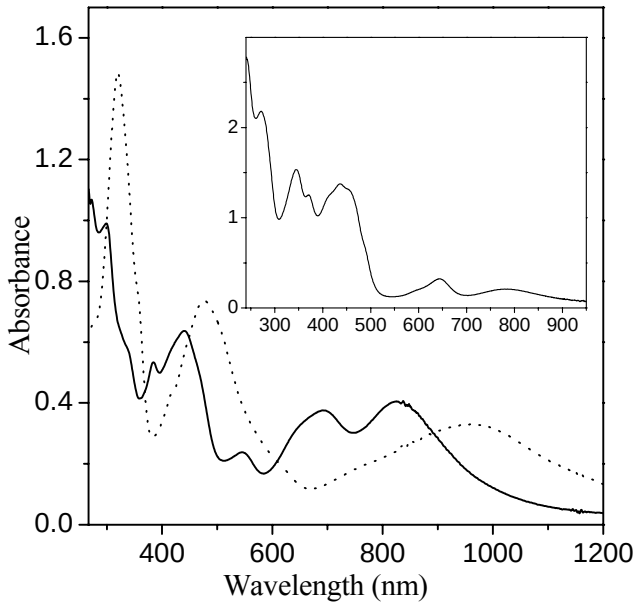

Fig. 5.6. Electronic spectra of **10** (inset), **11** (solid line) and **12** (dotted line).

5.4.8. Structural characterization of 12

Unlike **8** and **9, 12** is a dinuclear complex (Figure 5.7). In **12** the each metal ion is in a square-planar N_2O_2 environment constituted by an amide-N atom, an imine-N atom and two deprotonated amide-O atoms. It crystallizes in the $P2_1/c$ space group. The asymmetric unit contains a dinuclear complex molecule and an acetone molecule. Selected bond parameters associated with the metal centers are listed in Table 5.7. Two halves of the dinuclear molecule is connected by a single C(sp2)-C(sp2) bond. The C3-C26 bond length is 1.486(13) Å. The two halves of the molecule are not exactly orthogonal to each other (Figure 5.7). The dihedral angle between them is 68.4(2)º. The Ni-N distances in both halves are not identical. These are 1.803(9), 1.806(9), 1.821(8) and 1.821(8) Å. However, the same values in each half indicate the delocalization of the negative charge in the six membered chelate ring. The small difference present in the two sets of Ni−N distances is possibly due to the different conformations of the two halves of **12**. One half of this molecule

is almost planar with slightly tilted phenyl rings (the dihedral angles are 16.41(7) and 12.88(46)º) whereas the other half has a greater amount of distortion and has a bow like structure. The Ni-N distances in **12** are smaller than the Ni-N distances observed in all other nickel(II) complexes reported in this chapter. The Ni−N and N−O distances are comparable with a similar dinuclear system reported before.[21] The four C-C bonds (C2-C3, C3-C4 and C26-C27, C25-C26) in **12** are little shorter than that of the other nickel(II) complexes (**8**, **9**, **13**, **14** and **15**) because here one of these is a double bond or in other words delocalized bond with bond order more than one.[21]

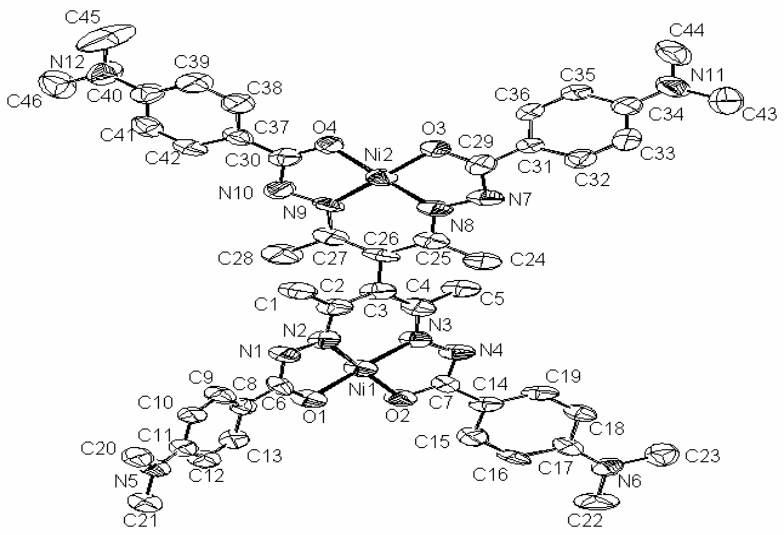

Fig. 5.7. Molecular structure of **12** with the atom labeling scheme. All non−hydrogen atoms are represented by their 40% probability thermal ellipsoids.

The packing of the neutral molecules of **12** in the crystal lattice is rather interesting. Two dinuclear molecules of **12** form centerosymmetric pair of discrete dimers *via* an intermolecular weak stacking interaction between two halves of **12** (Figure 5.8). The distance between Ni1 and its centerosymmetric counterpart (Ni1') is 3.631(2) Å. As the formal oxidation state of Nickel in this complex is +3, metal−metal interaction together with

π–π interaction between the chelate rings is possibly responsible for such discrete dimer formation.[21]

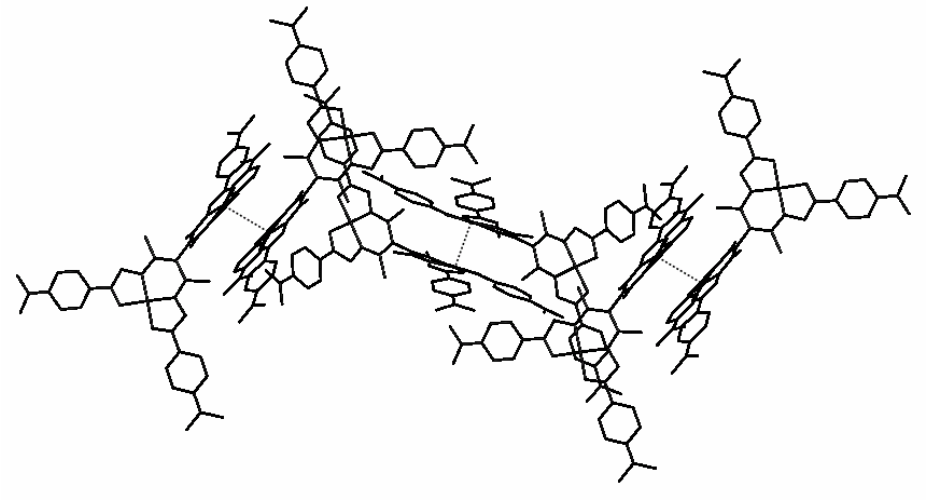

Fig. 5.8. Discrete dimers of **12**

Table 5.7. Selected bond lengths (Å) and bond angles (°) for 12·$(CH_3)_2CO$

Bond lengths			
Ni(1)-N(2)	1.803(9)	Ni(2)-N(9)	1.821(8)
Ni(1)-N(3)	1.806(9)	Ni(2)-N(8)	1.821(8)
Ni(1)-O(2)	1.843(7)	Ni(2)-O(3)	1.846(6)
Ni(1)-O(1)	1.845(7)	Ni(2)-O(4)	1.856(6)
Bond angles			
N(2)-Ni(1)-N(3)	97.3(5)	N(9)-Ni(2)-N(8)	95.6(5)
N(2)-Ni(1)-O(2)	177.9(4)	N(9)-Ni(2)-O(3)	175.9(3)
N(3)-Ni(1)-O(2)	84.8(4)	N(8)-Ni(2)-O(3)	84.7(4)
N(2)-Ni(1)-O(1)	84.4(4)	N(9)-Ni(2)-O(4)	84.2(4)
N(3)-Ni(1)-O(1)	177.7(4)	N(8)-Ni(2)-O(4)	177.2(3)
O(2)-Ni(1)-O(1)	93.5(4)	O(3)-Ni(2)-O(4)	95.2(3)

5.4.9. EPR spectral characteristics of 10, 11 and 12

The solid state magnetic moments of **10**, **11** and **12** at 300 K are very similar (~1.80 μ_B per nickel) and indicate an S = 1/2 spin state of each metal center in these complexes. A non-innocent nature of the ligands in complexes with tetradentate Schiff bases derived from acetylacetone has been noted before.[21,27,28] Thus, to resolve the ambiguity between an authentic nickel(III) complex and a nickel(II) stabilized ligand radical system we have examined the EPR spectral features of **10**, **11** and **12** (Figures 5.9 and 5.10). At room temperature (300 K) in the powdered phase all the complexes display an isotropic signal centered at around g = 2.01. The peak-to-peak separations for these signals are around 70 G. At low temperature (115 K) these signals become rhombic (Figure 5.9). The corresponding g values are listed in Table 5.8. Like the solid samples, the dichloromethane solutions (Figure 5.10) of the complexes at room temperature also display a similar isotropic signal at around g = 2.01. However, the peak-to-peak width (~17 G) for these signals are significantly smaller compared to that in the solid state spectra. The spectra of the complexes in frozen (115 K) dichloromethane solutions are again rhombic in character (g values are listed in Table 5.8). However, in these spectra, for **10** and **12**, the lowest field signals are well resolved and the highest field signals are significantly broadened compared to the corresponding signals observed in the spectra obtained from the solid samples of the complexes at the same temperature (Figure. 5.9). The observed g values are very close to those for a nickel(II) stabilized ligand radical species.[29-32] However, the peak-to-peak width for the isotropic signals observed at room temperature in the solid state spectra is rather large for a ligand radical system.[29] Although the room temperature isotropic signals displayed by the dichloromethane solution of **10**, **11** and **12** are sufficiently narrow, they are devoid of any nitrogen hyperfine structure to suggest ligand radical systems. In addition, at low temperature both solid state and frozen solution spectra are rhombic in character. Such rhombic spectra are not unusual for square-planar

nickel(III) complexes, due to distortion from the square-planar geometry or weak coordination at the apical site.[32] Considering all the EPR features it is difficult to describe **10**, **11** and **12** as genuine nickel(III) species or nickel(II) stabilized ligand radical systems. Thus the best description for **10**, **11** and **12** may perhaps be that they are border-line between the two possible situations. However, the typical rhombic nature of both low temperature solid state and frozen solution spectra suggests that these complexes may be slightly biased towards the nickel(III) side.

Table 5.8. EPR spectroscopic data of 10, 11 and 12 (g values)

Complex		g values
10	Powder at 115 K	2.02, 2.01 and 1.98
	Frozen soution at 115 K	2.02, 2.01 and 1.98
11	Powder at 115 K	2.02, 2.009 and 1.98
	Frozen soution at 115 K	2.02, 2.006 and 1.98
12	Powder at 115 K	2.01, 2.007 and 1.98
	Frozen soution at 115 K	2.02, 2.009 and 1.99

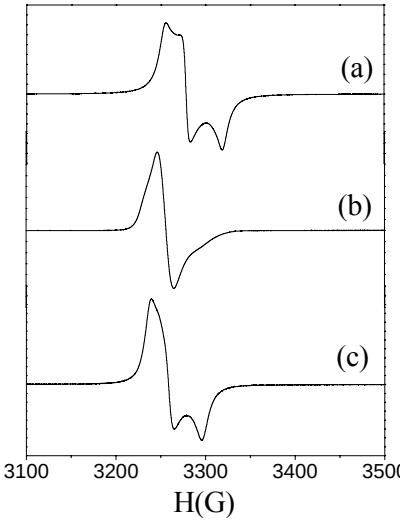

Fig. 5.9. EPR spectra of (a) **10,** (b) **11** and (c) **12** in powder phase at 115K.

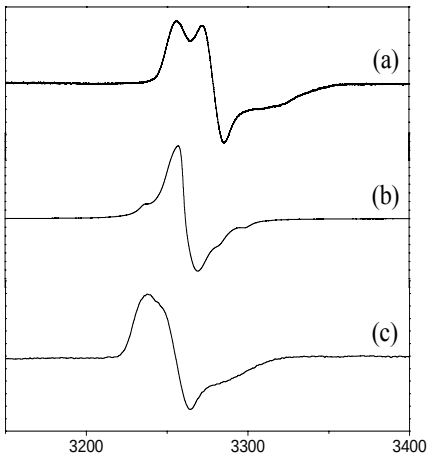

Fig. 5.10. EPR spectra of (a) **10,** (b) **11** and (c) **12** in frozen (115K) dichloromethane solution.

5.4.10. Magnetic property of 10

Magnetic susceptibility measurements with a powdered sample of **10** were performed in the temperature range 2-300K at a constant magnetic field of 5 KG. The effective magnetic moment (μ_{eff}) of **10** at 300 K is 2.55 μ_B. On cooling the moment of **10** gradually decreases and the μ_{eff} value at 2 K is 1.94 μ_B. The curve obtained is shown in Figure 5.11. The nature of the curve indicates a small but definite antiferromagnetic interaction in **10.** The data of **10** was fitted using the expressions for χ_M vs T derived from the isotropic spin-exchange Hamiltonian $H = -2JS_1 \cdot S_2$, where $S_1 = S_2 = 1/2$.[33] The best least-squares fits[34] were obtained with $J = -1.4(1)$ cm^{-1} and $g = 2.079(1)$.

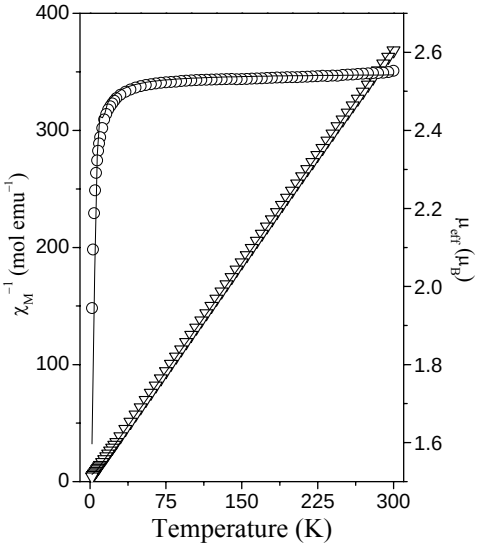

Fig. 5.11. Temperature dependence of the effective magnetic moments (○) and inverse molar susceptibilities (∇) of **10**. The solid lines were generated from the best least-squares fit parameters given in the text.

5.4.11. Synthesis and characterization of 13, 14 and 15

Slow evaporation of wet dichloromethane–acetonitrile (1:1) solutions of **10**, **11** and **12** in air produced three brown crystalline substances **13**, **14** and **15**, respectively. However, if the same procedure was performed using dry solvents under moisture free atmosphere in the presence or absence of oxygen, the unchanged **10**, **11** and **12** were recovered. Interestingly all these paramagnetic complexes remain unchanged in wet solvent under dinitrogen atmosphere. Thus, the complexes (**13**, **14** and **15**) were formed in the presence of both moister and oxygen. Solid state magnetic susceptibility measurements with these crystalline substances indicate the diamagnetic character of these materials. In acetonitrile solutions, these new species are electrically non-conducting. Thus these brown complexes are most likely neutral square-planar nickel(II) complexes. In the electronic absorption spectra, **13**, **14** and **15** display a weak absorption in the range 530-580 nm. This absorption has been

assigned to the spin-allowed d–d transition ($^1A_{1g}$—$^1A_{2g}$). All these complexes show intense bands in the range 440–223 nm. These absorptions are possibly due to ligand-to-metal charge transfer and intra-ligand transitions. The infrared spectra of the solids do not display any peak that could be associated with the N–H group. The absence of an N–H group indicates deprotonation of the amide functionalities in the ligand. However, in all of the three complexes, one medium intensity peak observed near 1650 cm^{-1}, is very likely due to a C=O group. The origin of another medium intensity peak in the range 1585-1595 cm^{-1} is most likely the C=N moieties of the ligand. It is known that under aerobic conditions in square-planar bivalent 3d metal ion complexes of formula [ML] (H_2L = acetylacetone bis(thiosemicarbazone)), the central methylene group of the acetylacetone residue of L^{2-} gets oxidized and a keto group is formed.[15,35] The infrared spectra and other physical properties indicate that the crystalline materials (**13**, **14** and **15**) obtained from **10**, **11** and **12** are possibly similar square-planar nickel(II) complexes [Ni(L_nO)] (**13** (n=1), **14**(n=2) and **15**(n=3)] with the oxidized ligand L_nO^{2-}.

5.4.12. Molecular structures of 13, 14 and 15

We have determined the X-ray structures of these three brown complexes (**13**, **14** and **15**) to confirm the above conjecture. The structures reveal that indeed the middle C-atom of the acetylacetone residue of the all three complexes has been oxidized with the formation of a keto group (Figures 5.12 − 5.14). Both **14** and **15** crystallize in $P2_1/n$ space group whereas **13** crystallizes in $P\bar{1}$. **15** is crystallized with a $CHCl_3$ molecule in the asymmetric unit. These complex molecules are square-planar nickel(II) species with a tetradentate dianionic ligand. Selected bond parameters are listed in Table 5.9. Intra-ligand bond distances and angles are unexceptional and consistent with the deprotonation of both amide functionalities and the middle carbon of the acetylacetone moiety containing the O−atom being a keto group.[23,24] The ligands bind the metal ions *via* two amide-O atoms and two imine-N atoms

providing an N_2O_2 square-plane around the metal ion. In this process, it forms two five-and one six-membered chelate rings. The chelate bite angles for the five membered rings of **13**, **14** and **15** are essentially identical (Table 5.9) and are smaller than that of the six-membered ring. In all the three complexes there is essentially no displacement of the nickel(II) centre from the N_2O_2 square plane. However, these molecules as a whole are not perfectly planar. The two phenyl ring planes are slightly tilted from the mean plane constituted by the rest of the molecule. The dihedral angles thus formed are in the range 1.70 – 8.72°.

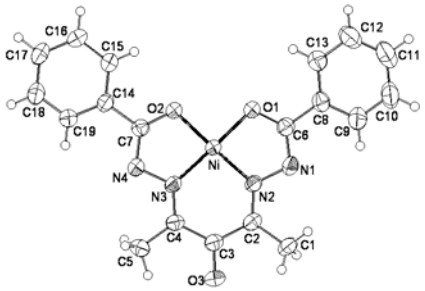

Fig. 5.12. Molecular structure of **13** with the atom labeling scheme. All non−hydrogen atoms are represented by their 40% probability thermal ellipsoids.

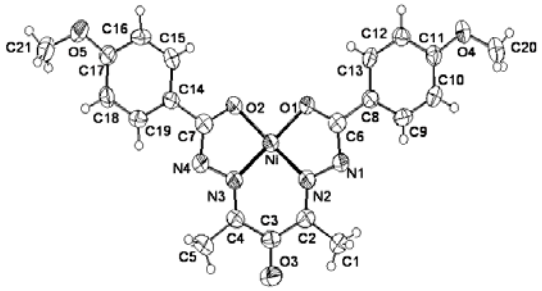

Fig. 5.13. Molecular structure of **14** with the atom labeling scheme. All non−hydrogen atoms are represented by their 40% probability thermal ellipsoids.

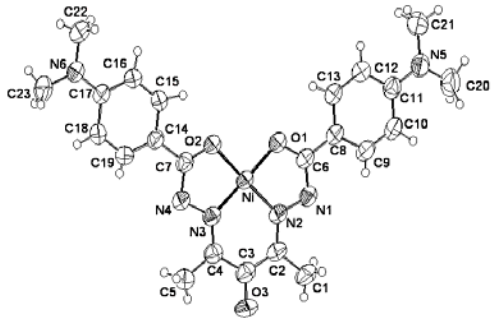

Fig. 5.14. Molecular structure of **15** with the atom labeling scheme. All non−hydrogen atoms are represented by their 40% probability thermal ellipsoids.

Table 5.9. Selected bond lengths (Å) and bond angles (°) for 13, 14 and 15·$CHCl_3$

Bond lengths					
13		**14**		**15·$CHCl_3$**	
Ni–O(1)	1.841(19)	Ni(1)-N(3)	1.830(4)	Ni(1)-N(2)	1.838(2)
Ni–O(2)	1.847(19)	Ni(1)-N(2)	1.838(4)	Ni(1)-N(3)	1.840(2)
Ni–N(2)	1.841(2)	Ni(1)-O(1)	1.856(3)	Ni(1)-O(2)	1.843(19)
Ni–N(3)	1.836(2)	Ni(1)-O(2)	1.860(3)	Ni(1)-O(1)	1.855(19)
Bond angles					
13		**14**		**15·$CHCl_3$**	
O(1)–Ni–O(2)	93.15(8)	N(3)-Ni(1)-N(2)	96.57(17)	N(2)-Ni(1)-N(3)	97.35(9)
O(1)–Ni–N(2)	84.77(9)	N(3)-Ni(1)-O(1)	177.86(15)	N(2)-Ni(1)-O(2)	178.13(9)
O(1)–Ni–N(3)	177.79(9)	N(2)-Ni(1)-O(1)	84.49(15)	N(3)-Ni(1)-O(2)	84.40(9)
O(2)–Ni–N(2)	177.90(9)	N(3)-Ni(1)-O(2)	84.54(15)	N(2)-Ni(1)-O(1)	84.42(9)
O(2)–Ni–N(3)	84.69(9)	N(2)-Ni(1)-O(2)	178.63(16)	N(3)-Ni(1)-O(1)	178.13(8)
N(2)–Ni–N(3)	97.40(10)	O(1)-Ni(1)-O(2)	94.42(13)	O(2)-Ni(1)-O(1)	93.84(8)

5.4.13. Self-assembly of [Ni(L_nO)] via non−covalent interaction

These complex molecules do not have any good conventional hydrogen bond donor. However, intermolecular C–H···π interactions[36] lead to the self-assembly of the molecules of **13** into a one-dimensional array in the crystal lattice. In this one-dimensional arrangement, two methyl C–H groups of each molecule are interacting with the phenyl rings of the two adjacent molecules in a reciprocal manner (Figure 5.15). The H···centroid (cg) distances are 2.801 and 2.952 Å for C1–H···cg (of C8–C12 ring) and C5–H···cg (of C13–C17 ring) interactions, respectively. The corresponding C–H···cg angles are 137.2° and 125.4°, respectively. The Ni···Ni distance for the pair of molecules involved in C1–H···cg interactions is 4.142 Å and that for the pair of molecules involved in C5–H···cg interactions is 3.586 Å. The differences in the structural parameters associated with the two C–H···π interactions and the tilted nature of the two phenyl rings compared to the rest of the molecule (vide supra) are possibly responsible for the alternating short and long Ni···Ni distances in the chain-like arrangement of the metal ions.

Fig. 5.15. One-dimensional ordering of **13** via C–H···π interactions.

In the crystal lattice of **14**, the molecules exist in a helical fashion through C−H···O hydrogen bonding (Fig. 5.16). The methyl hydrogen of one of the methoxy group is acting as a donor and the oxygen atom (O5) of the methoxy group, from another molecule, is acting as an acceptor. The H···O5 and C20···O5 distances are 2.57 and 3.48 Å, respectively. The C20-H···O5 angle is 159.3º. This hydrogen bonding interaction leads to a helical arrangement of **14** parallel to *b* axis.

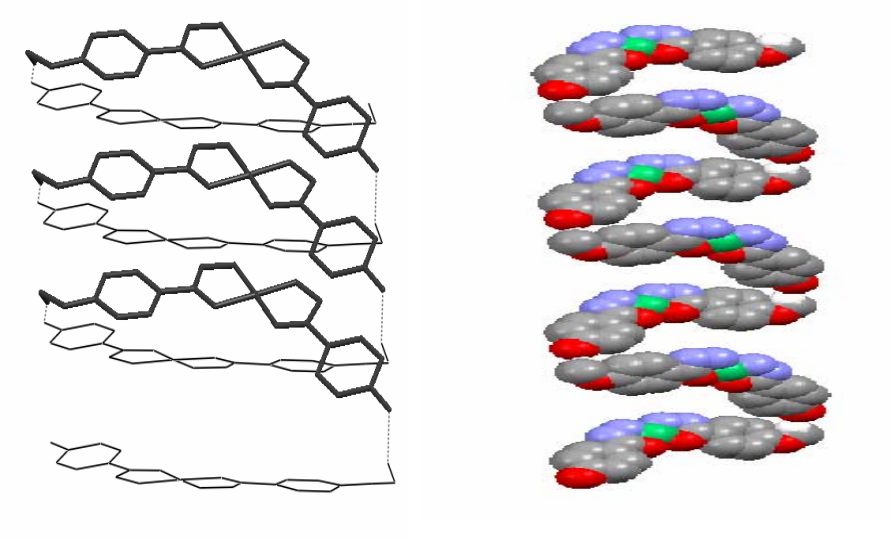

(**a**) (**b**)

Fig. 5.16. Helical arrangement of **14**. (a) Propagation of the helix through the hydrogen bonding interactions and (b) Space-filling model of the helix. Hydrogens that do not participate in hydrogen bonding interaction are omitted for clarity.

In the crystal lattice of **15**, the molecules form a one−dimensional assembly *via* C−H···O hydrogen bonding interaction (Figure 5.17). One C−H group of the NMe_2 fragment and the oxygen atom (O3) of the keto group are involved in this

hydrogen bonding. The H···O3 and C21···O3 distances are 2.34(4)and 3.206(6) Å, respectively. The C21−H···O3 angle is 147°.

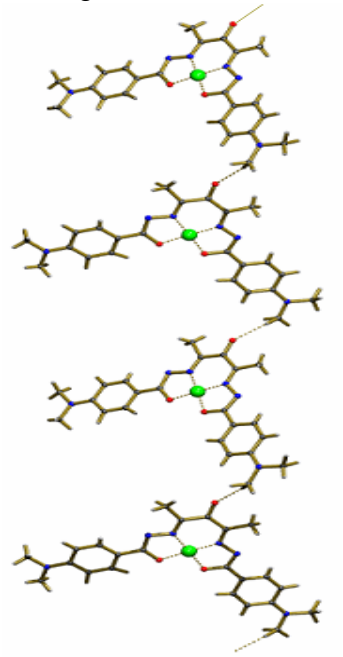

Fig. 5.17. One-dimensional ordering of **15** via C–H···O interactions.

5.5. Conclusion

Our objective was to study the nickel coordination chemistry with the Schiff bases acetylacetone bis(aroylhydrazone) containing two higher oxidation state promoting amide functionalities. In our attempt to prepare these Schiff bases from acetylacetone and *para*-substituted aroylhydrazine, we have isolated 3,5-substituted pyrazolines. Treatment of these pyrazolines with nickel acetate tetrahydrate leads to metal ion assisted pyrazoline ring opening and the formation of a series of neutral complexes of nickel in both +2 ([Ni(HL_n)]) and formal +3 oxidation ([NiL_n−L_nNi]) states. The molecular formula and the magnetic moment of the dinuclear [NiL_n-L_nNi] species are consistent with the +3 formal oxidation state of the metal ions in these

complexes. However, the EPR spectral characteristics of these complexes indicate a border-line situation between a nickel(III) species and a nickel(II) stabilized ligand radical species. In wet dichloromethane–acetonitrile solution, the C–C bridge of the ligand in [NiL_n-L_nNi] gets oxidized to –C(=O)– and a series of square-planar mononuclear nickel(II) complexes having the common formula [$Ni(L_nO)$] are formed. Considering the border-line nature of [NiL_n−L_nNi] and the need of moisture for this transformation to take place, a possible mechanism for this oxidation could be as follows: shift of the unpaired electrons from the nitrogen atoms to the carbon atoms of the ligand, followed by homolytic cleavage of the C–C bond and addition of water to form –CH(OH)–, and finally a 2e, $2H^+$ oxidation to the keto group by oxygen. Similar mechanisms have been suggested for platinum(IV) and ruthenium(III) assisted conversion of a methine group to a keto group in guanine.[37,38]

Although the oxidation of the methylene group to a keto group for the complexes [ML] of the deprotonated acetylacetone bis(thiosemicarbazone) (H_2L) in the presence of oxygen has been observed before,[15,20] nothing has been reported about the nature of the intermediate involved during the formation of [MLO] from [ML]. In this work, we have been able to isolate and establish the nature of these intermediates ([Ni(HLn)]) and [NiLn−LnNi]), which provides us some clues about the possible pathways for the formation of the final complex of the oxidized ligand.

5.6. References

1. J. R. Lancaster (Ed.), *The Bioinorganic Chemistry of Nickel,* VCH, New York, 1988.
2. A. E. Przybyla, J. Robbins, N. Menon and H. D. Peck Jr., *FEMS Microbiol. Rev*., 1992, **88**, 109.
3. H. Yoon, T. R. Wagler, K. J. O'Connor and C. J. Burrows, J. Am. Chem. Soc., 1990, **112**, 4568.
4. P. J. Chmielewski and L. Latos-Grazynski, *Inorg. Chem*., 1997, **36**, 840.

5. D. W. Margerum, *Pure. Appl. Chem*., 1983, **32**, 297,
6. W.E. Hatfield, in: E.A. Boudreaux and L.N. Mulay (Eds.), *Theory and Applications of Molecular Paramagnetism,* Wiley, New York, 1976, p. 491.
7. L.J. Farrugia, *J. Appl. Crystallogr*. 1999, **32**, 837.
8. *SMART* V5.630 and *SAINT-plus* V6.45, Bruker-Nonius Analytical X-ray Systems Inc.: Madison, WI, USA, 2003.
9. G. M. Sheldrick, *SADABS*, Empirical Absorption Correction Program, University of Göttingen, Göttingen, Germany, 1997.
10. G. M. Sheldrick, *SHELX-97*, *Structure Determination Software*, University of Göttingen, Göttingen, Germany, 1997.
11. P. McArdle, *J. Appl. Crystallogr.*, 1995, **28**, 65.
12. A. L. Spek, *PLATON*, *A Multipurpose Crystallographic Tool*, Utrecht University, Utrecht, The Netherlands, 2002.
13. H. Buttkus and R. J. Bose, *J. Org. Chem.,* 1971, **36**, 3895.
14. D. H. Hunter, C. McRoberts and J. J. Vittal, *Can. J. Chem*., 1998, **76,** 522.
15. S. C. Davies, M. C. Durrant, D. L. Hughes, A. Pezeshk and R. L. Richards, *J. Chem. Res. (S),* 2001, 100.
16. E. C. Constable, M. J. Doyle, S. M. Elder and P. R. Raithby, *J. Chem. Soc., Chem. Commun.,* 1989, 1376.
17. K. C. Joshi, R. Bohra and B. S. Joshi, *Inorg. Chem*., 1992, **31**, 598.
18. W. Kemp, *Organic Spectroscopy, Macmillan*, Hampshire, 1987, p. 65.
19. M. B. Hursthouse, M. A. Laffey, P. T. Moore, D. B. New, P. R. Raithby, and P. Thornton, *J. Chem. Soc. Dalton Trans*., 1982, 307.
20. V. B. Arion, N. V. Gerbeleu, V. G. Levitsky, Y. A. Simonov, A. A. Dvorkin and P. N. Bourosh, *J. Chem. Soc, Dalton Trans*., 1994, 1913.
21. V. B. Arion, K. Weighardt, T. Weyhermueller, E. Bill, V. Leovac and A. Rufinska, *Inorg. Chem*., 1997, **36**, 661.
22. A. Mukhopadhyay, G. Padmaja, S. N. Pal and S. Pal, *Inorg. Chem. Commun.*, 2003, **6,** 381.
23. H. Yin and S. -X. Liu, *Chinese J. Inorg. Chem*., 2002, **18**, 269.

24. S. Pal, *Proc. Ind. Acad. Sci. (Chem. Sci.),* 2002, **114**, 417.
25. S. N. Pal and S. Pal, *Eur. J. Inorg. Chem*., 2003, 4244.
26. K. Nakamoto, *Infrared and Raman Spectra of Inorganic and Coordination Compounds,* Wiley, New York, 1986, pp. 241–244.
27. U. Knof, T. Weyhermuller, T. Wolter, K. Weighardt, E. Bill, C. Butzlaff and A. X. Trauwein, *Angew. Chem. Int. Ed. Engl.,* 1993, **32**, 1635.
28. U. Knoff, T. Weyhermueller, T. Wolter, K. Wieghardt, E. Bill, C. Butzalff, A. Trautwein, *Angew. Chem. Int. Ed. Engl*., 1993, **32**, 1635.
29. R. R. Gagne and D. M. Ingle, *Inorg. Chem*., 1981, **20**, 420.
30. J. A. McCleverty, *Prog. Inorg. Chem*., 1968, **10**, 49.
31. R. S. Drago and I. Baucom, *Inorg. Chem*., 1972, **11**, 2064.
32. Y. Shimazaki, F. Tani, K. Fukui, Y. Naruta and O. Yamauchi, *J. Am. Chem. Soc*., 2003, **125**, 10512.
33 C. J. O'Connor, *Prog. Inorg. Chem.,* 1982, **29**, 203.
34. G. V. R. Chandramouli, C. Balagopalakrishna, M. V. Rajasekharan, P. T. Manoharan, *Comput. Chem.,* 1996, **20**, 353.
35. V. B. Arion, N. V. Gerbeleu and K.M. Indrichan, *Russ. J. Inorg. Chem.,* 1985, **30**, 70.
36. M. Nishio, *Cryst. Eng. Comm*., 2004, **6**, 130
37. S. Choi, S. Delaney, L. Orbai, E. J. Padgett and A. S. Hakemian, *Inorg. Chem.,*2001, **40**, 5481.
38. K. C. Cariepy, M. A. Curtin and M. J. Clarke, *J. Am. Chem. Soc*., 1989, **111**, 4947.

Appendix

AI

Table AI. 1. Structural Data Related to Intramolecular M···H–C Interaction in d^8 Metal Ion Complexes discussed in Chapter 4.

refcode	M(II)	M···H dist. (Å)	M···H–C angle (deg)	Ψ (deg)
COPGET	Ni(II)	2.668	125.102	33.573
DAWGUD	Ni(II)	2.885	102.297	85.365
ERURAK	Ni(II)	2.885	94.712	87.400
ERUREO	Ni(II)	2.733	109.016	77.854
FAKVIW	Ni(II)	2.894	93.133	85.339
GIGVEX10	Ni(II)	2.859	107.358	88.293
IFAFIE	Ni(II)	2.476	136.801	12.763
KIYQUE	Ni(II)	2.792	129.004	36.500
KOHHAQ	Ni(II)	2.810	128.477	55.681
LOKZOA	Ni(II)	2.919	101.781	88.010
LUQJOW	Ni(II)	2.833	90.816	86.319
MIYQEQ	Ni(II)	2.607, 2.972	123.717, 99.198	31.403, 31.403
NOKVOY	Ni(II)	2.663	105.555	77.495
QOZROM	Ni(II)	2.353	140.411	14.618
RORHUB	Ni(II)	2.869	90.055	86.797
SENHIC	Ni(II)	2.874	114.987	75.856
SOSVAX	Ni(II)	2.786	90.748	37.947
SOSVAX1	Ni(II)	2.786	90.750	37.948
TISPEQ	Ni(II)	2.844	111.106	77.368
TISPIU	Ni(II)	2.967	108.425	82.605
VETPEP	Ni(II)	2.979	97.906	90.369
BABDIS	Pd(II)	2.703	119.125	73.137
BECGEV	Pd(II)	2.949	117.971	70.944
CAPVOE	Pd(II)	2.585, 2.732	125.092, 115.835	15.776, 1.934
DAGGUN	Pd(II)	2.946	112.824	15.596
DUHYUA	Pd(II)	2.783	102.092	43.831
DUNWAK	Pd(II)	2.944	99.833	45.921

continued ….

EFODEI	Pd(II)	2.884	107.519	31.598
HAPNIV	Pd(II)	2.926	115.268	16.080
HOZNUF	Pd(II)	2.880, 2.836	100.278, 96.338	85.396, 84.995
JEDDIF	Pd(II)	2.865	102.679	79.360
KIMXOT	Pd(II)	2.871	132.141	54.848
LANBIL	Pd(II)	2.968	108.260	79.553
LIJHUH	Pd(II)	2.946	106.715	88.674
NINMAY	Pd(II)	2.933, 2.744	119.920, 128.876	69.726, 62.872
NOKGUP	Pd(II)	2.823	108.391	57.224
SUGWEW	Pd(II)	2.596	133.835	54.013
TURKIA	Pd(II)	2.679	122.982	68.115
UGIKOK	Pd(II)	2.983, 2.953, 2.843	110.515, 114.306, 122.513	14.014, 10.811, 3.029
XODPEL	Pd(II)	2.815	107.154	48.564
YIYHIX	Pd(II)	2.833	117.149	72.866
ZODQOY	Pd(II)	2.868	101.858	86.739
HAPZPT10	Pt(II)	2.966	90.958	68.292
HIXJUT	Pt(II)	2.854, 2.976	125.650, 131.625	12.480, 33.951

Appendix II

AII

Tables for Atomic coordinates (x 10^4) and equivalent isotropic displacement parameters (A^2 x 10^3). U(eq) is defined as one third of the trace of the orthogonalized Uij tensor.

Table AII.1. $[Ni(paap)_2]\cdot CH_3COOH\cdot H_2O$ (1) (Chapter 2)

Atom	x	y	z	U(eq)
Ni	5302(1)	1296(1)	2636(1)	50(1)
O(1)	7039(4)	634(2)	2457(3)	59(1)
O(2)	6263(4)	1941(2)	3716(3)	58(1)
O(3)	8634(7)	1286(5)	1276(7)	141(4)
O(4)	10132(17)	503(7)	1423(13)	285(9)
O(5)	7834(7)	988(3)	4853(4)	96(2)
N(1)	3294(5)	1588(3)	3039(4)	51(1)

N(2)	4793(5)	347(2)	3364(4)	48(1)
N(3)	4481(5)	1006(3)	1286(4)	54(1)
N(4)	5927(5)	2206(3)	1888(4)	49(1)
C(1)	2567(7)	2234(4)	2890(5)	66(2)
C(2)	1216(8)	2315(5)	3156(6)	87(3)
C(3)	617(9)	1709(6)	3611(7)	97(3)
C(4)	1363(7)	1049(5)	3775(6)	70(2)
C(5)	2701(6)	996(3)	3491(5)	53(2)
C(6)	3603(7)	318(3)	3674(5)	54(2)
C(7)	5871(7)	-202(3)	3465(4)	52(2)
C(8)	5836(8)	-872(3)	4017(5)	65(2)
C(9)	6995(8)	-1346(4)	4098(6)	70(2)
C(10)	8162(9)	-1147(4)	3623(6)	76(2)
C(11)	8192(8)	-504(4)	3065(5)	68(2)
C(12)	7033(6)	-6(3)	2958(5)	54(2)
C(13)	3719(7)	399(4)	979(6)	68(2)
C(14)	3252(8)	304(5)	83(6)	77(2)
C(15)	3565(8)	859(5)	-567(6)	84(2)
C(16)	4341(8)	1514(4)	-257(6)	70(2)
C(17)	4782(6)	1566(4)	636(5)	55(2)
C(18)	5629(7)	2213(3)	1029(5)	57(2)
C(19)	6752(6)	2738(3)	2421(5)	58(2)
C(20)	7435(7)	3391(4)	2039(6)	66(2)
C(21)	8226(7)	3858(3)	2632(7)	74(2)
C(22)	8354(7)	3694(4)	3573(7)	70(2)
C(23)	7706(6)	3066(4)	3952(5)	61(2)
C(24)	6888(6)	2561(3)	3363(5)	55(2)
C(25)	9840(11)	1129(6)	1196(8)	101(3)
C(26)	10632(15)	1634(10)	700(12)	188(7)

Table AII.2. $[Ni(paab)_2]\cdot 2H_2O$ (2) (Chapter 2)

Atom	x	y	z	U(eq)
Ni	5550(1)	9820(1)	7336(1)	54(1)
O(1)	3753(5)	9145(4)	8534(3)	70(1)
O(2)	1815(11)	8232(17)	9314(10)	321(11)
O(3)	4206(6)	11088(5)	6995(4)	82(1)
O(4)	2707(15)	12615(10)	7258(13)	266(8)
O(5)	311(10)	9096(11)	11335(10)	194(5)
O(6)	497(15)	5773(11)	10697(11)	221(6)
N(1)	7296(5)	10369(4)	5907(4)	53(1)
N(2)	5314(5)	8702(4)	6266(4)	52(1)

continued ….

N(3)	6810(5)	8669(4)	7991(4)	53(1)
N(4)	5917(5)	10916(4)	8349(4)	52(1)
C(1)	8267(8)	11169(6)	5718(6)	68(2)
C(2)	9250(8)	11503(7)	4688(6)	75(2)
C(3)	9261(8)	10964(7)	3806(6)	70(2)
C(4)	8243(8)	10130(6)	3978(5)	68(2)
C(5)	7284(7)	9835(5)	5032(5)	55(1)
C(6)	6186(7)	8960(6)	5289(5)	56(2)
C(7)	4243(7)	7827(5)	6520(5)	57(2)
C(8)	4326(10)	7029(6)	5750(6)	81(2)
C(9)	3291(12)	6206(7)	5950(9)	98(3)
C(10)	2156(11)	6137(7)	6938(9)	91(2)
C(11)	2104(8)	6862(6)	7725(7)	74(2)
C(12)	3130(7)	7704(6)	7561(5)	61(2)
C(13)	2916(8)	8408(10)	8522(7)	96(3)
C(14)	7285(8)	7530(6)	7791(6)	70(2)
C(15)	7939(8)	6858(7)	8420(7)	84(2)
C(16)	8118(8)	7339(7)	9264(6)	78(2)
C(17)	7646(8)	8485(7)	9486(6)	72(2)
C(18)	6989(6)	9124(5)	8836(4)	53(1)
C(19)	6488(7)	10379(5)	8994(5)	54(1)
C(20)	5555(7)	12169(5)	8384(5)	60(2)
C(21)	6230(9)	12869(6)	8855(6)	79(2)
C(22)	5878(12)	14070(7)	8925(9)	101(3)
C(23)	4878(14)	14574(8)	8523(9)	114(3)
C(24)	4234(12)	13924(7)	8045(8)	102(3)
C(25)	4543(8)	12675(6)	7952(5)	66(2)
C(26)	3782(11)	12066(8)	7373(8)	98(3)

Table AII.3. [Ni(bhac)(Hdmpz)] (3) (Chapter 3)

Atom	x	y	z	U(eq)
Ni	5305(1)	2350(1)	1561(1)	40(1)
O(1)	6116(1)	1749(2)	1974(1)	51(1)
O(2)	4460(1)	2971(2)	1196(1)	41(1)
N(1)	4905(1)	942(2)	1288(2)	44(1)
N(2)	4233(1)	1018(2)	932(2)	46(1)
N(3)	5693(1)	3903(2)	1672(2)	42(1)
N(4)	5829(1)	4445(2)	2412(2)	45(1)
C(1)	6980(2)	388(4)	2378(2)	76(1)
C(2)	6266(2)	627(3)	2013(2)	54(1)

C(3)	5846(2)	-263(3)	1739(2)	57(1)
C(4)	5175(2)	-124(3)	1371(2)	51(1)
C(5)	4789(2)	-1186(3)	1058(2)	70(1)
C(6)	4051(2)	2118(3)	916(2)	42(1)
C(7)	3365(2)	2444(3)	557(2)	43(1)
C(8)	3082(2)	1820(3)	-110(2)	56(1)
C(9)	2455(2)	2168(4)	-465(2)	68(1)
C(10)	2096(2)	3123(4)	-154(3)	70(1)
C(11)	2359(2)	3734(3)	512(2)	68(1)
C(12)	2993(2)	3399(3)	862(2)	58(1)
C(13)	6247(2)	6331(3)	3016(2)	79(1)
C(14)	6070(2)	5546(3)	2299(2)	51(1)
C(15)	6094(2)	5716(3)	1450(2)	54(1)
C(16)	5859(2)	4684(3)	1079(2)	46(1)
C(17)	5816(2)	4367(3)	173(2)	61(1)

Table AII.4. [Ni(bhac)(Himdz)] (4) (Chapter 3)

Atom	x	y	z	U(eq)
Ni	2016(1)	1783(1)	8340(1)	42(1)
O(2)	2899(2)	3373(7)	7851(2)	45(1)
O(1)	1151(3)	208(8)	8837(2)	53(1)
N(1)	1925(3)	37(8)	7499(2)	40(1)
N(3)	2256(3)	3641(9)	9199(2)	44(1)
N(2)	2526(3)	704(8)	6950(2)	41(1)
N(4)	2353(3)	4771(10)	10355(2)	55(1)
C(1)	135(5)	-2749(13)	9155(3)	70(2)
C(2)	729(4)	-1651(12)	8594(3)	52(2)
C(3)	813(4)	-2627(11)	7911(3)	51(2)
C(4)	1405(4)	-1829(11)	7373(3)	46(1)
C(5)	1451(4)	-3208(11)	6676(3)	54(2)
C(6)	3024(4)	2442(10)	7209(3)	40(1)
C(7)	3786(3)	3404(10)	6790(3)	40(1)
C(8)	4193(4)	2109(11)	6248(3)	50(1)
C(9)	4931(4)	2994(14)	5876(3)	69(2)
C(10)	5291(4)	5139(16)	6066(3)	74(2)
C(11)	4903(4)	6421(11)	6609(3)	57(2)
C(12)	4149(4)	5600(12)	6956(3)	51(2)
C(13)	2681(4)	5752(12)	9240(3)	54(2)
C(14)	2750(4)	6459(12)	9959(3)	57(2)
C(15)	2067(4)	3112(12)	9890(3)	49(1)

continued ….

Table AII.5. [Ni(bhac)(phim)] (5) (Chapter 4)

Atom	x	y	z	U(eq)
Ni(1)	1629(1)	2533(1)	4650(1)	37(1)
O(1)	1250(1)	2584(1)	3172(2)	39(1)
O(2)	2017(1)	2505(1)	5965(2)	48(1)
N(1)	1320(1)	672(2)	3197(2)	41(1)
N(2)	1605(1)	1023(2)	4196(2)	39(1)
N(3)	1600(1)	4095(2)	5204(2)	39(1)
N(4)	1435(1)	5749(2)	5860(3)	45(1)
C(1)	2500(1)	1835(4)	7421(6)	74(1)
C(2)	2187(1)	1606(2)	6317(3)	51(1)
C(3)	2097(1)	542(2)	5807(4)	54(1)
C(4)	1808(1)	242(2)	4814(3)	46(1)
C(5)	1725(1)	-972(2)	4504(5)	60(1)
C(6)	1153(1)	1554(2)	2737(3)	38(1)
C(7)	1825(1)	4890(2)	5071(4)	50(1)
C(8)	1725(1)	5898(2)	5474(4)	53(1)
C(9)	1363(1)	4647(2)	5700(3)	37(1)
C(10)	1065(1)	4190(2)	6033(3)	40(1)
C(11)	796(1)	4821(2)	5567(4)	53(1)
C(12)	512(1)	4396(3)	5855(4)	70(1)
C(13)	495(1)	3355(3)	6599(4)	71(1)
C(14)	759(1)	2729(3)	7066(4)	64(1)
C(15)	1045(1)	3139(2)	6795(3)	50(1)
C(16)	836(1)	1432(2)	1722(3)	40(1)
C(17)	615(1)	2260(2)	1851(3)	48(1)
C(18)	315(1)	2146(3)	943(4)	56(1)
C(19)	236(1)	1214(3)	-114(4)	59(1)
C(20)	454(1)	404(2)	-258(4)	57(1)
C(21)	752(1)	499(2)	649(3)	48(1)

Table AII.6. [Ni(ahac)(phim)] (6) (Chapter 4)

Atom	x	y	z	U(eq)
Ni(1)	812(1)	6671(1)	4761(1)	32(1)
O(1)	1197(2)	4863(5)	4977(2)	37(1)
O(2)	417(2)	8506(6)	4557(2)	40(1)
N(1)	1366(3)	7991(7)	5088(2)	33(2)
N(2)	1222(3)	9619(7)	5021(2)	35(2)
N(3)	175(3)	5507(7)	4391(2)	33(2)
N(4)	-445(3)	4196(7)	3883(2)	43(2)
C(1)	1909(4)	3150(9)	5389(3)	69(3)
C(2)	1700(3)	4799(9)	5266(3)	37(2)

C(3)	2024(3)	6035(9)	5450(2)	37(2)
C(4)	1867(3)	7640(9)	5359(2)	30(2)
C(5)	2279(3)	8897(8)	5580(2)	43(2)
C(6)	716(4)	9693(10)	4737(3)	43(2)
C(7)	-349(4)	5499(9)	4451(3)	42(2)
C(8)	-741(4)	4715(9)	4137(3)	44(2)
C(9)	110(4)	4675(9)	4036(3)	34(2)
C(10)	546(4)	4294(9)	3844(2)	38(2)
C(11)	439(4)	3163(11)	3540(3)	65(3)
C(12)	851(6)	2718(13)	3368(4)	92(4)
C(13)	1380(5)	3429(14)	3490(4)	88(4)
C(14)	1497(4)	4580(14)	3788(4)	83(3)
C(15)	1084(4)	5005(11)	3961(3)	60(3)
C(16)	464(4)	11306(9)	4619(3)	69(3)
Ni(2)	1548(1)	6588(1)	2167(1)	36(1)
O(3)	1933(2)	4801(6)	2388(2)	44(2)
O(4)	1180(2)	8430(7)	1935(2)	46(1)
N(6)	1702(3)	9436(8)	2582(2)	46(2)
N(5)	1863(3)	7794(8)	2633(2)	43(2)
N(7)	1178(3)	5532(7)	1646(2)	38(2)
N(8)	591(3)	4308(7)	1098(2)	42(2)
C(17)	2547(4)	3055(10)	2882(3)	70(3)
C(18)	2261(4)	4659(11)	2773(3)	46(2)
C(19)	2376(4)	5815(12)	3069(3)	54(3)
C(20)	2178(4)	7359(11)	2999(3)	50(2)
C(21)	2362(4)	8571(11)	3359(3)	82(3)
C(22)	1339(4)	9597(10)	2210(3)	47(2)
C(23)	1397(4)	5576(10)	1318(3)	50(2)
C(24)	1042(4)	4810(10)	982(3)	48(2)
C(25)	674(4)	4747(9)	1498(2)	34(2)
C(26)	277(4)	4380(9)	1729(3)	38(2)
C(27)	-226(4)	3573(11)	1538(3)	73(3)
C(28)	-596(5)	3160(14)	1760(4)	100(4)
C(29)	-463(5)	3561(13)	2169(4)	84(4)
C(30)	22(5)	4396(12)	2359(3)	74(3)
C(31)	387(4)	4787(10)	2144(3)	52(3)
C(32)	1089(4)	11161(9)	2062(3)	70(3)
Ni(3)	3670(1)	8445(1)	1268(1)	39(1)
O(5)	3500(2)	6664(6)	1503(2)	47(1)
O(6)	3825(2)	10248(6)	1015(2)	52(2)
N(10)	3203(3)	11298(7)	1331(2)	47(2)
N(9)	3205(3)	9721(8)	1451(2)	38(2)
N(11)	4148(3)	7243(7)	1028(2)	40(2)

continued ….

N(12)	4810(3)	5826(7)	886(3)	51(2)
C(33)	3054(4)	4922(9)	1850(3)	62(3)
C(34)	3135(4)	6540(11)	1705(2)	43(2)
C(35)	2837(4)	7778(10)	1794(3)	46(2)
C(36)	2871(3)	9359(10)	1670(3)	43(2)
C(37)	2498(4)	10591(9)	1781(3)	67(3)
C(38)	3528(4)	11440(11)	1095(3)	50(2)
C(39)	3953(4)	6812(10)	610(3)	48(2)
C(40)	4354(4)	5950(10)	523(3)	52(3)
C(41)	4682(4)	6621(10)	1192(3)	45(2)
C(42)	5063(4)	6741(13)	1624(3)	61(3)
C(43)	4970(5)	7780(20)	1892(4)	199(10)
C(44)	5350(8)	7930(30)	2300(5)	228(11)
C(45)	5830(6)	6999(19)	2444(5)	129(6)
C(46)	5908(7)	5991(17)	2180(6)	176(9)
C(47)	5544(6)	5914(15)	1761(4)	135(6)
C(48)	3582(4)	13013(10)	911(3)	81(3)
Ni(4)	3844(1)	8363(1)	4381(1)	42(1)
O(7)	3561(2)	6569(7)	4541(2)	55(2)
O(8)	4126(2)	10182(7)	4216(2)	56(2)
N(14)	3281(3)	11196(8)	4262(2)	50(2)
N(13)	3228(3)	9614(8)	4371(2)	42(2)
N(15)	4545(3)	7258(7)	4412(2)	44(2)
N(16)	5289(3)	6105(8)	4322(3)	60(2)
C(49)	2944(4)	4869(10)	4751(3)	68(3)
C(50)	3069(4)	6445(11)	4608(3)	46(2)
C(51)	2690(4)	7656(10)	4572(3)	46(2)
C(52)	2764(4)	9214(10)	4457(3)	43(2)
C(53)	2300(4)	10410(11)	4422(3)	72(3)
C(54)	3756(4)	11353(11)	4188(3)	52(2)
C(55)	4949(5)	6964(12)	4792(3)	78(3)
C(56)	5413(4)	6267(13)	4746(3)	84(4)
C(57)	4763(4)	6714(10)	4121(3)	48(2)
C(58)	4515(5)	6808(13)	3672(3)	78(3)
C(59)	4854(7)	6690(30)	3429(5)	247(13)
C(60)	4638(8)	6930(30)	2991(5)	250(13)
C(61)	4048(7)	6960(20)	2809(5)	181(9)
C(62)	3709(5)	7050(14)	3030(4)	94(4)
C(63)	3946(4)	6962(12)	3469(4)	74(3)
C(64)	3919(4)	12930(10)	4057(3)	74(3)

Table AII.7. 1-benzoyl-3,5-dimethyl-5-(10-benzoyl-hydrazido)pyrazoline (7) (Chapter 5)

Atom	x	y	z	U(eq)
O(2)	1854(2)	6653(1)	880(1)	42(1)
N(3)	974(2)	5134(1)	637(1)	33(1)
N(4)	-87(2)	4438(1)	604(1)	36(1)
N(2)	3060(2)	4385(1)	899(1)	36(1)
O(1)	1866(2)	5030(1)	1729(1)	55(1)
N(1)	2438(2)	3706(1)	1234(1)	36(1)
C(1)	1235(2)	3291(2)	1961(1)	37(1)
C(2)	428(3)	3669(2)	2319(1)	60(1)
C(3)	-227(3)	2990(2)	2619(1)	69(1)
C(4)	-86(3)	1924(2)	2574(1)	64(1)
C(5)	731(3)	1541(2)	2226(1)	64(1)
C(6)	1387(3)	2210(2)	1919(1)	51(1)
C(7)	1876(2)	4077(2)	1640(1)	37(1)
C(8)	2229(2)	4626(2)	484(1)	33(1)
C(9)	1706(2)	3616(2)	254(1)	37(1)
C(10)	318(2)	3591(2)	403(1)	36(1)
C(11)	884(2)	6083(2)	861(1)	33(1)
C(12)	-379(2)	6447(2)	1072(1)	37(1)
C(13)	-635(2)	7522(2)	1038(1)	48(1)
C(14)	-1750(3)	7931(2)	1244(1)	68(1)
C(15)	-2584(3)	7292(3)	1491(1)	79(1)
C(16)	-2329(3)	6234(3)	1536(1)	73(1)
C(17)	-1231(2)	5808(2)	1324(1)	54(1)
C(18)	-541(2)	2663(2)	333(1)	52(1)
C(19)	3008(2)	5288(2)	130(1)	47(1)

Table AII.8. $[Ni^{II}L_1]\cdot H_2O$ (8) (Chapter 5)

Atom	x	y	z	U(eq)
Ni(1)	2285(1)	2500	7500	45(1)
O(1)	1675(1)	1996(1)	6621(4)	50(1)
N(1)	2871(2)	1994(2)	6610(5)	49(1)
N(2)	2595(2)	1516(2)	5799(5)	53(1)
C(4)	1968(2)	1564(2)	5903(5)	48(1)
C(2)	3494(2)	2021(2)	6614(6)	53(1)
C(5)	1572(2)	1097(2)	5151(5)	52(1)
C(6)	1866(3)	654(2)	4234(6)	68(1)
C(10)	908(2)	1102(2)	5323(6)	59(1)
C(1)	3902(2)	1579(2)	5744(6)	69(1)
C(8)	836(3)	235(2)	3692(7)	79(2)

continued ….

C(9)	547(3)	670(2)	4593(7)	74(2)
C(3)	3837(3)	2500	7500	62(2)
C(7)	1493(3)	227(2)	3520(8)	80(2)
O(2)	0	2500	7500	405(9)

Table AII.9. [$Ni^{II}L_2$] (9) (Chapter 5)

Atom	x	y	z	U(eq)
Ni(1)	3164(1)	4328(1)	199(1)	34(1)
O(1)	4325(2)	4094(1)	979(1)	40(1)
O(2)	3367(2)	2856(1)	-75(1)	40(1)
O(3)	7559(2)	5071(1)	3744(1)	51(1)
O(4)	2253(2)	-1536(1)	-1741(1)	48(1)
N(1)	3713(2)	5967(1)	1083(1)	39(1)
N(2)	2964(2)	5776(1)	476(1)	35(1)
N(3)	1941(2)	4530(1)	-559(1)	35(1)
N(4)	1732(2)	3556(1)	-923(1)	39(1)
C(1)	2224(3)	7755(2)	490(1)	48(1)
C(2)	2255(2)	6629(2)	189(1)	37(1)
C(3)	1430(3)	6525(2)	-457(1)	43(1)
C(4)	1266(2)	5438(2)	-797(1)	37(1)
C(5)	317(3)	5457(2)	-1426(1)	47(1)
C(6)	4398(2)	5029(2)	1294(1)	36(1)
C(7)	2559(2)	2740(2)	-624(1)	36(1)
C(8)	5266(2)	5050(2)	1931(1)	36(1)
C(9)	5770(2)	6061(2)	2209(1)	40(1)
C(10)	6549(2)	6106(2)	2809(1)	42(1)
C(11)	6818(2)	5120(2)	3149(1)	39(1)
C(12)	6322(3)	4107(2)	2878(1)	44(1)
C(13)	5570(3)	4070(2)	2273(1)	41(1)
C(14)	2528(2)	1630(2)	-934(1)	37(1)
C(15)	3311(3)	698(2)	-643(1)	41(1)
C(16)	3222(3)	-336(2)	-928(1)	42(1)
C(17)	2345(2)	-472(2)	-1509(1)	39(1)
C(18)	1595(3)	453(2)	-1811(1)	45(1)
C(19)	1698(3)	1485(2)	-1523(1)	45(1)
C(20)	8144(4)	6081(2)	4032(1)	58(1)
C(21)	1413(3)	-1694(2)	-2347(1)	50(1)

Table AII.10. [NiL_3-L_3Ni]·$(CH_3)_2CO$ (12)·(Chapter 5)

Atom	x	y	z	U(eq)
Ni(1)	7971(1)	2990(1)	880(1)	68(1)
O(1)	8263(6)	3677(3)	1475(5)	76(2)

O(2)	8750(6)	3092(3)	249(5)	76(2)
N(1)	7205(7)	3356(4)	2092(7)	73(3)
N(2)	7232(6)	2911(4)	1528(7)	67(3)
N(3)	7739(7)	2314(3)	311(7)	67(3)
N(4)	8229(8)	2200(4)	-238(7)	76(3)
N(5)	8857(9)	5665(5)	4438(8)	97(4)
N(6)	11055(10)	2595(5)	-2286(9)	112(4)
C(1)	6096(9)	2536(4)	2100(8)	79(4)
C(2)	6702(9)	2474(5)	1528(9)	68(3)
C(3)	6646(8)	1991(5)	957(9)	67(3)
C(4)	7173(9)	1924(5)	372(9)	69(3)
C(5)	7132(9)	1370(4)	-129(9)	101(4)
C(6)	7806(10)	3741(6)	2022(9)	70(3)
C(7)	8763(9)	2647(6)	-212(9)	69(3)
C(8)	8039(9)	4238(5)	2624(8)	60(3)
C(9)	7554(9)	4394(6)	3180(9)	80(4)
C(10)	7821(11)	4856(6)	3775(9)	91(4)
C(11)	8604(11)	5195(6)	3868(9)	72(4)
C(12)	9097(9)	5041(5)	3311(9)	76(4)
C(13)	8818(9)	4573(5)	2720(8)	70(3)
C(14)	9322(9)	2627(5)	-767(8)	68(3)
C(15)	9811(11)	3082(5)	-843(9)	94(4)
C(16)	10353(11)	3081(5)	-1360(10)	103(5)
C(17)	10495(11)	2608(6)	-1803(9)	85(4)
C(18)	9992(10)	2152(6)	-1729(10)	84(4)
C(19)	9434(9)	2155(5)	-1236(9)	72(3)
C(20)	8409(11)	5799(6)	5071(11)	144(6)
C(21)	9691(12)	5984(5)	4570(9)	122(5)
C(22)	11588(15)	3078(6)	-2350(14)	209(11)
C(23)	11213(11)	2093(6)	-2717(10)	141(6)
Ni(2)	4721(1)	445(1)	807(1)	66(1)
O(3)	3611(5)	117(3)	-253(5)	69(2)
O(4)	4832(5)	-61(3)	1784(5)	68(2)
N(7)	3708(7)	898(4)	-1062(7)	64(3)
N(8)	4570(7)	962(4)	-137(7)	66(3)
N(9)	5754(6)	793(4)	1880(6)	63(3)
N(10)	6075(6)	544(4)	2811(7)	67(3)
N(11)	-642(7)	26(3)	-4265(7)	60(2)
N(12)	5732(8)	-1071(4)	6057(7)	78(3)
C(24)	4813(8)	1762(4)	-935(8)	89(4)
C(25)	5167(9)	1404(5)	2(9)	72(3)
C(26)	6007(9)	1523(5)	944(9)	73(3)
C(27)	6272(9)	1232(5)	1862(9)	71(3)

continued ….

C(28)	7198(8)	1364(4)	2825(8)	80(4)
C(29)	3239(8)	444(5)	-1050(8)	59(3)
C(30)	5515(9)	93(5)	2677(9)	59(3)
C(31)	2278(8)	311(5)	-1929(8)	57(3)
C(32)	1769(9)	687(4)	-2702(8)	67(3)
C(33)	809(9)	601(4)	-3456(8)	60(3)
C(34)	312(9)	119(5)	-3505(9)	59(3)
C(35)	830(10)	-274(4)	-2757(9)	68(3)
C(36)	1771(10)	-177(4)	-1981(8)	67(3)
C(37)	5620(8)	-210(5)	3557(9)	59(3)
C(38)	5089(8)	-693(5)	3420(9)	72(3)
C(39)	5127(8)	-969(4)	4255(10)	69(3)
C(40)	5693(8)	-793(5)	5243(9)	62(3)
C(41)	6240(7)	-295(5)	5363(8)	65(3)
C(42)	6183(8)	-18(4)	4532(9)	65(3)
C(43)	-1217(7)	450(4)	-4998(7)	73(3)
C(44)	-1200(8)	-477(4)	-4342(7)	76(3)
C(45)	5037(10)	-1512(5)	5882(9)	121(5)
C(46)	6367(9)	-891(5)	7078(9)	94(4)
C(47)	6801(16)	7236(9)	4711(14)	242(13)
C(48)	6815(16)	7575(13)	3901(18)	178(10)
C(49)	7048(14)	8146(8)	4051(14)	180(8)
O(5)	6616(14)	7349(6)	3134(14)	237(8)

Table AII.11. [$Ni^{II}OL_1$] (13) (Chapter 5)

Atom	x	y	z	U(eq)
Ni	2523(1)	409(1)	5300(1)	34(1)
O(2)	2300(3)	1613(2)	6700(2)	41(1)
O(1)	3608(3)	1690(2)	4707(2)	41(1)
O(3)	831(4)	-3922(2)	3800(2)	67(1)
N(4)	1055(3)	-286(2)	7081(2)	39(1)
N(3)	1427(3)	-820(2)	5937(2)	34(1)
N(2)	2804(3)	-739(2)	3894(2)	35(1)
N(1)	3646(3)	-130(2)	3146(2)	41(1)
C(15)	2137(5)	3168(3)	8987(3)	54(1)
C(16)	1950(6)	3956(3)	10089(3)	65(1)
C(17)	955(6)	3405(4)	10805(3)	63(1)
C(18)	175(5)	2065(3)	10401(3)	59(1)
C(19)	359(5)	1274(3)	9292(3)	48(1)
C(14)	1354(4)	1821(3)	8577(2)	40(1)
C(7)	1583(4)	1010(3)	7386(2)	37(1)
C(4)	931(4)	-2096(3)	5452(3)	37(1)
C(3)	1350(4)	-2728(3)	4245(3)	41(1)

C(2)	2382(4)	-2009(3)	3530(3)	39(1)
C(6)	3952(4)	1147(3)	3654(3)	39(1)
C(8)	4726(4)	2001(3)	2980(3)	43(1)
C(9)	4928(5)	1462(4)	1789(3)	56(1)
C(10)	5627(6)	2265(4)	1168(4)	72(1)
C(11)	6145(6)	3609(4)	1728(4)	74(1)
C(12)	5945(5)	4165(4)	2910(4)	68(1)
C(13)	5223(5)	3364(3)	3534(3)	51(1)
C(5)	-35(5)	-2968(3)	6051(3)	50(1)
C(1)	2822(5)	-2806(3)	2407(3)	52(1)

Table AII.12. [$Ni^{II}OL_2$] (14) (Chapter 5)

Atom	x	y	z	U(eq)
Ni(1)	6240(1)	10319(1)	9049(1)	39(1)
O(1)	5514(4)	9916(2)	7919(2)	45(1)
O(2)	7418(4)	9412(2)	9411(2)	44(1)
O(3)	5255(5)	12579(2)	10449(2)	72(1)
O(4)	1853(4)	9678(2)	3991(2)	60(1)
O(5)	11998(4)	7087(2)	11874(2)	57(1)
N(1)	4361(5)	11162(2)	7788(3)	45(1)
N(2)	5091(4)	11211(2)	8664(3)	38(1)
N(3)	6913(4)	10686(2)	10182(2)	40(1)
N(4)	7916(5)	10165(2)	10701(3)	44(1)
C(1)	3932(10)	12548(4)	8680(6)	56(2)
C(2)	4874(6)	11870(3)	9096(3)	41(1)
C(3)	5567(6)	11960(3)	10053(3)	45(1)
C(4)	6600(6)	11364(3)	10559(3)	42(1)
C(5)	7256(11)	11557(5)	11501(4)	61(2)
C(6)	4636(6)	10445(3)	7476(3)	43(1)
C(7)	8105(5)	9514(3)	10218(3)	41(1)
C(8)	3849(5)	10247(3)	6573(3)	40(1)
C(9)	2870(7)	10796(3)	6083(4)	49(1)
C(10)	2147(6)	10625(3)	5227(4)	49(1)
C(11)	2430(6)	9895(3)	4835(3)	44(1)
C(12)	3356(7)	9340(3)	5332(4)	49(1)
C(13)	4065(6)	9515(3)	6180(4)	46(1)
C(14)	9118(5)	8874(3)	10659(3)	39(1)
C(15)	9565(6)	8212(3)	10185(4)	42(1)
C(16)	10538(6)	7633(3)	10609(4)	44(1)
C(17)	11056(6)	7690(3)	11517(3)	42(1)
C(18)	10605(7)	8346(3)	11995(4)	54(2)
C(19)	9652(7)	8922(4)	11567(4)	56(2)
C(20)	1077(9)	10278(4)	3430(5)	66(2)

continued ….

C(21)	12480(11)	7116(5)	12818(5)	72(2)

Table AII.13. $[Ni^{II}OL_3]\cdot CHCl_3$ (15) (Chapetr 5)

Atom	x	y	z	U(eq)
Ni(1)	6035(1)	1306(1)	9759(1)	50(1)
O(1)	5150(1)	2476(3)	9314(1)	57(1)
O(2)	6463(1)	1038(3)	9036(1)	58(1)
O(3)	6891(2)	-6(4)	11817(1)	87(1)
N(1)	4857(1)	2409(3)	10324(1)	57(1)
N(2)	5576(1)	1584(3)	10462(1)	51(1)
N(3)	6929(1)	163(3)	10178(1)	50(1)
N(4)	7437(1)	-309(3)	9781(1)	53(1)
N(5)	1890(2)	6647(4)	8773(1)	74(1)
N(6)	8863(1)	-684(3)	7219(1)	61(1)
C(1)	5389(3)	1399(7)	11570(2)	77(1)
C(2)	5843(2)	1111(4)	11055(1)	57(1)
C(3)	6632(2)	283(4)	11244(1)	62(1)
C(4)	7138(2)	-227(3)	10784(1)	55(1)
C(5)	7891(3)	-1144(5)	11058(2)	68(1)
C(6)	4693(2)	2860(3)	9703(1)	51(1)
C(7)	7127(2)	226(3)	9189(1)	50(1)
C(8)	3968(2)	3824(3)	9464(1)	52(1)
C(9)	3478(2)	4350(4)	9873(2)	60(1)
C(10)	2805(2)	5281(4)	9652(1)	62(1)
C(11)	2571(2)	5721(4)	8999(1)	58(1)
C(12)	3058(2)	5190(4)	8584(2)	62(1)
C(13)	3738(2)	4280(4)	8811(1)	59(1)
C(14)	7575(2)	-85(3)	8682(1)	49(1)
C(15)	7323(2)	641(4)	8076(1)	63(1)
C(16)	7745(2)	450(4)	7597(1)	62(1)
C(17)	8446(2)	-494(3)	7698(1)	49(1)
C(18)	8698(2)	-1233(3)	8313(2)	55(1)
C(19)	8268(2)	-1027(4)	8784(2)	54(1)
C(20)	1337(2)	6938(7)	9191(3)	87(1)
C(21)	1597(3)	6878(9)	8096(2)	101(2)
C(22)	9606(2)	-1591(7)	7334(2)	81(1)
C(23)	8613(3)	127(7)	6602(2)	82(1)
C(24)	9383(3)	2843(6)	8845(2)	96(1)
Cl(1)	10055(1)	1938(3)	9473(1)	172(1)
Cl(2)	9798(2)	3343(3)	8200(1)	203(1)
Cl(3)	8954(1)	4621(2)	9105(1)	161(1)

Publications

1. Square−planar nickel(II) complexes with a tridentate Schiff base and Monodentate heterocycles: Self-assembly to dimeric and one-dimensional array via hydrogen bonding.

   A. Mukhopadhyay, G. Padmaja, S. Pal and S. Pal,

   Inorg.Chem.Commun., 2003,**6,**381.

2. Complexes of nickel with tetradentate ligands formed by ring opening of 1-benzoyl-3,5-dimethyl-5-(1′-benzoylhydrazido)pyrazoline.

   A. Mukhopadhyay and S. Pal,

   Polyhedron, 2004, **23**, 1997.

3. Nickel(II) complexes with N,N,O-donor Schiff bases. Self-assembly to two-dimensional network via hydrogen bonding.

   A. Mukhopadhyay and S. Pal,

   J. Chem. Crystallogr., 2005, **35**, 737.

4. Intramolecular apical M···H–C interaction in square planar nickel(II) complexes with dibasic tridentate ligands and 2-phenyl-imidazole.

   A. Mukhopadhyay and S.Pal,

   Submitted

5. Square planar nickel(II) radical complexes with a non−innocent ligand system: Synthesis, characterization and DFT study.

   A. Mukhopadhyay and S. Pal,

   (Manuscript under preparation)